Impressum
TU Dortmund University
www.bci.tu-dortmund.de
Redaktion: Prof. Joerg C. Tiller
Publication date: Juli 2026

TU Dortmund University

2025

SCIENTIFIC HIGHLIGHTS

Annual Report

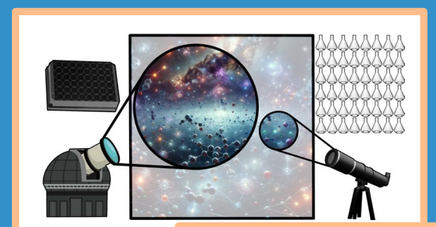

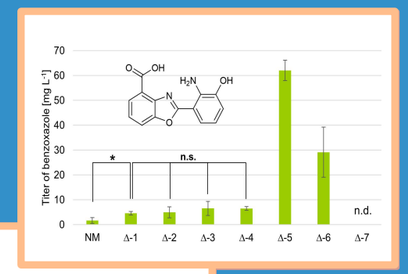

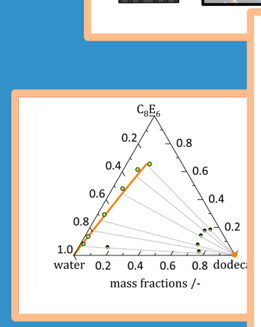

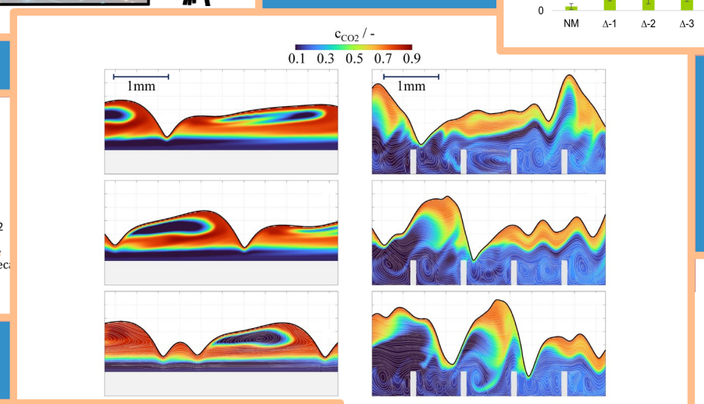

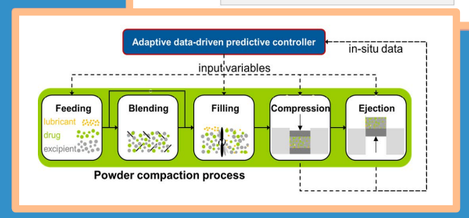

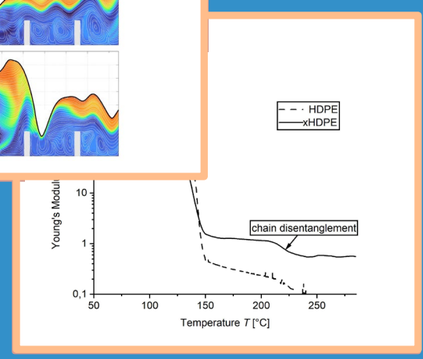

SCIENTIFIC HIGHLIGHTS 2025

Department of Biochemical- and Chemical Engineering

Content


Hannsjörg Freund


Toni Goßmann


Kai Langenbach


Oliver Kayser


Norbert Kockmann


Sergio Lucia


Stephan Lütz


Markus Nett


Gabriele Sadowski


Elsa Sánchez García


Gerhard Schembecker


Markus Thommes


Jörg C. Tiller


Dieter Vogt


Alba Diéguez Alonso

Department of BCI

Preface

Dear Reader,

The Department of Biochemical and Chemical Engineering (BCI) of TU Dortmund University presents the Scientific Highlights of the year 2025 in this issue as a long going tradition since the Highlights of the year 2010. This is the first issue that is created without the great help of Dr. Paul Kerzel. We wish him all the best for his retirement. The presented engineering science that covers a broad range from catalysis, fluid and solid production processes and separation, genetic engineering, computational engineering, drug discovery and formulation, and materials science is a unique combination that also reflects the wide knowledge of our undergraduate and graduate students who participated most in these investigations. As every year, we hope that the presented scientific success attracts current and future collaboration partners from industry and academia.

Enjoy the reading

Prof. Joerg C. Tiller

Equipment Design (AD)

Numerical simulation of two-phase flow and temperature distribution in microfluidic reactors.

Improved temperature measurement and two-phase capillary flow in microreactor systems.

Otto Mierka, Stefan Turek, Julia Surkamp, Lisa Schulz, Thorsten Röder, Norbert Kockmann

Numerical simulations give unrevealed details and enhanced understanding of complex technical systems. Simple tasks as temperature measurement or mixing of components depend on transport of heat and mass, which can be very complex, in particular on small length scales. Numerical simulations give detailed insights and can lead to optimized and efficient technical solutions.

The exact measurement of the temperature in laboratory continuous flow processes is of high importance for many investigations. The smaller the technical systems get, the less accurate the measurements will get and external influences get more important. Since the temperature is often the decisive parameter, accurate measurement is essential. The inline temperature measurement using a conventional Pt100 sensor with 1.6 mm outer diameter and 20 mm measuring length is illustrated in Fig. 1 for a T-piece in a continuous flow reactor on the micro-scale.

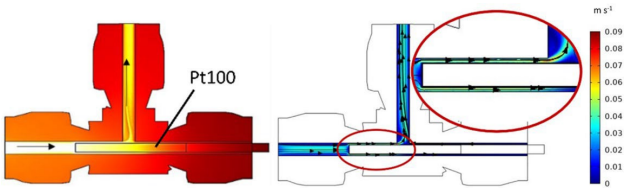

Figure 1. Simulated temperature profiles for side-on Pt100 positions inside the T-piece without insulation. (a); CFD simulation of the fluid flow velocity field at a flow rate of 5 mL min-1 for the side-on Pt100 position with a right-angle fluid flow. Flow direction is depicted by black arrows. The red circles show an enlarged section of the flow around the Pt100 (diameter: 1.6 mm) inside the channel for both side-on and head-on position.

Extensive fluid flow and heat transfer simulation in different flow configuration indicated the importance of thermal insulation for the measurement accuracy. The shown 90° installation in Fig 1 together with thermal insulation result in the optimal temperature measurement.

Mass transfer simulation is very demanding on small scale due to the different time scale of momentum and species transfer, described by the dimensionless Schmidt number Sc. For gaseous flow, Sc=1 and can easily simulated with CFD methods. For liquid flow, the Sc number is approx. 3 orders of magnitude larger and the simulations need a much higher temporal and spatial resolution. Hence, fluid dynamic simulation coupled with particle tracking methods give a good approximation of mixing processes, as shown for the liquid phase in Fig. 2 for gas-liquid Taylor flow in 1.6 mm helical capillaries with a 90° bend. This type of tubular reactor is called Coiled Flow Inverter, which is a central investigation object in the Laboratory of Equipment Design. Together with the research group in numerical mathematics, the dynamic behavior of the mixing was described for the first time and gives unique insights to the detailed local dispersion process, see Fig. 2.

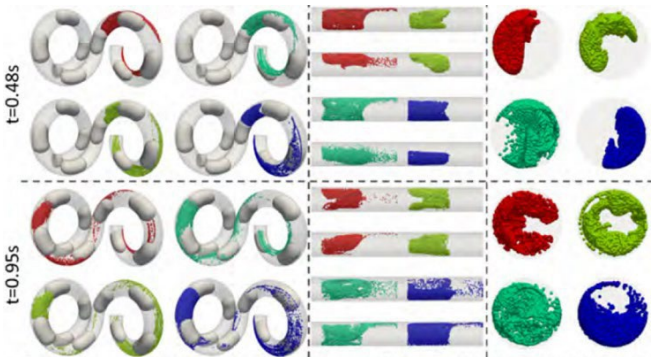

Figure 2. Dispersion analysis with the use of particle tracing method demonstrated for the 2-phase CFI flow. The leftmost column shows the particle dynamics in the physical geometry. The middle and right columns show the particle dynamics in the “backtransformed” geometry (with straight capillary display) in the axial and cross-sectional direction, respectively, by tracking the initially seeded liquid slug segment. The evolution of the particle distribution is visualized in the top-to-bottom direction for the time levels 0.00 s, 0.48 s, 0.95 s, and 1.43 s.

The impact of secondary flow vortices of Dean and Taylor nature on mixing and dispersion is very good to observe with direct numerical simulation based on a finite element method. The helical flow with the influence of the centrifugal force and pitch (Dean flow) as well as the capillary two-phase flow (Taylor bubble) is described and characterized by particle dispersion in the axial and radial direction. The full 3D resolution of the flow field and detailed examination of particle dispersion provides valuable insights into mixing dynamics, in particular the deflection of flow velocity from the center axis contributes is followed by tracking of particle with defined starting positions, aiding in flow visualization and dispersion characterization.

julia.surkamp@tu-dortmund.de
stefan.turek@tu-dortmund.de
norbert.kockmann@tu-dortmund.de

Publications:
Nuredin, V.; Schulz, L.; Kockmann, N.; Röder, T., Best practice approach for temperature measurement in flow chemistry based on CFD simulation. J. Flow Chem., 15, 47-58 (2025). https://doi.org/10.1007/s41981-024-00341-0
Mierka, O.; Münster, R.; Surkamp, J.; Turek, S.; Kockmann, N., Direct numerical simulation of dispersion and mixing in gas-liquid Dean-Taylor flow with influence of a 90° bend. Chem. Eng. Sci. 301, 120691 (2025). https://doi.org/10.1016/j.ces.2024.120691

Variations in modular crystallization and related process development.

The Plentitude, Abundance, and Wealth of Crystallization Equipment and Continuous Processes.

Laura Marsollek, P. L. Knappstein, M. Hubmann, Norbert Kockmann

Modular plants offer adaptable and efficient production systems enabling rapid process development through interchangeable Process Equipment Assemblies (PEAs). In combination with crystallization, novel process concepts can already be developed and validated on laboratory scale with consistent pathway to small-scale production.

To extend the modular concept to solid product manufacturing, a lab-scale Draft Tube Baffle Crystallizer (DTBC) with an inner volume of 2.1 L was modularized for continuous evaporation crystallization (Fig. 1). A gate system was developed for the reliable continuous solid removal. The fine grain dissolution (FGD) had to be adapted to the hydrostatic conditions in a scaled down DTBC. By utilizing a geodetic height of 1.4 m, a small operating window for the FGD was defined, achieving dissolution of 98 % of fine particles < 90 µm and a solid fraction of 0.5 wt%. The evaporation rate has a significant influence on the crystallization kinetics and were determined by thermal characterization of the lab-scale DTBC. Together with classification behavior studies under varying parameters such as rotation speed of the stirrer and product removal rate, these results form the basis for describing evaporation crystallization in modular DTBC systems.

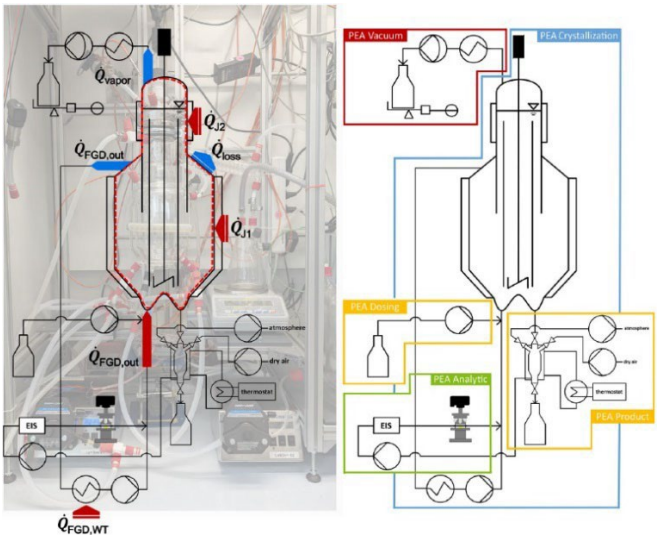

Figure 1. Experimental setup of the DTBC with illustrated heat flows (left) and modular division into various PEAs (right) [Marsollek et al., CIT, 2025]

More equipment studies can be found in Kockmann et al., MDPI crystals journal in 2025.

Solubility data are the base for crystallization process development. The study of solid–liquid equilibria for L-tryptophan, which possesses an α-amino group, an α-carboxylic acid group, and an indole compound, presents significant challenges. Transitioning from batch to continuous processes allows for improved scalability and resource management. The solubility and cooling crystallization characteristics of L-tryptophan from 1-propanol/water and iso-propanol/water solvent mixtures in the temperature range from 60 °C to 20 °C (Fig. 2).

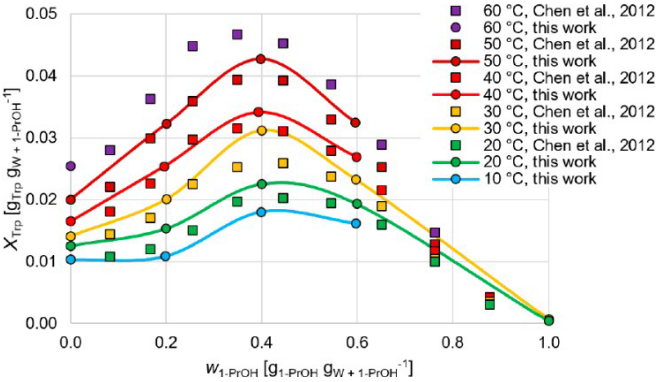

Figure 2. Comparison of the experimentally determined solubility data ("this work" in the legend) and the literature data for the solubilities of L-Trp in water/1-PrOH mixtures according to Chen et al., Fluid Phase Equilib. 2012.

By adding the alcohols, the solubility can be drastically increased by more than 100% compared to the solubility in pure water. Lab-scale crystallization experiments in both batch and continuous operation allow for the assessment of the process feasibility and solvent impacts on the process and product. The focus is on process development that emphasizes material savings through strategic solvent selection and co-solvent choices.

laura.marsollek@tu-dortmund.de
norbert.kockmann@tu-dortmund.de

Publications:
Marsollek, L.; Knappstein, P.; Duncker, P.; Lamprecht, J.; Westkämper, N.; Kockmann, N.
Conceptual Approach for Lab-Scale Vacuum DTB Crystallizer with Online Monitoring and Flexible Process Functionalities for Rapid Process Adjustment.
Chem. Ing. Technik, 97, 1103-1109 (2025).
https://doi.org/10.1002/cite.70033
Marsollek, L.; Hubmann, M.; Buchhorn, K.; Kockmann, N.
Automated and Selective Product Removal for Lab-Scale Draft Tube Baffle Crystallizer Under Vacuum Operation.
MDPI-crystals, 15, 893 (2025).
https://doi.org/10.3390/cryst15100893
Kockmann, N.; Schmalenberg, M.; Strakeljahn, B.; Wohlgemuth, K.
Energy and Resource Efficient Continuous Cooling Crystallization with Modular Lab-scale Equipment.
MDPI-crystals, 15, 421 (2025).
https://doi.org/10.3390/cryst15050421
Hohmann, L.; Antpusat (née Hampel), R.; Kockmann, N.
Process Design for Continuous Crystallization of l-Tryptophan in Water–Alcohol Solvent Mixtures.
MDPI-crystals, 15(4), 355 (2025).
https://doi.org/10.3390/cryst15040355

Research Data Management and Semantics for Smarter Catalysis Research.

Enhanced data interoperability and precise reaction classification through refined chemical ontologies.

Hendrik Borgelt, Frederick G. Kitel, Norbert Kockmann

Semantic analysis enhances catalysis research by refining and extending chemical ontologies, enabling automated identification of functional groups and more generalized reaction classification. The main benefit for researchers is improved data interoperability and usability through semantic structuring and a user-friendly interface that supports precise querying and reasoning over complex catalytic reactions.

The Findability, Accessibility, Interoperability, and Reusability (FAIR) [1] of research data is becoming more important to accelerate research processes in general. Metadata standards are important for research data management derived from domain-specific vocabulary. The Reac4Cat ontology established a generic data pattern for modeling reactions and enabling the classification of reactions occurring in a reaction experiment, which is enlarged in this research. Based on PubChem and KEGG as knowledge sources, chemical reactions are described in machine- and human-readable format, see the table in Figure 1, which only shows some of the information provided from the KEGG database.

Entry	R12516 Reaction
Name	3-methylbutyl acetate acetohydrolase
Definition	Isoamyl acetate + H2O <=> 3-Methylbutanol + Acetate
Equation	C12296 + C00001 <=> C07328 + C00033
	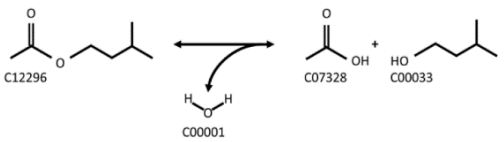

Figure 1. Sketch of a reaction entry in the KEGG reaction database. In this case, the most relevant information from reaction R12516 [Genes, K. Genomes R12516-KEGG Entry] is depicted. The reactants and products of the example reaction can be seen in the “equation” row, with their respective KEGG-specific chemical IDs.

To differentiate between reference reactions and experimental data, two distinct data patterns are employed: chemical entities and their respective functional group residues. Logical axioms and class hierarchy represent the data pattern for reference reactions, where new reference data should be classified via axioms of the respective reaction classes. This enables various permutations of a reaction to be introduced and still classified as the same reaction. Specifically, permutations of chemical entities are presented by the axioms here.

Figure 2 presents the data pattern used for experimental reactions. This model is derived from the Reac4Cat ontology and is intentionally different from the reference data pattern. For purposes of simplicity, Figure 2 only sketches the design pattern. The primary objective of this differentiation is to prevent the drawing of inferences that should not be drawn. For reference reactions, it can be assumed that all data are available. However, experimental data may be incomplete. Reasoning based on such incomplete information may cause inconsistencies and should, therefore, be avoided. By using different data patterns and thereby different relations between instances describing reference datasets and experimental datasets, the axioms and thus the logic can differentiate between different data patterns.

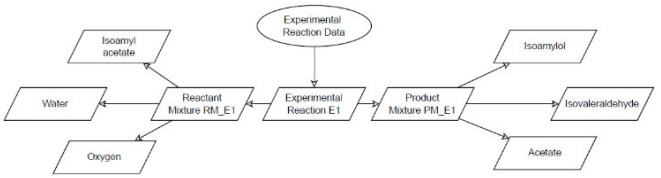

Figure 2. Depiction of the data pattern used for experimental reactions. This pattern follows the Reac4Cat ontology [Behr et al. Datenbank Spektrum 2024] data pattern and as such is only sketched here. The data pattern differs from that of reference reactions in that it includes instances that describe the reactant and product mixture composition.

A key advantage of this approach is the direct link to existing ontologies, as SHACL shapes represent an artifact that can be imported into the OWL language, unlike pure SPARQL queries. Two example reactions were used to show how this can be applied. While this methodology represents a continuation and refinement of existing approaches to processing reaction datasets in knowledge graphs, it is worth noting the approach’s extensibility. Through more detailed reaction descriptions, more complex modeling can be implemented in both the OWL and the SHACL-SPARQL query.

hendrik.borgelt@tu-dortmund.de
norbert.kockmann@tu-dortmund.de

Publications:
Borgelt, H.; Kitel, F.G.; Kockmann, N. Ontology-Based Data Pipeline for Semantic Reaction Classification and Research Data Management. MDPI-computers,14, 311, (2025). https://doi.org/10.3390/computers14080311
Strömert, P.; Borgelt, H.; Linke, D.; Doerr, M.; Katabathuni, B.; Koepler, O.; Kockmann, N. ChemDCAT-AP: Enabling Semantic Interoperability with a Contextual Extension of DCAT-AP. 19th International Conference on Metadata and Semantics Research, December 16–19, 2025, MTSR2025, Thessaloniki, Greece. https://doi.org/10.48550/arXiv.2602.01822

Stirred cell mini-reactor with modular setup for liquid-liquid reactions.

Modular reactor systems for development of continuous processes.

Mathias Schmitz, Lennart Regenitter, Anil Can Karsli, Neetika Sain, Norbert Kockmann

Modularization of chemical plants has gained increased interest due to its flexibility and shorter time-to-market. This contribution resents a stirred-pulsed DN15 extraction cell (SPEC) operated as a continuous stirred-tank reactor (CSTR) within a modular plant concept. The main objective is to demonstrate the transferability of an extraction column to reaction processes and to showcase the associated service-based automation concept using Module Type Package (MTP) principles.

The SPEC consists of six stirred compartments separated by sieve plates and equipped with a pulsation unit, conceptually resembling a cascade of CSTRs and aiming to enhance mass transfer. Saponification of ethyl acetate with sodium hydroxide is used as a test reaction, which proceeds either as a single-phase second-order reaction or as a two-phase pseudo-first-order reaction depending on the reactant ratio. Conversion is monitored via conductivity measurements, from which kinetic parameters are derived and further processed for simulation purposes. The experimental setup is divided into several Process Equipment Assemblies (PEAs), including a reactor PEA, three feeding PEAs, a temperature PEA, and a pulsation PEA. For the different PEAs were services as their base functionalities defined. The services are orchestrated into different recipes for the particular process, either extraction or reaction.

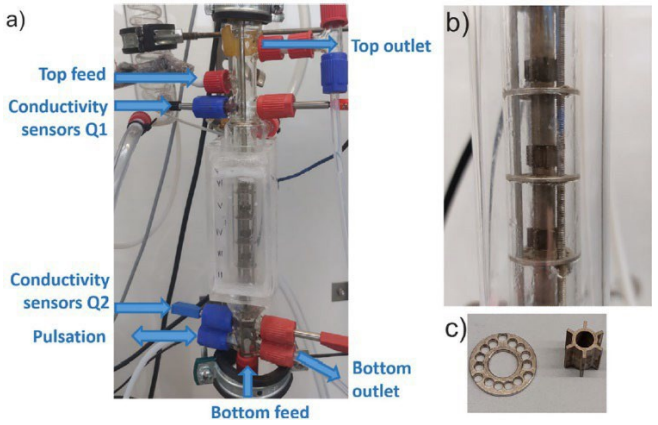

Figure 1. a) Stirred-pulsed extraction cell with inlet and outlet streams and their respective direction for the extraction process. The pulsation is connected in the bottom of the SPEC. The conductivity sensors are at the bottom and head of the SPEC and between the compartments and the inlet and outlets. b) Close-up of the internals inside of the SPEC. c) Internals of the six compartments. Each compartment consists of a stirrer and a sieve plate with 2-mm holes.

In contrast to the traditional CSTR the SPEC offers multiple operation modes which are beneficial for increased mass transport between two liquid phases. Single- and two-phase operations in co-current and counter-current modes are investigated, showing that co-current operation provides more stable measurement signals, while counter-current operation achieves faster conversion but exhibits stronger fluctuations due to phase separation effects. The flexible reconfiguration of the PEAs depending on the selected operation mode is also described.

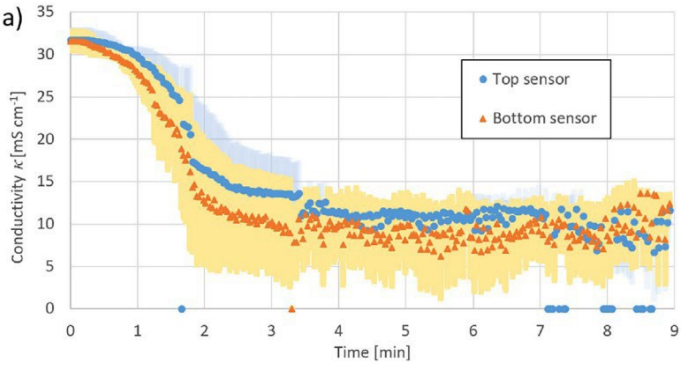

Figure 2. Measured conductivity for a two-phase liquid-liquid saponification in countercurrent operation mode. The experiment was done three times and the mean values are plotted together with the standard deviation.

The application of an extraction column as a CSTR was demonstrated which is a sparsely used concept for a reactor but exhibits promising results in comparison to traditional STRs. This is especially interesting in terms of modularization, as the same PEA can be used for different unit operations. In addition, the allocation of components to PEAs was discussed in order to maximize flexibility and maintain modular interoperability.

mathias.schmitz@tu-dortmund.de
norbert.kockmann@tu-dortmund.de

Publications:
Schmitz, M.; Regenitter, L.; Karsli, A.C.; Sain, N.; Kockmann, N. Stirred cell mini-reactor with modular setup for liquid-liquid reactions.
Chem. Ing. Technik, 97, 444-453 (2025).
https://doi.org/10.1002/cite.202400142

AI-assisted Image recognition for emulsion processes.

Modular sensor system for process development and production quality control.

Inga Burke-Oeing, Norbert Kockmann

The developed AI-based sensor system can monitor and optimize liquid–liquid mixing processes in real time, helping produce emulsions such as those used in cosmetics. By combining image recognition with a dynamic micromixer, the study showed how digital technologies enable faster, more efficient, and flexible small-scale emulsion production.

Smart sensor systems are increasingly important for real-time process analysis in the chemical industry. An image-based sensor integrated into an emulsification setup was developed and evaluated using different YOLO object detection models on an edge device. The inclusion of digital images and synthetic datasets improved model robustness. The potential of real-time object detection was demonstrated for monitoring liquid–liquid emulsification processes. An important application for emulsions is cosmetics, which are shown for small-scale-production in the following. The laboratory setup including a detailed view of the micromixer and the optical analysis method is presented in Fig.1.

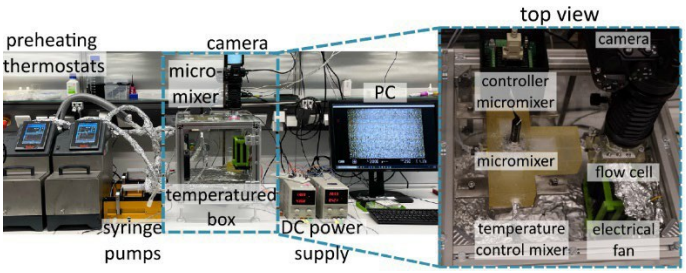

Figure 1 Lab setup including a detailed view of the micromixer and the optical analysis method including an optical measurement flow cell and camera setup.

A modified, microstructured annular gear pump from HNP Mikrotechnik, Schwerin, was investigated as an active micromixer, allowing independent adjustment of mixing power to study droplet size distribution under varying process conditions. Using AI-based image recognition for real-time emulsion characterization, optimal operation ranges and design parameters for liquid–liquid mixing can be rapidly identified and optimized.

The dynamic micromixer was investigated for continuous emulsification of almond oil–water, coconut oil–water, and lotion with droplet sizes between 3 and 75 µm under varying process conditions. The defined operation window with rotor speed of 6000–12000 min^{-1}, a total flow rate of 0.5–1.5 mL min^{-1}, and an oil fraction of 10–18.4 wt% demonstrated the mixer's suitability for flexible emulsion production in rapidly changing applications. Examples of the droplet size distribution is shown in Fig. 2 as histogram and exemplarily AI-based detected droplets in the flow cell.

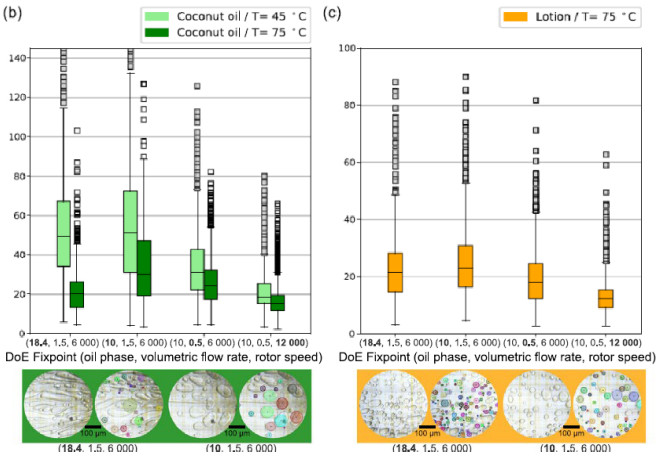

Figure 2. The figure shows the droplet size distribution for different process parameters at different temperature levels. Below, example droplet images for the different process states after the AI-based object detection. left: the substance system coconut oil–water and the lotion. The light color indicates the results for TT = 45 °C and the dark color for TT = 75 °C.

The emulsification process produced stable droplets within a broad size range, confirming efficient and controllable mixing performance. The integration of AI-based inline optical analysis enabled rapid and reliable characterization of emulsions in real time. Overall, the results demonstrated the general applicability of the dynamic micromixer for continuous emulsion production across various substance systems.

inga.burke@tu-dortmund.de
norbert.kockmann@tu-dortmund.de

Publications:
Burke-Oeing, I.; Derkum, S.; Olusanya, T.O.O.; Kockmann, N. AI- and Image-Based Analysis of Emulsification Processes: Opportunities and Challenges. Chem. Ing. Technik, 97, 1070-1084 (2025). https://doi.org/10.1002/cite.70018

Burke, I.; Brockerhoff, L.; Kockmann, N. Fast liquid-liquid dispersion for low volumina in an active micromixer – AI-based investigation. Chem. Eng. & Proc.-PI, 215, 110362 (2025). https://doi.org/10.1016/j.cep.2025.110362

Augmented reality and mobile teaching in fluid mechanical education.

Evaluating effectiveness and appeal of teaching units.

Konrad Boettcher, Alexander Sommer-Behr, Daniel Aurich

The works demonstrate how mobile virtual and augmented reality laboratories expand fluid-mechanics experiments in a scalable, location-independent, and pedagogically effective way by making invisible flow phenomena visible and linking real measurement data with interactive 3D simulations. Both approaches enhance motivation and conceptual understanding by translating complex fluid-mechanics concepts into intuitive learning environments that can be experienced directly.

To make invisible flow phenomena in real laboratory experiments (Fig. 1) visible, CFD simulation data are implemented in professional game engines and made interactable. The current flow quantities in the wind tunnel are measured and transmitted via WiFi to the AR app. The associated teaching unit is designed on the basis of constructive alignment, and the SOLO taxonomy is used to identify the cognitive processes in order to formulate learning objectives that promote deep rather than surface learning.

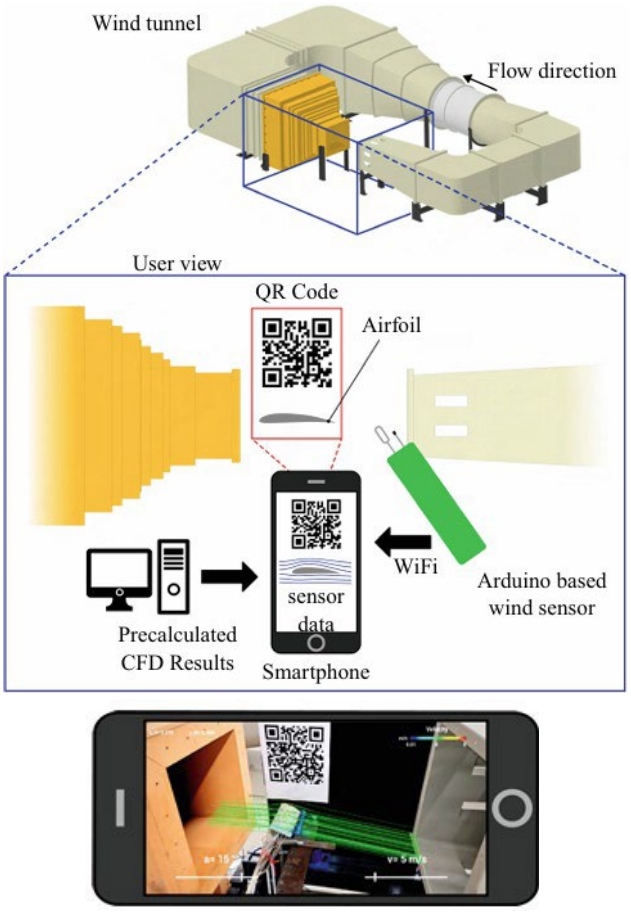

Figure 1. A wind tunnel with a dedicated measurement section is used, and the operating principle is illustrated in the upper schematic. An Arduino-based thermo-anemometer transmits the incoming flow velocity via WiFi to the smartphone, which retrieves the corresponding data. A QR code provides spatial registration. The streamlines are projected into the smartphone's camera view, enabling an intuitive understanding of pressure fields, velocity distributions, and flow separation.

The app AR-Flow (Fig. 2) enables students to interactively explore small multi-scale flow phenomena on their own mobile devices in fluid-mechanics courses. It aims to foster functional understanding through a modular, level-based learning design that integrates digital lab manuals, AR visualizations, and context-specific learning tasks. The resulting environment combines script-based learning with interactive laboratories in a quest-based format that guides students from superficial learning toward relational and extended-abstract understanding (deep learning) of core fluid-mechanics concepts. Student motivation is rated highly positive, with an average of 4.42/5. In pre- and post-tests targeting tasks at the extended-abstract cognitive level, students achieved partially substantial improvements, with effect sizes between d = 0.1 and d = 0.7.

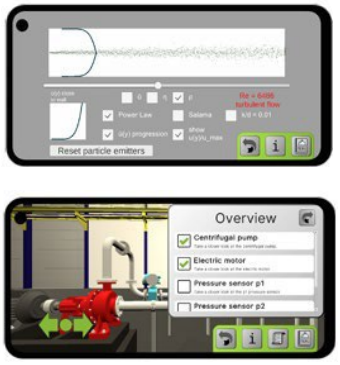

Figure 2. AR-App experiment on turbulent flows and quest system within the pump test rig level.

konrad.boettcher@tu-dortmund.de
alexander.behr@tu-dortmund.de
daniel.aurich@tu-dortmund.de

Publications:
Aurich, D., Sommer-Behr, A., Neumann, J., Boettcher, K. E. R., Brümmer, A. (2025). Evaluating Effectiveness and Appeal of a Virtual Laboratory in an Undergraduate Fluid Mechanics Course. International J. of Eng. Ped. (iJEP), 15(8), pp. 65–75. https://doi.org/10.3991/ijep.v15i8.59067
Aurich, D., Lehr, C., Wolny, M.M., Boettcher, K., Brümmer, A. (2024). Immersive Airfoil Student Laboratory: Augmented Reality Application with Real-Time Measurement Data Access. In: May, D., Auer, M.E., Kist, A. (eds) Online Laboratories in Engineering and Technology Education. Lecture Notes in Networks and Systems, vol 1135. Springer, Cham. https://doi.org/10.1007/978-3-031-70771-1_14

Awards:
GOLC International Online Laboratory Awards 2026
Best Paper Award Smart Technology in Education 2026

2025

Peer Reviewed Journal Articles

Burke-Oeing, I.; Derkum, S.; Olusanya, T.O.O.; Kockmann, N.
AI- and Image-Based Analysis of Emulsification Processes: Opportunities and Challenges.
Chem. Ing. Technik, 97, 1070-1084 (2025).
https://doi.org/10.1002/cite.70018

Marsollek, L.; Knappstein, P.; Duncker, P.; Lamprecht, J.; Westkämper, N.; Kockmann, N.
Conceptual Approach for Lab-Scale Vacuum DTB Crystallizer with Online Monitoring and Flexible Process Functionalities for Rapid Process Adjustment.
Chem. Ing. Technik, 97, 1103-1109 (2025).
https://doi.org/10.1002/cite.70033

Marsollek, L.; Hubmann, M.; Buchhorn, K.; Kockmann, N.
Automated and Selective Product Removal for Lab-Scale Draft Tube Baffle Crystallizer Under Vacuum Operation.
MDPI-crystals, 15, 893 (2025).
https://doi.org/10.3390/cryst15100893

Borgelt, H.; Kitel, F.G.; Kockmann, N.
Ontology-Based Data Pipeline for Semantic Reaction Classification and Research Data Management.
MDPI-computers,14, 311, (2025).
https://doi.org/10.3390/computers14080311

Burke, I.; Brockerhoff, L.; Kockmann, N.
Fast liquid-liquid dispersion for low volumina in an active micromixer – AI-based investigation.
Chem. Eng. & Proc.-PI, 215, 110362 (2025).
https://doi.org/10.1016/j.cep.2025.110362

Kockmann, N.; Schmalenberg, M.; Strakeljahn, B.; Wohlgemuth, K.
Energy and Resource Efficient Continuous Cooling Crystallization with Modular Lab-scale Equipment.
MDPI-crystals, 15, 421 (2025).
https://doi.org/10.3390/cryst15050421

Hohmann, L.; Antpusat (née Hampel), R.; Kockmann, N.
Process Design for Continuous Crystallization of l-Tryptophan in Water–Alcohol Solvent Mixtures.
MDPI-crystals, 15(4), 355 (2025).
https://doi.org/10.3390/cryst15040355

Schmitz, M.; Regenitter, L.; Karsli, A.C.; Sain, N.; Kockmann, N.
Stirred cell mini-reactor with modular setup for liquid-liquid reactions.
Chem. Ing. Technik, 97, 444-453 (2025).
https://doi.org/10.1002/cite.202400142

Nuredin, V.; Schulz, L.; Kockmann, N.; Röder, T.
Best practice approach for temperature measurement in flow chemistry based on CFD simulation.
J. Flow Chem., 15, 47-58 (2025).
https://doi.org/10.1007/s41981-024-00341-0

Mierka, O.; Münster, R.; Surkamp, J.; Turek, S.; Kockmann, N.
Direct numerical simulation of dispersion and mixing in gas-liquid Dean-Taylor flow with influence of a 90° bend.
Chem. Eng. Sci. 301, 120691 (2025).
https://doi.org/10.1016/j.ces.2024.120691

Peer-reviewed Conference Contributions

Strömert, P.; Borgelt, H.; Linke, D.; Doerr, M.; Katabathuni, B.; Koepler, O.; Kockmann, N. **ChemDCAT-AP: Enabling Semantic Interoperability with a Contextual Extension of DCAT-AP.**
19th International Conference on Metadata and Semantics Research, December 16–19, 2025, MTSR2025, Thessaloniki, Greece.
https://doi.org/10.48550/arXiv.2602.01822

2024

Peer Reviewed Journal Articles

Schulz, L.; Kockmann, N.; Röder, T.
Model-based scale-up of a homogeneously catalysed Sonogashira coupling reaction in a 3D printed continuous-flow reactor.
ACS Engineering Au, 4, 519-523 (2024).
https://doi.org/10.1021/acsengineeringau.4c00027

Marsollek, L.; Lamprecht, J.; Kockmann, N.
Investigation of AI Algorithms for Photometric Online Analysis in a Draft Tube Baffle Crystallize.
MDPI-crystals, 14, 1045 (2024).
https://doi.org/10.3390/cryst14121045

Oldach, B.; Fortmann, R.; Pleie, T.; Timm, P.; Kockmann, N.
Design and Rapid Prototyping of 3D-Printed Microfluidic Systems for Multiphase Flow.
MDPI-chemistry, 6, 1458–1476 (2024).
https://doi.org/10.3390/chemistry6060088

Burke, I.; Dhayaparan, T.; Youssef, A.S.; Schmidt, K.; Kockmann, N.
Two deep learning methods in comparison to characterize droplet sizes in emulsification flow processes.
J. Flow Chem. 14, 597-613 (2024).
https://doi.org/10.1007/s41981-024-00330-3

Boga. B.; Baur, K.; Timiş, E.-C.; Lund, H.; Peppel, T.; Cristea, V.-M.; Kockmann, N.; Steinfeldt, N.
Photocatalytic antibiotic degradation in coated open microchannels by applying 2D and 3D flow modeling with kinetics.
J. Environmental Chem. Eng. 12(6), 114173 (2024).
https://doi.org/10.1016/j.jece.2024.114173

Behr, A.S.; Chernenko, D.; Koßmann, D.; Neyyathala, A.; Hanf, S.; Schunk, S.A.; Kockmann, N.
Generating knowledge graphs through AI-assisted text mining of catalysis research related literature.
Catalysis Science & Technology, 14, 5699-5713 (2024).
https://doi.org/10.1039/D4CY00369A

Oldach, B.; Wintermeyer, P.; Kockmann, N.
Transfer of Periodic Phenomena in Multiphase Capillary Flows to a Quasi-Stationary Observation Using U-Net.
MDPI-computers, 13(9), 230 (2024).
https://doi.org/10.3390/computers13090230

Surkamp, J.; Wellmann, L.; Lütz, S.; Rosenthal, K.; Kockmann, N.
Ethanol production using *Zymomonas mobilis* and in situ extraction in a capillary microreactor.
MDPI-micromachines, 15, 1255 (2024).
https://doi.org/10.3390/mi15101255

Burke, I.; Salzer, S.; Stein, S.; Olusanya, T.O.O.; Thiel, O.F.; Kockmann, N.
AI-Based Integrated Smart Process Sensor for Emulsion Control in Industrial Application.
MDPI-processes, 12(9), 1821 (2024).
https://doi.org/10.3390/pr12091821

Höving, S.; Ronnewinkel, P.; Kockmann, N.
From Batch to Continuous Small-Scale Production of Particles: Mixer Design Methodology for Robust Operation.
MDPI-crystals, 14(5), 398 (2024).
https://doi.org/10.3390/cryst14050398

Oldach, B.; Chiang, Y.-Y.; Ben-Achour, L.; Chen, T.-J.; Kockmann, N.
Performance of Different Microfluidic Devices in Continuous Liquid-Liquid Separation.
J. Flow Chem, 14, 547-557 (2024).
https://doi.org/10.1007/s41981-024-00326-z

Burke, I.; Assies, C.; Kockmann, N.
Rapid prototyping of a modular optical flow cell for image-based droplet size measurements in emulsification processes.
J. Flow Chem, 14, 515-528 (2024).
https://doi.org/10.1007/s41981-024-00323-2

Behr, A.S.; Borgelt, H.; Kockmann, N.
Reac4Cat-Ontology: Harnessing the Power of Ontological Description Logic in Catalysis Research as a Practical Approach to Knowledge Inferences.
Datenbank-Spektrum, 24, 139-150 (2024).
https://doi.org/10.1007/s13222-024-00476-3

Boga, B. Baur, K.; Cristea, V.-M.; Steinfeldt, N.; Kockmann, N.
Experimental and numerical investigations of flow behavior in an open falling film microreactor equipped with curved flow splitting elements.
Chem. Eng. Sci., 298, 120338 (2024).
https://doi.org/10.1016/j.ces.2024.120338

Dinter, R.; Helwes, L.; de Vries, S.; Jegatheeswaran, K.; Jibben, H.; Kockmann, N.
3D-printed open-source sensor flow cells for microfluidic temperature, electrical conductivity, and pH value determination.
J. Flow Chem, 14, 469-479 (2024).
https://doi.org/10.1007/s41981-024-00319-y

Behr, A.S.; Borgelt, H.; Kockmann, N.
Ontologies4Cat: Investigating the Landscape of Ontologies for Catalysis Research Data Management.
J. Cheminformatics, 16(1), 16 (2024).
https://doi.org/10.1186/s13321-024-00807-2

Behr, A.S.; Surkamp, J.; Abbaspour E.; Häußler, M.; Lütz, S.; Pleiss, J.; Kockmann, N.; Rosenthal, K.
Fluent Integration of Laboratory Data into Biocatalytic Process Simulation Using EnzymeML, DWSIM, and Ontologies.
MDPI-processes, 12, 597 (2024).
https://doi.org/10.3390/pr12030597

2023

Peer Reviewed Journal Articles

Dinter, R.; Götte, K.; Gronke, F.; Justen, L.; Brunschweiger, A.; Kockmann, N.
Development of an Automated Flow Chemistry Affinity-Based Purification Process for DNA-Encoded Chemistry.
J. Flow Chem, 13, 361–373 (2023).
https://doi.org/10.1007/s41981-023-00282-0

Behr, A.S.; Völkenrath, M.; Kockmann, N.
Ontology extension with NLP-based concept extraction for domain experts in catalytic sciences.
Knowledge and Information Systems, 65(12), 5503–5522 (2023).
https://doi.org/10.21203/rs.3.rs-3491129/v1

Neuendorf, L.M.; Khaydarov, V.; Schlander, C.; Kock, T.; Fischer. J.; Urbas, L.; Kockmann, N.
Artificial Intelligence-based Module Type Package (MTP)-compatible Smart Sensors in the Process Industry.
Chem. Ing. Technik, 95(10), 1546-1554 (2023).
https://doi.org/10.1002/cite.202300047

Dinter, R.; Willems, S.; Nissalk, T.; Hastuerk, O.; Brunschweiger, A.; Kockmann, N.
Development of a Microfluidic Photochemical Flow Reactor Concept by Rapid Prototyping.
frontiers in chemistry, 11, 1244043 (2023).
https://doi.org/10.3389/fchem.2023.1244043

Höving, S.; Schmidt, T.; Peters, M.; Lapainis, H.; Kockmann, N.
Small-scale Solids Production Plant with Cooling Crystallization, Washing, and Drying in a Modular, Continuous Plant.
MDPI-processes, 11(8), 2457 (2023).
https://doi.org/10.3390/pr11082457

Klose, A.; Wagner-Stürz, D.; Neuendorf, L.M.; Oeing, J.; Khaydarov, V.; Schleehahn, M.; Kockmann, N.; Urbas, L.
Automated Evaluation of Biochemical Plant KPIs based on DEXPI Information.
Chem. Ing. Technik, 95(7), 1165-1171 (2023).
https://doi.org/10.1002/cite.202200239

Oeing, J.; Brandt, K.; Wiedau, M.; Tolksdorf, G.; Welscher, W.; Kockmann, N.
Graph Learning in Machine-Readable Plant Topology Data.

Chem. Ing. Technik, 95(7), 1049-1060 (2023).
https://doi.org/10.1002/cite.202200223

Neuendorf, L.M.; Höving, S.; Bennemann, L.; Kockmann, N.
Detecting crystals in suspensions: convolutional neural networks vs. a gravity based approach for size distribution detection.
Chem. Ing. Technik, 95(7), 1146-1153 (2023).
https://doi.org/10.1002/cite.202200235

Oeing, J.; Holtermann, T.; Welscher, W.; Kockmann, N.
preHAZOP: Graph-based safety analysis for early integration into automated engineering workflows.
Chem. Ing. Technik, 95(7), 1083-1095 (2023).
https://doi.org/10.1002/cite.202200222

Neuendorf, L.M.; Hammal, Z.; Fricke, A.; Kockmann, N.
AI-based supervision for a stirred extraction column assisted with population balance-based simulation.
Chem. Ing. Technik, 95(7), 1134-1145 (2023).
https://doi.org/10.1002/cite.202200241

Bortz, M.; Dadhe, K.; Engell, S.; Gepert, V.; Kockmann, N.; Müller-Pfefferkorn, R.; Schindler, T.; Urbas, L.
AI in Process Industries – Current Status and Future Prospects.
Chem. Ing. Technik, 95(7), 975-988 (2023).
https://doi.org/10.1002/cite.202200247

Dobler, T.; Höving, S.; Dreiser, C.; Gleiß, M.; Gröschen, M.; Henkel, A.; Hörne, M.; Schäfer, M.; Sonnenschein, J.; Wiese, G.; Wohlgemuth, K.; Kockmann, N.; Nirschl, H.
From Lab to Pilot Scale: Commissioning of an Integrated Device for the Generation of Crystals.
Chem Eng. & Technol., 46(7), 1511-1520 (2023).
https://doi.org/10.1002/ceat.202200616

Bittorf, L.; Oeing, J.; Kock, T.; Garreis, R.; Kockmann, N.
Design of MTP services for modular downstream units and process analytic technology following VDI/VDE/NAMUR 2658.
Chem. Eng. & Technol., 46(7), 1502-1510 (2023).
https://doi.org/10.1002/ceat.202200390

Elhami, V.; Neuendorf, L.M.; Kock, T.; Kockmann, N.; Schuur, B.
Separation of Crotonic Acid and 2-Pentenoic Acid Obtained by Pyrolysis of Bio-Based Polyhydroxyalkanoates Using a Spinning Band Distillation Column.
ACS Sustain. Chem. Eng., 11(12), 4699-4706 (2023).
https://doi.org/10.1021/acssuschemeng.2c07046

Dinter, R.; Willems, S.; Hachem, M.; Streltsova, Y.; Brunschweiger, A.; Kockmann, N.
Development of a two-phase flow reaction system for DNA-encoded amide coupling.
Reac. Chem. & Eng., 8, 1334-1340 (2023).
https://doi.org/10.1039/D3RE00020F

Frede, T.A.; Weber, C.; Christ, T.; Brockhoff, T.; Ludwig, D.; Kockmann, N.
Data Management of a Microcalorimeter Using a Modular Open-Source IoT Platform.
MDPI-processes, 11(1), 279 (2023).
https://doi.org/10.3390/pr11010279

Sakthithasan, P.; Orth, L.; Venhuis, M.; Kockmann, N.
Design of a process intensified liquid-liquid extraction cell for higher temperature and pressure.
Chem. Eng. & Technol., 46(5), 882-890 (2023).
https://doi.org/10.1002/ceat.202200550

Höving, S.; Bolien, P.; Siebers, P.; Kockmann, N.
Simplified Approach to Characterize the Cooling Crystallization in a Modular Mini-Plant.

MDPI-crystals, 13(1),147 (2023).
https://doi.org/10.3390/cryst13010147

Höving, S.; Neuendorf, L.M.; Betting, T.; Kockmann, N.
Determination of Crystal Size Distributions of Bulk Samples using Micro-Computed Tomography and Artificial Intelligence.
MDPI-materials, 16(3), 1002 (2023).
https://doi.org/10.3390/ma16031002

Korel, L.; Yorsh, U.; Behr, A.S.; Kockmann, N.; Holeňa, M.
Text-to-Ontology Mapping via Natural Language Processing with Application to Search for Relevant Ontologies in Catalysis.
MDPI-computers, 12, 14 (2023).
https://doi.org/10.3390/computers12010014

Schulz, L.; Stähle, P.; Reining, S.; Sawall, M.; Kockmann, N.; Röder, T.
Multivariate curve resolution for kinetic modeling and scale-up prediction.
J. Flow Chem., 13, 13-19 (2023).
https://doi.org/10.1007/s41981-022-00252-y

Frede, T.A.; Nikbin, N.; Kockmann, N.;
Reactor Performance Estimation in Microscale Flow Calorimeter for Rapid Characterization of Exothermic Reactions.
J. Flow Chem., 13, 31-44 (2023).
https://doi.org/10.1007/s41981-022-00251-z

Achternbosch, M.; Zibula, L.; Schmidt, A.; Krieger, W.; Kockmann, N.; Strohmann, C.
Selective monosubstitution on a trichlorosilane with highly reactive organolithium compounds in a microflow reactor.
J. Flow Chem., 13, 9-12 (2023).
https://doi.org/10.1007/s41981-022-00254-w

Peer-reviewed Conference Contributions

Behr, A.S.; Abbaspour, E.; Rosenthal, K.; Pleiss, J.; Kockmann, N.
Ontology-Based Laboratory Data Acquisition with EnzymeML for Process Simulation of Biocatalytic Reactors.
1st Conf. Research Data Infrastructure - CoRDI, Karlsruhe, 12.-14.9.2023.
https://doi.org/10.52825/cordi.v1i.324

Behr, A.S.; Borgelt, H.; Petrenko, T.; Dörr, M.; Kockmann, N.
Investigating the Landscape of Ontologies for Catalysis Research Data Management.
1st Conf. Research Data Infrastructure - CoRDI, Karlsruhe, 12.-14.9.2023.
https://doi.org/10.52825/cordi.v1i.232

Oldach, B.; Höving, S.; Boettcher, K.E.R.; Kockmann, N.
Ultra-Concurrent Remote Laboratory for Microfluidic Applications.
20th Intl. Conf. Remote Eng. & Virtual Instrum., REV23, Thessaloniki, Greece, 1.-3.3.2023.
https://doi.org/10.1007/978-3-031-42467-0_43

Behr, A.S.; Neuendorf, L.M.; Sakthithasan, P.; Karan, M.; Fang, Q.; Boettcher, K.E.R.; Terkowsky, C.; Kockmann, N.
Uniting Knowledge and Application in a Hybrid Laboratory Experiment in Virtual Reality - A Cross-Reality Laboratory with Applications of Artificial Intelligence for Industry 4.0.
20th Intl. Conf. Remote Eng. & Virtual Instrum., REV23, Thessaloniki, Greece,1.-3.3.2023.
https://doi.org/10.1007/978-3-031-42467-0_26

Books & Book chapters

Baerns, M.; Behr, A.; Brehm, A.; Gmehling, J.; Hinrichsen, K.-O.; Hofmann, H.; Kleiber, M.; Kockmann, N.; Onken, U.; Palkovits, R.; Renken, A.; Vogt, D. **Technische Chemie.**
Wiley-VCH, Weinheim, 2023.
ISBN 978-3-527-34574-8

Kockmann, N.; Schuler, J.; Oldach, B. X-Ray Based Investigations on Multiphase Capillary Flows.
in G.H. Yeoh, J.B. Joshi (Eds.) Handbook of Multiphase Flow Science and Technology, SpringerNature, 2023. https://doi.org/10.1007/978-981-4585-86-6_29-1

Plant and Process Design (APT)

Development of a Novel Rotor Design for Counter-Current Centrifugal Extraction Based on Computational Fluid Dynamics Simulation.

Sophia Volpert, Lisa Nordhausen, Richard Alfsmann, Gerhard Schembecker

Counter-Current Centrifugal Extraction (CCE) is a novel concept for continuous multistage liquid–liquid extraction that combines the benefits of mixer-settler cascades and centrifugal extractors in one compact apparatus. The working principle builds on Centrifugal Partition Chromatography (CPC), where two immiscible liquid phases are contacted inside a rotating rotor. Unlike the established Centrifugal Partition Extraction (CPE), both phases flow alternately through a single duct connecting the chambers, eliminating the need for check valves. CFD simulations using the Volume of Fluid method were used to validate the concept and develop an optimized chamber geometry, confirming the hydrodynamic feasibility of CCE.

Continuous liquid–liquid extraction is a key unit operation in downstream processing. Centrifugal extractors accelerate phase separation by up to 300-fold compared to static settlers, but are limited in the number of achievable separation stages. The existing Centrifugal Partition Extraction (CPE) concept addressed this by realizing a counter-current flow inside a single rotating apparatus, but required crossing ducts and numerous check valves inside the rotor, leading to leakages and blockages.

The novel CCE concept replaces this complex design with a single duct between chambers, adapted from standard CPC rotor geometry. Three design requirements were formulated: (1) chamber volume must greatly exceed duct volume; (2) dispersion must be maximized to create a large interfacial area; (3) chambers must be as compact as possible to enable stacking of multiple rotors. Starting from the original CPE chamber, a three-step CFD-guided optimization was performed. First, the chamber height was halved from 12 mm to 6 mm, improving the utilization as a dispersion zone from ~45 % to 100 %. Second, due to the Coriolis force acting on the inflowing lamellae, the chambers were tilted by 35° to the radial direction, with an inlet angle of 20° to ensure centered inflow in both operating modes as shown in Figure 1.

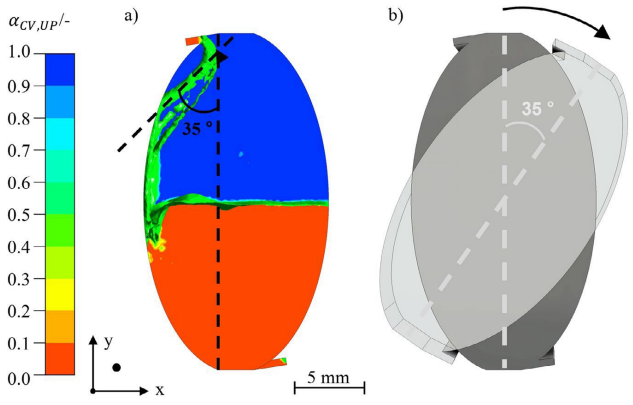

Figure 1. Determination of the inclining angle of the chamber. (A) An example of the determination of the angle of the incoming lamella. (B) Schematical inclination of the chamber.

Third, baffles were placed opposite each inlet to guide flow centrally, reduce dead zones, and stabilize the coalescence zone. The final geometry is shown in Figure 2 as an elliptical chamber inclined at 35°, with a height of 6 mm and a volume of 1.43 mL. A simulation of five consecutive mode-switches confirmed the feasibility: the phase ratio alternates stably between α ≈ 0.57 (ascending) and α ≈ 0.48 (descending), recovering reproducibly after each switch.

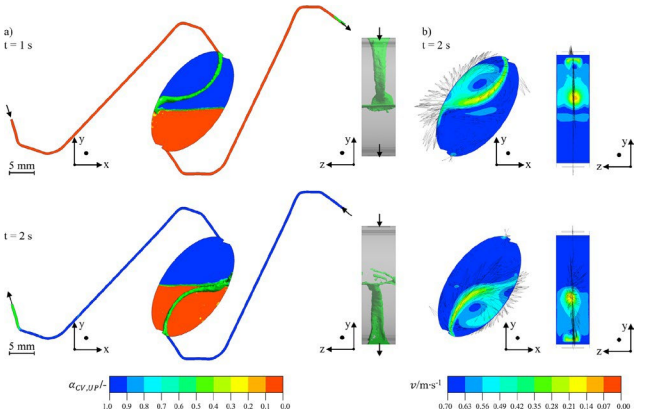

Figure 2. (A) Flow patterns for a chamber oriented at 35◦ with baffles and an inlet angle of 20◦ in descending mode (top) and ascending mode (bottom). (B) Velocity profiles represented by contours and their direction shown as vectors.

Compared to CPE, the CCE eliminates all check valves, doubles the achievable separation stages per housing, and enables additive manufacturing of modular rotors. Future work will include experimental validation and first separation tests.

gerhard.schembecker@tu-dortmund.de

Publications:
Volpert S., Nordhausen L., Alfsmann R., Schembecker G. Development of a Novel Rotor Design for Counter-Current Centrifugal Extraction Based on Computational Fluid Dynamics Simulations. Journal of Separation Science, 48, e70339 (2025). https://doi.org/10.1002/jssc.70339

2025

Peer Reviewed Journal Articles

Volpert S., Nordhausen L., Alfsmann R., Schembecker G.
Development of a Novel Rotor Design for Counter-Current Centrifugal Extraction Based on Computational Fluid Dynamics Simulations.
Journal of Separation Science, 48:e70339, (2025)
https://doi.org/10.1002/jssc.70339

Heming R., Yilmaz O., Wohlgemuth K.
The impact of process parameters on the performance of a wash column in an integrated suspension melt crystallization pilot plant.
Separation and Purification Technology, 377, 134411, (2025)
https://doi.org/10.1016/j.seppur.2025.134411

Kockmann N., Schmalenberg M., Strakeljahn B., Wohlgemuth K.
Energy and Resource Efficient Continuous Cooling Crystallization with Modular Lab-Scale Equipment.
Journal Crystals, 15, 421, (2025)
https://doi.org/10.3390/cryst15050421

Heming R., Yousf A., Wohlgemuth K.
Understanding the impact of process parameters on the crystallization process within an integrated suspension melt crystallization pilot plant.
Separation and Purification Technology, 369, 133096, (2025)
https://doi.org/10.1016/j.seppur.2025.133096

Schlüter M., Zimmer J., Held C., Wohlgemuth K.
Enhancing Sustainability in PET Glycolysis by closed-loop Recycling.
Chemical Engineering Science, 307, 121337, (2025)
https://doi.org/10.1016/j.ces.2025.121337

Schlüter M., Held C., Wohlgemuth K.
BHET Crystallization in Water-Free PET Glycolysis Systems.
Industrial & Engineering Chemistry Research, 64, 1189-1201, (2025)
https://doi.org/10.1021/acs.iecr.4c03250

2024

Peer Reviewed Journal Articles

Maria Schlüter, Shartak Bhutani, Kerstin Wohlgemuth, Christoph Held
Predicting Kinetics of the PET Glycolysis Reaction Using an Activity-Based Model and Experimental Validation
Industrial & Engineering Chemistry Research 2024, 63, 35, 15458-15465
pubs.acs.org/doi/10.1021/acs.iecr.4c02382

Felix Buthmann, Philip Laby, Djamal Hamza, Jörg Koop, Gerhard Schembecker
Spatially and Temporally Resolved Analysis of Bleeding in a Centrifugal Partition Chromatograph
Separations 2024, 11(2), 56
doi.org/10.3390/separations11020056

Felix Buthmann, Jan Hohlmann, Sophia Volpert, Mareen Neuwald, Djamal Hamza, Gerhard Schembecker
Counteracting Bleeding in Centrifugal Partition Chromatography: Redosing of the Stationary Phase
Separations 2024, 11(4), 98
doi.org/10.3390/separations11040098

Tobias Pyka, André Bieberle, Rouven Loll, Christoph Held, Markus Schubert, Gerhard Schembecker
Distributor Effects on Liquid Hold-Up in Rotating Packed Beds
Industrial and Engineering Chemistry Research 2024, 63(4), 2000–2010
doi.org/10.1021/acs.iecr.3c03996

Felix Buthmann, Jan Hohlmann, Mareen Neuwald, Gerhard Schembecker
Optimizing Chromatographic Separation with Redosing: Effects on Separation Efficiency of a Model System in Centrifugal Partition Chromatography
Separations 2024, 11(4), 111
doi.org/10.3390/separations11040111

Felix Buthmann, Sophia Volpert, Jörg Koop, Gerhard Schembecker
Prediction of Bleeding via Simulation of Hydrodynamics in Centrifugal Partition Chromatography
Separations 2024, 11(1), 16
doi.org/10.3390/separations11010016

Maria Schlüter, Sarthak Bhutani, Jasmin Bahr, Kerstin Wohlgemuth, Christoph Held
Measurement and PC-SAFT Modeling of the Solubility of BHET monomer, BHET dimer and PET in single solvents
Journal of Chemical & Engineering 2024, 69, 3, 1326-1334
doi.org/10.1021/acs.jced.3c00627

Maria Schlüter, Ryota Enomoto, Shin Makino, Lisa Weihs, Cyra Lina Stamm, Kerstin Wohlgemuth, Christoph Held
Boosting the kinetics of PET glycolysis
Reaction Chemistry and Engineering 2024, 9, 3038-3046
doi.org/10.1039/D4RE00235K

2023

Peer Reviewed Journal Articles

Hina Qammar, Tobias Pyka, Jörg Koop, Andrzej Górak, Gerhard Schembecker
Radial Temperature Profile Measurements to Understand Mass Transfer in Rotating Packed Bed Distillation
Industrial and Engineering Chemistry Research 2023, 62(38), 15588-15599
doi.org/10.1021/acs.iecr.3c01068

Rouven Loll, Lisa Nordhausen, André Bieberle, Markus Schubert, Tobias Pyka, Jörg Koop, Christoph Held, Gerhard Schembecker
Analysis of Flow Patterns in Structured Zickzack Packings for Rotating Packed Beds Using γ-Ray Computed Tomography
Industrial and Engineering Chemistry Research 2023, 62(38), 15625-15634
doi.org/10.1021/acs.iecr.3c02252

Jörg Koop, Ninja Bera, Erik Quickert, Marvin Schmitt, Maria Schlüter, Christoph Held, Gerhard Schembecker
Separation of Volatile Organic Compounds from Viscous Liquids with RPB Technology
Industrial and Engineering Chemistry Research 2023, 62(34), 13637-13645
doi.org/10.1021/acs.iecr.3c01597

Tobias Pyka, Alexander Ressemann, Christoph Held, Gerhard Schembecker, Jens-Uwe Repke
Impact of Vapor Bypasses on Separation Performance of Rotating Packed Beds in Distillation
Industrial and Engineering Chemistry Research 2023, 62(33), 13274-13279
doi.org/10.1021/acs.iecr.3c01947

Tobias Pyka, Manuel Brunert, Jörg Koop, André Bieberle, Christoph Held, Gerhard Schembecker
Novel Liquid Distributor Concept for Rotating Packed Beds
Industrial and Engineering Chemistry Research 2023, 62(14), 5984-5994
doi.org/10.1021/acs.iecr.3c00248

Tobias Pyka, Vincent Backhaus, Christoph Held, Gerhard Schembecker
Impact of Number of Rotors in Rotating Packed Beds on Separation Performance in Distillation
Industrial and Engineering Chemistry Research, 2023, 62(46), 19855-10861
doi.org/10.1021/acs.iecr.3c03173

Anne Cathrine Kufner, Marc Meier, Kerstin Wohlgemuth
End-to-End Continuous Small-Scale Drug Substance Manufacturing: From a Continuous In Situ Nucleator to Free-Flowing Crystalline Particles
Crystals 2023, 13(12), 1675
doi.org/10.3390/cryst13121675

Astrid Ina Seifert, Hannes Wegener, Katharina Brühl, Thomas Seidensticker, Kerstin Wohlgemuth
Polymer-Grade Bio-Monomers from Oleochemicals by Combining Homogeneous Catalysis and Selective Product Crystallization in an Integrated Process
Processes 2023, 11 (10), 2861
doi.org/10.3390/pr11102861

Anne Cathrine Kufner, Michael Rix, Kerstin Wohlgemuth
Modeling of continuous slug flow cooling crystallization towards pharmaceutical applications
Processes 2023, 11(9), 2637
doi.org/10.3390/pr11092637

Astrid Ina Seifert, Anna Wehning, Jan Gutsch, Kerstin Wohlgemuth
Focusing impurities during inert gassing crystallization of complex mixtures
Organic Process Research & Development 2023, 27, 8, 1485-1498
doi.org/10.1021/acs.oprd.3c00171

Anne Cathrine Kufner, Nico Westkämper, Henrik Bettin, Kerstin Wohlgemuth
Prediction of Particle Suspension State for Various Particle Shapes Used in Slug Flow Crystallization
Chem Engineering 2023, 7(2), 34
doi.org/10.3390/chemengineering7020034

Timo Dobler, Stefan Höving, Christian Dreiser, Marco Gleiß, Mathias Gröschen, Alexander Henkel, Manuel Hörne, Martin Schäfer, Jana Sonnenschein, Georg Wiese, Kerstin Wohlgemuth, Norbert Kockmann and Hermann Nirschl
From Lab to Pilot Scale: Commissioning of an Integrated Device for the Generation of Crystals
Chemical Engineering & Technology 2023, 46(7), 1511-1520
doi.org/10.1002/ceat.202200616

Astrid Ina Seifert, Justin Simons, Jan Gutsch, Kerstin Wohlgemuth
Inert gassing crystallization for improved product separation of oleo-chemicals towards an efficient circular economy
Organic Process Research & Development 2023, 27, 1, 136-147
https://doi.org/10.1021/acs.oprd.2c00312

Biomaterials and Polymer Science (BMP)

Beyond Glass Transition and Melting: α-Relaxation as a Shape Memory Trigger.

Achieving Reversible, Solid-State Morphological Changes in Crosslinked High-Density Polyethylene.

M. Maricanov, R. D. L. Jerusalem, C. Meykranz, L. Schultz, J. C. Tiller, F. Katzenberg

Shape memory polymers represent an important class of smart or adaptive materials. Typically, they are mechanically transformed into a certain "programmed" shape, but they always remember their original shape. The programmed shape is stabilized if the polymer is below its glass transition (T_α) or melting temperature (T_m). Exceeding this by heating results in a transformation back to the original shape. Since these temperatures are fix for each polymer, every application requires a different polymer. Here, we demonstrate that it is feasible to use a the α-relaxation of semi-crystalline thermoplastics as an independent trigger using crosslinked high-density polyethylene (xHDPE). This establishes α-relaxation as a genuine switching mechanism, opening new possibilities for the design of multi-shape memory materials.

Previous research on crosslinked low-density polyethylene (xLDPE) suggested that the α-relaxation could serve as a shape memory trigger. However, because the α-relaxation of xLDPE partially overlaps with its melting range, the contribution of crystal melting could not be completely ruled out. To clarify this, xHDPE was investigated. Due to its higher melting temperature, xHDPE allows for programming and triggering at a temperature distinctively between T_α and the onset of melting.

Unlike LDPE, HDPE cannot be homogeneously crosslinked by simply adding peroxides directly into the extruder due to its higher processing temperature. To overcome this, a specific swelling method was applied: thin pieces of HDPE were first soaked in a di-tert-butyl peroxide (DTBP) bath at room temperature to ensure a uniform initial distribution. The DTBP-impregnated HDPE was then extruded and subsequently cured in a heating press at 160 °C under the exclusion of air, resulting in successful chemical crosslinking.

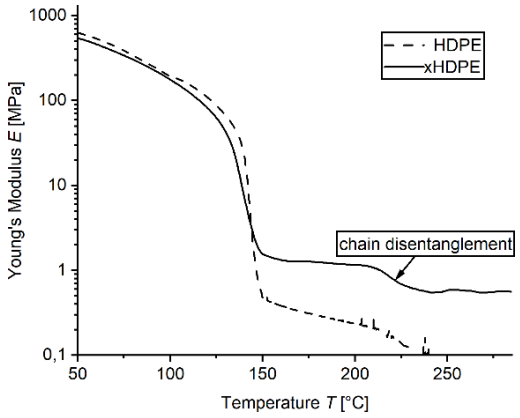

Figure 1. Young's modulus versus temperature plot of HDPE and xHDPE showing successful crosslinking.

To understand the structural changes during the shape memory cycle, TEM and SAXS measurements were conducted.

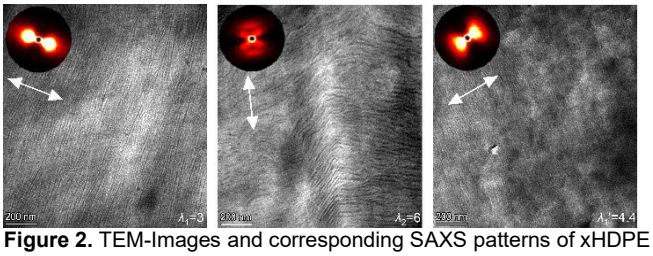

Figure 2. TEM-Images and corresponding SAXS patterns of xHDPE in its intermediate shape (left), in its temporary shape (center), and after switching to its new intermediate shape (right).

These imaging techniques confirm that the transition between intermediate and temporary shapes is accompanied by a reversible change in morphology. Stretching the samples into their temporary shape leads to a heavily distorted morphology and shearing of the lamellae crystals. Upon reheating above T_α, the material retracts to its intermediate shape, and a stacked lamellae morphology is restored without significant distortions. Thermomechanical cycles revealed that the programmed xHDPE samples exhibit strain fixity ratios (R_f) close or equal to 100%. Similar to xLDPE, a conditioning cycle is required to achieve full shape recovery. While the recovery ratio after the first cycle is lower, the lamellar morphology reorganizes so that subsequent cycles achieve recovery ratios between 90% and 100%. This switching was efficiently performed at T_α + 15°C, well below the melting range.

This work firmly establishes α-relaxation as a novel, genuine switching mechanism in semi-crystalline SMPs. Remarkably, this morphological change and full recovery of plastically deformed morphologies occur entirely in the solid state, without the need for any melting and recrystallization cycles. Although the strain storage capacity (up to 30%) is lower than that of conventional T_α- or T_m-switched SMPs, it provides a valuable additional switching option within the temperature range between T_α and T_μ.

michail.maricanov@tu-dortmund.de
frank.katzenberg@tu-dortmund.de

Publication:
Maricanov, M.; Jerusalem, R.D.L.; Meykranz, C.; Schultz, L.; Tiller, J.C.; Katzenberg, F., Switching the shape of crosslinked high-density polyethylene using α-relaxation. Polymer 2025. https://doi.org/10.1016/j.polymer.2025.129287

Maximizing strength and toughness of Poly(2-Ethyl-2-Oxazoline) based double network hydrogels.

This is a new design principle for ultra-tough double network hydrogels, achieved through controlled network architecture and polymerisation strategy.

Sebastian Weckes, Cornelius Rawert, Joerg C Tiller

Double network hydrogels (DNHs) are among the most mechanically resilient hydrogel systems. Although numerous examples are found to literature, little is known on the influence of the architecture of the networks on their mechanical performance. To shed some light on this, different cross-linking strategies and polymer synthesis methods were applied to obtain similar DNHs with varying network architectures. The results clearly show that the way of the synthesis of DNHs is crucial for their performance and dependent of the nature of the functional groups.

Two different primary networks were synthesized, an end-group cross-linked low-molecular-weight PEtOx and a backbone cross-linked high molecular weight architecture (Figure 1)

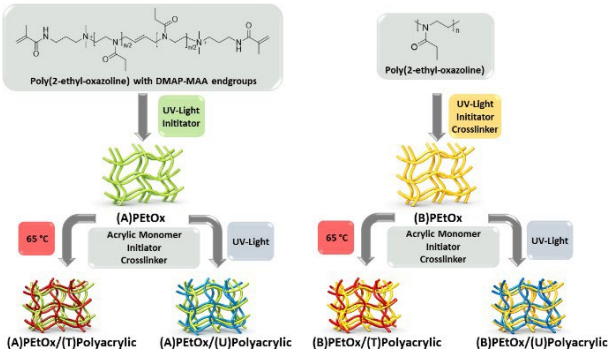

Figure 1. Overview of the synthesis routes for double network hydrogels. The first network was either UV-cross-linked or backbone cross-linked, while the second network was formed by UV (U) or thermal (T) polymerization, yielding four network combinations.

Although both single networks showed similar swelling and tensile properties, the backbone cross-linked system exhibited a six-fold increase in fracture energy and more than double the compressive strength, attributed to a high density of trapped entanglements that enhance energy dissipation. Based on this architecture, double network hydrogels were prepared using different acrylic second networks poly(acrylic acid) (PAA), poly(acrylamide) (PAAm), and a co-polymer of 2-hydroxyethylacrylamide and acrylamide (P(HEAAm$_{90}$-co-AAm$_{10}$)), polymerized either by UV or thermal initiation to directly assess the influence of radical concentration and internetwork interactions. The results reveal a pronounced monomer-specific effect of the polymerization method. For PEtOx/PAA systems, UV-induced polymerization significantly increased fracture energy and compressive strength, reaching up to 48 MPa (Figure 2), likely due to additional inter-network connections formed at high radical concentrations that reinforce hydrogen bonding.

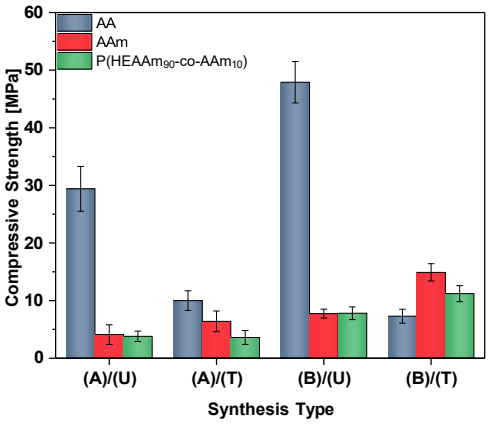

Figure 2. Comparison of compressive strength (A) and fracture energy (B) of all DNHs for each synthesis route. The second network was polymerized either photochemically (U) or thermally (T). Mechanical tests were performed on water-swollen samples at room temperature (mean ± SD, n = 4).

In contrast, PEtOx/PAAm and PEtOx/P(HEAAm$_{90}$-co-AAm$_{10}$) systems showed superior toughness and strength when the secondary network was polymerized thermally. Here, mechanical performance is governed by entanglement-driven energy dissipation, while additional covalent interconnections formed during UV polymerization restrict network mobility and reduce toughness.

Overall, this study establishes clear structure property relationships for PEtOx-based double networks and demonstrates that mechanical performance can be maximized by deliberately tailoring backbone entanglement and polymerization strategy. The backbone cross-linking approach enables the design of mechanically robust hydrogels for load-bearing and advanced soft material applications.

sebastian.weckes@tu-dortmund.de
joerg.tiller@tu-dortmund.de

Publications:
Benitez-Duif, P.A.; Weckes, S.; Ferreira, R.M.P.; Kurka, D.; Tiller, J.C., Insights on the Influence of Functional Side Groups on the Mechanical Performance of Poly(2-oxazoline)/Poly(acrylate) Double Network Hydrogels. https://doi.org/10.1016/j.polymer.2024.12801

Cross-Linked Shape Memory Polymer Blends with Tunable Heating Rate Sensitivity.

Robert D.L. Jerusalem, Michail Maricanov, Frank Katzenberg, Joerg C Tiller

What if materials could anticipate change instead of merely reacting to it? This study presents cross-linked blends of poly(vinylidene fluoride) (PVDF) and poly(2-ethyl-2-oxazoline) (PEtOx) that respond not only to temperature but also to heating rate. By tailoring composition and crystallization kinetics, these predictive shape-memory polymers translate thermal speed into mechanical behavior. They "read" their environment and adjust their recovery accordingly a breakthrough toward self-regulating systems, adaptive actuators, and next-generation intelligent matter.

This work introduces predictive shape-memory polymers based on co-cross-linked blends of semicrystalline PVDF and amorphous PEtOx. Unlike traditional homopolymers such as syndiotactic polypropylene or PET, these networks allow independent tuning of glass transition (T_g), melting (T_m), and cold crystallization (T_{cc}) temperatures simply by varying composition. Dynamic mechanical analysis confirmed robust cross-linking with stable plateau moduli above *Tm*. Differential scanning calorimetry revealed that increasing PVDF content decreases both T_g and T_{cc}, enabling control over crystallization kinetics from fully amorphous states to partially crystalline morphologies.

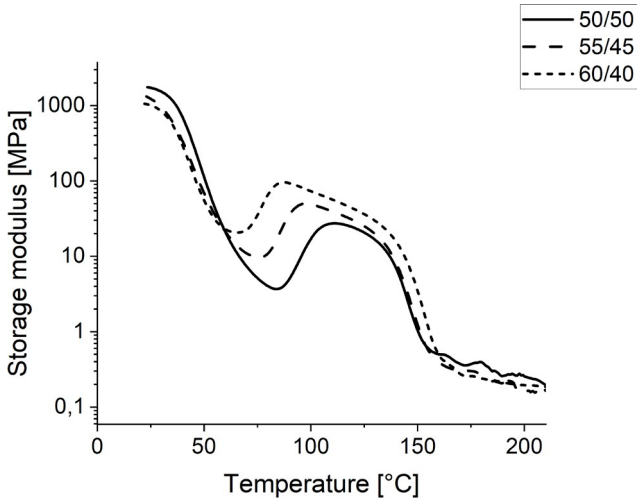

Figure 1. *E'* versus *T* plots of the three differently composed PVDF/PEtOx networks. Samples heated with a heating rate of 5 K min^{-1}.

When programmed under strain and quenched below T_g, the materials exhibit remarkable rate-dependent recovery between 1-100 K min^{-1}. Slow heating promotes gradual relaxation; rapid heating shifts recovery onset upward due to competing recrystallization processes that stabilize intermediate shapes. Each blend effectively encodes its thermal history within its dimensional response acting as a physical "memory" of environmental dynamics.

Wide-angle X-ray scattering confirmed the absence of large crystals after quenching but indicated oriented amorphous regions contributing to temporary shape fixation. The interplay between relaxation-driven retraction and crystallization-induced stabilization defines the kinetic sensitivity range for each blend ratio.

By adjusting PVDF content, the responsive temperature window can be finely tuned from around 120 °C to 150 °C.

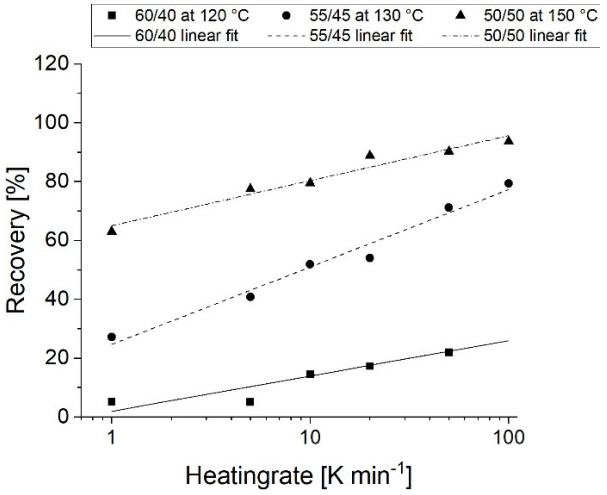

Figure 2. Measured recovery of the 60/40, 55/45 and 50/50 PVDF/PEtOx samples at a temperature of 120 °C, 130 °C and 150 °C respectively in dependence on the applied heating rate.

Such tailored responsiveness transforms passive SMPs into active sensors for kinetic stimuli. Predictive polymer blends can be customized for specific sensitivity ranges by adjusting network composition, offering new design freedom for safety materials detecting overheating rates or soft robotic components requiring controlled actuation speed.

robert.jerusalem@tu-dortmund.de
michail.maricanov@tu-dortmund.de
frank.katzenberg@tu-dortmund.de
joerg.tiller@tu-dortmund.de

Publications:
Jerusalem, R.D.L.; Maricanov, M.; Katzenberg, F.; Tiller, J.C., Cross-Linked Shape Memory Polymer Blends with Tunable Heating Rate Sensitivity. ACS Applied Polymer Materials 2025. https://doi.org/10.1021/acsapm.4c03410

Protection of the Mechanical Failure of an Acid-Based Hydrogel by pH Changes.

Prevention of deprotonation of an acid within a double network hydrogel by structural optimization

Paola Benitez-Duif, Sebastian Weckes, Joerg C. Tiller

Cartilage is a hydrogel that has the compressive strength of concrete. Substituting such a material as artificial cartilage is highly challenging from the perspective of polymer science as well as from that of biomaterials. We have previously presented the first hydrogel, a double network hydrogel based on poly(2-methyl-oxazoline) (PMOx) and poly(acrylic acid) (PAA), that truly possesses the mechanical properties and the biocompatibility of cartilage. Downside of this hydrogel is the loss of its mechanical stability above pH 7.4. The present work shows an approach to stabilize this hydrogel even in media of pH 9 by systematically varying the composition of the acrylate phase.

The cartilage-like double network hydrogel PMOx/PAA DNH is presumed to derive its properties from the strong hydrogen bonds between the protonated carboxylate groups of PAA and the carbonyl function of PMOx. Given the molecular structural differences between PAA and PMOx it becomes clear that not all carboxylate groups have a binding partner (see Figure 1). These groups will eventually be easier, i.e., at lower pH values, deprotonated than the groups that form the hydrogen bonds with the PMOx network. The concept of this study is to exchange the excessive non-binding carboxylates by another hydrogen donor monomer to obtain an even higher shift in pKa of the PAA. As shown previously, PAAm is suited as DNHs partner for PMOx networks.

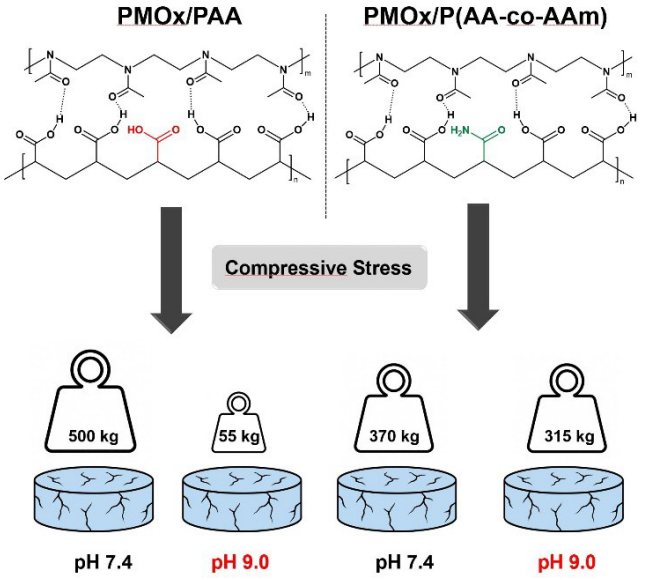

Figure 1. Concept of the structure-induced higher pH-stability of PMOx/PAA DNHs by addition of a minor fraction acryl amide.

Therefore, we chose acryl amide as comonomer for PAA to reduce the number of non-binding carboxic acid groups in the DNH. To find the optimal composition, a series of PMOx/P(AA-co-AAm) DHNs with varying ratios of AA:AAm was prepared according to previously published protocols. The resulting DNHs were studied regarding their mechanical properties under compression and strain in PBS buffer at different pH values. The introduction of acryl amide groups leads to somewhat decreased compressive strength at pH 7.4, but the pH sensitivity is already improved at only 5 wt% PAAM content and is highest at 10 wt%. Such DNHs are nearly independent in their compressive strength even up to pH 9.0. Higher PAAm contents afford a loss in pH sensitivity. A similar picture is found for strainability and toughness, measured as fractured energy (see Figure 2). DNHs with 10 wt% PAAm show nearly fully protonated carboxylate at pH 9.0, which is remarkable for acid groups that have a pKa value of 4.7

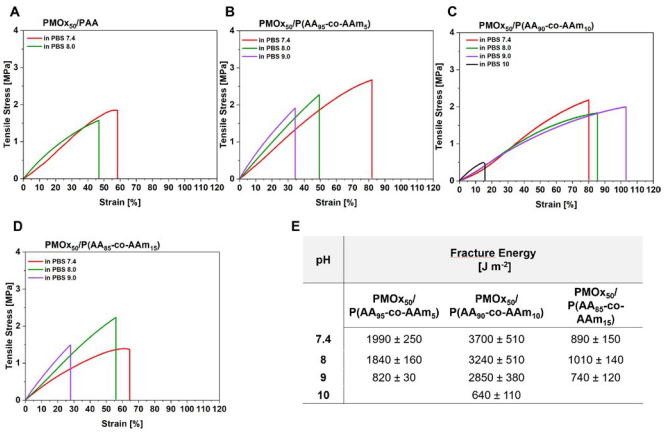

pH	Fracture Energy [J m^{-2}]		
	PMOx$_{50}$/P(AA$_{95}$-co-AAm$_5$)	PMOx$_{50}$/P(AA$_{90}$-co-AAm$_{10}$)	PMOx$_{50}$/P(AA$_{85}$-co-AAm$_{15}$)
7.4	1990 ± 250	3700 ± 510	890 ± 150
8	1840 ± 160	3240 ± 510	1010 ± 140
9	820 ± 30	2850 ± 380	740 ± 120
10		640 ± 110	

Figure 2. Stress strain curves of A)PMOx/PAA, B) PMOx/P(AA95-co-AAm5), C) PMOx/P(AA90-co-AAm10), D) PMOx/P(AA85-co-AAm15) and E) fracture energies of different PMOx/P(AA-co-AAm) DNHs in PBS buffer with different pH at room temperature

The results show that a very narrow range of acryl amide concentration peaking at 10 wt% in the AA monomer is suited to stabilize the high compressive strength and tensile toughness of PMOx/P(AA-co-AAm) DHNs to up to pH 9.0. This greatly improves the applicability of such DNHs in biological applications. It further shows, how much the mechanical properties of POx-based non-ionic DNHs depend on the exact matching between the two interpenetrating polymer phases.

paola.benitez@tu-dortmund.de
sebastian.weckes@tu-dortmund.de
joerg.tiller@tu-dortmund.de

Publications:
Benitez-Duif, P. A., Santhirasegaran, Weckes, S., Tiller, J. C. Extending the pH Stability of Poly(2-Oxazoline)/Poly(Acrylic Acid) Double-Network Hydrogels by Including Acrylamide as Comonomer. *Macromolecular Rapid Communications, 47 (1), e00593 (2025)*

2025

Peer Reviewed Journal Articles

Weckes, S., Rawert, C., Vieten, P., Tiller, J.C.
Maximizing strength and toughness fo Poly(2-Ethyl-2-Oxazoline) based double network hydrogels by varying cross-linking strategy of the primary network and polymerization method of the secondary acrylic network.
European Polymer Journal 237, 114194 (2025)
https://doi.org/10.1016/j.eurpolymj.2025.114194

Gramse, C., Wesselmann, J., Jerusalem, R. D. L., Weberskirch, R.
Core-Shell Functionalized Block Copolymer Micelles: A Versatile Approach Toward One-Pot Two-Step Tandem Reactions.
ChamCatChem 1, (23), e01129 (2025)
https://doi.org/10.1002/cctc.202501129

Maricanov, M., Jerusalem, R. D. L., Meykranz, C., Schultz, L., Tiller, J. C., Katzenberg, F.
Switching the shape of crosslinked high-density polyethylene using α-relaxation.
Polymer, 341, 129287 (2025)
https://doi.org/10.1016/j.polymer.2025.129287

Jerusalem, R. D. L., Maricanov, M. , Katzenberg, F., Tiller, J. C.
Cross-Linked Shape Memory Polymer Blends with Tunable Heating Rate Sensitivity.
ACS Appl. Polym. Mater 7 (2), 932-937 (2025)
https://doi.org/10.1021/acsapm.4c03410

Benitez-Duif, P. A., Santhirasegaran, Weckes, S., Tiller, J. C.
Extending the pH Stability of Poly(2-Oxazoline)/Poly(Acrylic Acid) Double-Network Hydrogels by Including Acrylamide as Comonomer.
Macromolecular Rapid Communications, 47 (1), e00593 (2025)
https://doi.org/10.1002/marc.202500593

Benitez-Duif, P. A., Weckes, S., Pinto Ferreira, R. M., Kurka, D., Tiller, J. C.
Insights on the influence of functional side groups on the mechanical performance of Poly(2-oxazoline)/Poly(acrylate) double networks hydrogels.
Polymer, 319, 128014 (2025)
https://doi.org/10.1016/j.polymer.2024.128014

2024

Peer Reviewed Journal Articles

Jerusalem , R. D. L., Maricanov, M., Raidt, T., Katzenberg, F., Tiller, J. C.
Heating Rate Sensitive Polyethylene Terephthalate.
Macromolecular Rapid Communications, 45 (20), 2400346 (2024)
https://doi.org/10.1002/marc.202400346

Maricanov, M., Becker, R., Jerusalem, R. D. L., Tiller, J. C., Katzenberg, F.
On the suitability of the α-relaxation as novel trigger for a shape memory polymer.
ACS Appl. Polym, 141 (46), e56241 (2024)
https://doi.org/10.1002/app.56241

Romanovska, A., Tophoven, J., Tiller, J. C.
Vitamin E-poly(2-oxazolin)-ciprofloxacin conjugates that enter bacterial cells via their efflux pumps.
Journal of Bioactive and Compatible Polymers, 39 (6), 536-550 (2024)
https://doi.org/10.1177/08839115241267807

Schneck, F. Kruse, P. O., Hesse-Hornich, D., Lopes Dias, N. F., Tillmann, W., Jerusalem, R. D. L., Maricanov, M., Katzenberg, F., Tiller, J. C., Handge, U. A.
Combination of Viscoelastic and a Tribological Analysis of a Low-Density Polyethylene with High Degree for Cross-linking.
Macromolecular Chemistry and Physics, 225 (13), 2400042 (2024)
https://doi.org/10.1002/macp.202400042

Romanovska, A., Schmidt, M., Brandt, V., Tophoven, J., Tiller, J. C.
Controlling the function of bioactive worm micelles by enzyme-cleavable non-covalent inter-assembly cross-linking.
Journal of Controlled Release, 368, 15-23, (2024)
https://doi.org/10.1016/j.jconrel.2024.02.013

2023

Milovanovic, M.; Tabakoglu, F.; Saki, F.; Pohlkoetter, E.; Buga, D.; Brandt, V.; Tiller, J. C.
Organic-inorganic double networks as highly permeable separation membranes with a chiral selector for organic solvents.
Journal of Membrane Science, 668, 121190 (2023)
https://doi.org/10.1016/j.memsci.2022.121190

Bioprocess Engineering (BPT)

Microtiter Plate Cultivation Systems Enable Chemically Diverse Metabolic Footprints During Bacterial Natural Product Discovery.

Secondary metabolite production profiling in microbioreactor systems.

Anton Lindig, Georg Hubmann, Stephan Lütz

Many bacterial natural products (NPs) are repeatedly rediscovered. To enhance the discovery of novel NPs, a variety of cultivation conditions can be tested in parallelized microtiter plate cultivation systems (MPCS). We compared the growth and metabolic footprints of four bacterial species in MPCS, shake flasks, and stirred-tank bioreactors. Growth was mostly consistent, but secondary metabolite (SM) formation varied considerably. Molecular networking visualized unique mass features (MFs) and structural modifications across the different systems. Filamentous bacteria exhibited greater variability than unicellular bacteria. MPCS produced fewer divergent SM profiles than shake flasks, supporting scalability. This study highlights the impact of cultivation systems on bacterial metabolism.

This study systematically investigated the effect of different cultivation systems on the growth dynamics and SM production of four bacterial species: *Bacillus amyloliquefaciens, Corallococcus coralloides, Streptomyces griseochromogenes*, and *Streptomyces cattleya*. All strains were cultivated in a complex medium at 30°C for five days using various formats, including shake flasks (SF), baffled shake flasks (BSF), stirred-tank bioreactors (STR), and MPCS, such as 24-deep well plates (24 DWP), 48-flower plates (FP), and 96-deep well plates (96 DWP). Biomass formation, glucose consumption, and metabolic footprints were monitored to evaluate the influence of system-specific parameters on bacterial physiology and metabolite space.

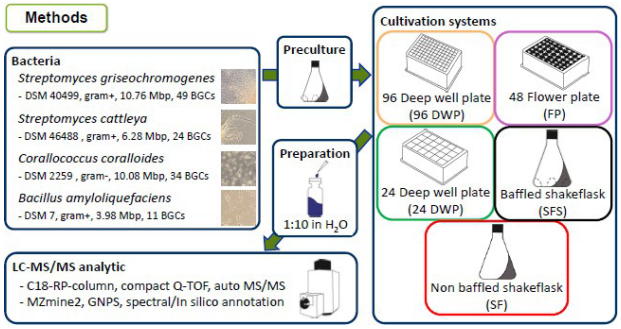

Figure 1. 'A journey through the metabolite space': The metabolic footprint reflects the biochemical potential of bacteria. Combining bioprocess engineering principles with insights into bacterial metabolite space, optimized cultivation strategies can overcome challenges in natural product discovery.

Although there was growth in all cultivation systems, entry into the stationary phase, final biomass concentrations, and residual glucose levels varied substantially between systems. Filamentous bacteria (*S. griseochromogenes* and *S. cattleya)* in particular exhibited pronounced variability in growth kinetics and morphology across systems; that is to say, they displayed dispersed or pellet-forming growth patterns, which were influenced by oxygen transfer capacity, shear stress, vessel geometry, and material properties. Metabolic footprint analysis revealed that cultivation conditions strongly influence SM diversity and abundance. Using untargeted LC–MS-based metabolomics combined with molecular network analysis, distinct sets of mass features (MFs) were detected in each system. Hierarchical clustering classified three temporal production profiles of SMs: early production during exponential growth, production and degradation throughout cultivation, and late production associated with stationary-phase metabolism. These profiles varied between systems, even for identical metabolites such as desferrioxamines or leupeptins, indicating that the cultivation system itself modulates the metabolite space. Further molecular network analysis elucidated the structural relationships among the detected metabolites, revealing families of related molecules that differ in terms of chain length modifications, amino acid substitutions, or cyclisation events. Such structural variations are known to significantly alter biological activity.

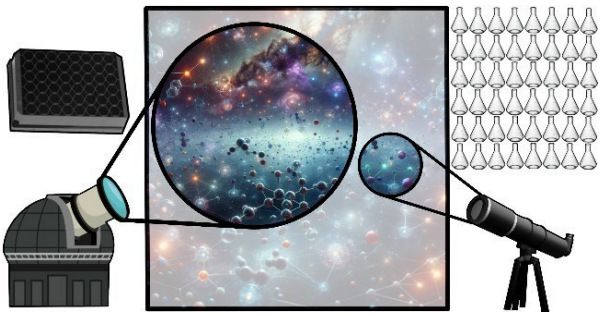

Figure 2. The utilization of microbioreactor cultivation systems in the discovery of NPs expands the secondary metabolic footprint.

Overall, this work highlights the profound impact of cultivation systems on bacterial metabolite space. In particular, microtiter plate cultivation systems facilitate the parallelization of bacterial cultivation and offer a greater degree of comparability with stirred tank bioreactors than shake flasks do.

anton.lindig@tu-dortmund.de
georg.hubmann@tu-dortmund.de
stephan.luetz@tu-dortmund.de

Publications:
Lindig, A., Hubmann, G., Lütz, S., Microtiter plate cultivation systems enable chemically diverse metabolic footprints during bacterial natural product discovery. Biotechnology and Bioengineering, 122: 2021-2036 (2025)
https://doi.org/10.1002/bit.29002
Front Cover Image, Volume 122, Number 8, August 2025.
https://doi.org/10.1002/bit.70022

2025

Peer-reviewed Journal Articles

- Lindig, A., Hubmann, G., Lütz, S.
  Microtiter plate cultivation systems enable chemically diverse metabolic footprints during bacterial natural product discovery. reactor.
  Biotechnology and Bioengineering, 122: 2021-2036 (2025)
  https://doi.org/10.1002/bit.29002

- Lindig, A., Hubmann, G., Lütz, S.
  Front Cover Image, Volume 122, Number 8, August 2025
  Biotechnology and Bioengineering, 122: i-i. (2025)
  https://doi.org/10.1002/bit.70022

- Brockhoff, T., Heinlein, M., Hubmann, G., Lütz, S., Lucia, S.
  Automatic design of robust model predictive control of a bioreactor via Bayesian optimization.
  IFAC-PapersOnLine 59(6):19–24 (2025)
  https://doi.org/10.1016/j.ifacol.2025.07.115

- Sánchez-Garcia, E., Lütz, S., Nett, M.
  Reaction Engineering of In Vitro Natural Product Biosynthesis: Challenges and Strategies.
  ChemBioChem, 26, e202500571 (2025)
  https://doi.org/10.1002/cbic.202500571

2024

Peer-reviewed Journal Articles

- Becker, M., Nowak, I., Hildebrand K., Lütz S., Rosenthal K.
  Development of a multi-enzyme cascade for 2′3′-cGAMP synthesis from nucleosides.
  Catalysis Science & Technology, 14, 3335-3345 (2024)
  https://doi.org/10.1039/D4CY00147H

- Behr, A.S., Surkamp, J., Abbaspour, E., Häußler, M., Lütz, S., Pleiss, J., Kockmann, N., Rosenthal, K.
  Fluent Integration of Laboratory Data into Biocatalytic Process Simulation Using EnzymeML, DWSIM, and Ontologies.
  Processes, 12 (3), 597 (2024)
  https://doi.org/10.3390/pr12030597

- Steinmetz, T., Lindig, A., Lütz, S., Nett, M.
  Molecular Networking-Guided Discovery of Kyonggic Acids in Massilia spp.
  European Journal of Organic Chemistry, 27 (17), (2024) e202400017
  https://doi.org/10.1002/ejoc.202400017

- Nerke, P., Korb, J., Haala, F., Hubmann, G., Lütz, S.
  Metabolic bottlenecks of Pseudomonas taiwanensis VLB120 during growth on d-xylose via the Weimberg pathway.
  Metabolic Engineering Communications 18, e00241 (2024)
  https://doi.org/10.1016/j.mec.2024.e00241

- Kinner, A., Lütz, S., Rosenthal, K.
  Biocatalytic Screening of the Oxidative Potential of Fungi Cultivated on Plant-Based Resources.
  AppliedChem, 4(3), 282-301 (2024)
  https://doi.org/10.3390/appliedchem4030018

- Bartsch, T., Lütz, S., Rosenthal, K.
  Cell-free protein synthesis with technical additives –expanding the parameter space of in vitro gene expression.
  Beilstein J. Org. Chem., 20, 2242-2253 (2024)
  https://doi.org/10.3762/bjoc.20.192

- Siedentop, R., Siska, M., Hermes, J., Lütz, S., von Lieres, E., Rosenthal, K.,
  Avoiding Replicates in Biocatalysis Experiments: Machine Learning for Enzyme Cascade Optimization.
  ChemCatChem, e202400777 (2024)
  https://doi.org/10.1002/cctc.202400777

- Surkamp, J., Wellmann, L., Lütz, S., Rosenthal, K., Kockmann, N.
  Ethanol production using Zymomonas mobilis and in situ extraction in a capillary microreactor.
  Micromaschines, 15(10), 1255, (2024)
  https://doi.org/10.3390/mi15101255

2023

Peer-reviewed Journal Articles

- Siedentop R., Prenzel T., Waldvogel S.R., Rosenthal K., Lütz S.
  Reaction Engineering and Comparison of Electroenzymatic and Enzymatic ATP Regeneration Systems.
  ChemElectroChem 10, e202300332 (2023).
  https://doi.org/10.1002/celc.202300332

- Siedentop R., Prenzel T., Waldvogel S.R., Rosenthal K., Lütz S.
  Reaction Engineering and Comparison of Electroenzymatic and Enzymatic ATP Regeneration Systems. (Coverprofil)
  ChemElectroChem 10, e202300587 (2023).
  https://doi.org/10.1002/celc.202300587

- Lindig A., Schwarz S., Hubmann G., Rosenthal K., Lütz S.
  Bivariate One Strain Many Compounds Designs Expand the Secondary Metabolite Production Space in Corallococcus coralloides.
  Microorganisms 11(10):2592 (2023).
  https://doi.org/10.3390/microorganisms11102592

- Rolf J., Handke J., Burzinski F., Lütz S., Rosenthal K.
  Amino acid balancing for the prediction and evaluation of protein concentrations in cell-free protein synthesis systems.
  Biotechnol. Prog. 39(6):e3373 (2023).
  https://aiche.onlinelibrary.wiley.com/doi/10.1002/btpr.3373

- Siedentop R., Siska M., Möller N., Lanzrath H., von Lieres E., Lütz S., Rosenthal K.
  Bayesian Optimization for an ATP-Regenerating In Vitro Enzyme Cascade.
  Catalysts 13(3):468 (2023).
  https://doi.org/10.3390/catal13030468

  Siedentop R., Dziennus M., Lütz S., Rosenthal K.
  Debottlenecking of an In Vitro Enzyme Cascade Using a Combined Model- and Experiment-Based Approach.
  Chemie Ingenieur Technik 95: 543-548 (2023).
  https://doi.org/10.1002/cite.202200170

Computational Bioengineering (CBE)

Molecular Interactions on Coinage Metal Surfaces: An Electrophilic Reactive Carbene vs. a Nucleophilic Stable Carbene

Two very different flavours of carbene reactivity were studied via computer simulations.

Yining Liu, Joel Mieres-Perez, and Elsa Sanchez-Garcia

Carbenes play important roles in synthetic chemistry and material science, among other applications. The reactivity and properties of carbenes highly depend on their environment and electronic structure. We studied the adsorption of two carbenes: cyclopentadienylidene (CP) and imidazol-2-ylidene (IMI) on three coinage metal surfaces: Cu(111), Ag(111), and Au(111), using plane-wave density functional theory. Our findings provide a foundation for on-surface catalysis strategies based on tailored reactivity of surface-bound carbenes.

Imidazol-2-ylidene (IMI) is a stable carbene at room temperature with a singlet ground spin-state. Cyclopentadienylidene (CP) is, however, highly reactive and has a triplet ground spin-state in the gas phase with a singlet-triplet gap ΔE_{ST} of 4.5 kcal/mol. These two molecules thus exemplify two extremes in carbene chemistry. Our calculations show that, in the presence of coinage metals, CP and IMI exhibit clear differences in adsorption configuration, adsorption energy, and charge transfer behavior.

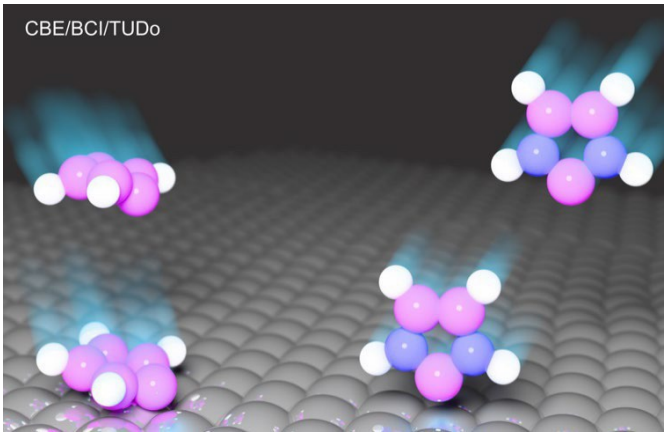

Figure 1. Adsorption of cyclopentadienylidene (CP, left) and imidazol-2-ylidene (IMI, right) on a coinage metal (111) surface. CP adopts a tilted adsorption geometry. IMI adsorbs perpendicularly to the on-top sites on the surfaces.

CP adsorbs tilted on all three (111) metal surfaces at hollow adsorption sites with strong carbene-surface interaction, which is consistent with our previous studies of fluorenylidene and diphenyl carbene on Ag(111) surfaces. The adsorption energies of CP on these three metal surfaces range from -77.2 kcal/mol (Ag) to -101.8 kcal/mol (Cu), with their modular values following the trend: Cu > Au > Ag. These large adsorption energies indicate the formation of strong bonds between carbenes and the metal surface.

We found that CP shows the strongest adsorption on Cu(111), exhibiting the shortest carbenic carbon–metal distance and the smallest adsorption angle amongst the three metal surfaces. Notably, upon adsorption on the (111) coinage metal surfaces, a spin-switching of CP from triplet (in the gas phase) to singlet can be induced.

Bader charge analysis shows that CP acts as an electron acceptor, withdrawing electron density from the surface. Charge density difference maps indicate that multiple metal atoms are involved in the interaction with the surface.

By contrast, IMI adsorbs perpendicularly at on-top sites with significantly smaller adsorption energies from −45.0 kcal/mol (Ag) to −54.2 kcal/mol (Cu and Au). IMI behaves as an electron donor. The interaction involved mostly only one atom at the on-top site on the metal surface.

The stronger binding of CP compared to that of IMI is attributed to the tilted adsorption geometry of CP due to its electrophilic properties, which enable multi-atom surface interactions, while IMI primarily interacts via σ-donation from its lone pair.

Our study indicates that carbene philicities fundamentally influence the adsorption mechanism, charge redistribution, and surface binding strength. Understanding these different adsorption behaviors provides insights essential for fine-tuning surface-bound carbene systems to design heterogeneous catalytic processes and functional materials.

yining.liu@tu-dortmund.de
joel.mieresperez@tu-dortmund.de
professors.cbe.bci@tu-dortmund.de

Publications:
Liu Y., Mieres-Perez, J., and Sanchez-Garcia, E., Interactions of Carbenes with Coinage Metal Surfaces: An Electrophilic Reactive Carbene vs. a Nucleophilic Stable Carbene. The Journal of Organic Chemistry, 90,14066−14073, (2025) https://doi.org/10.1021/acs.joc.5c01313

Understanding the Role of Osmolytes in Biocatalysis

Computational and experimental studies address the effect of osmolytes on two biocatalytic systems.

Julio C. Vieyto-Nuñez, Julio A. Perez-Erviti, Joel Mieres-Perez, and Elsa Sanchez-Garcia

Osmolytes can reshape biomolecular function not only by "stabilizing proteins" in a generic sense, but also by reorganizing local solvation. Here, we highlight two complementary studies that connect cosolvent organization at the molecular level to experimentally measurable outcomes in (i) protein–ligand binding and (ii) enzyme catalysis.

Cells use osmolytes to keep their proteins functional under stress, but the impact of osmolytes on ligand binding is not fully understood. We studied the binding of the competitive inhibitor proflavine to α-chymotrypsin (α-CT) in the presence of several biologically relevant osmolytes to resolve how distinct cosolvents modulate binding thermodynamics and kinetics.

The study combined experimental results from collaboration partners (R. Winter, CCB) with our extensive molecular dynamics (MD) simulations. Ligand dissociation kinetics were quantified computationally via τ-random acceleration molecular dynamics (τRAMD), enabling the prediction of relative residence times of proflavine at the catalytic site across different osmolyte solutions. Figure 1 shows the comparison of experimental ligand binding constants (K_b) with the computed residence times across different osmolytes, displaying a strong correlation between experiments and simulations ($R^2 = 0.89$).

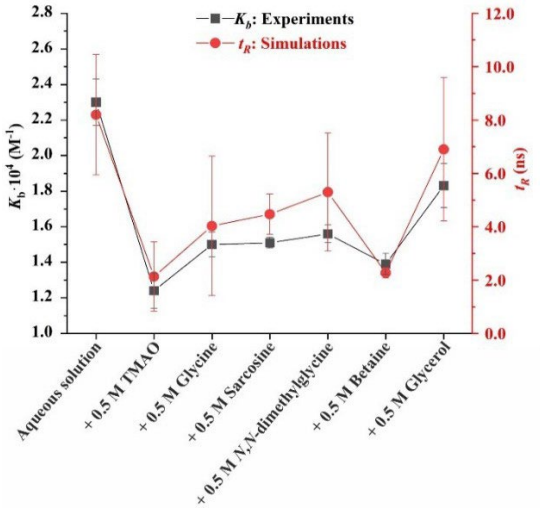

Figure 1. Computed residence times of proflavine in α-CT, in the presence of osmolytes vs. experimentally determined binding constants (K_b).

Our MD analysis also revealed how osmolytes reshape the local solvent composition around both the ligand and the catalytic site. Density maps and contact analyses showed that some osmolytes (such as glycerol) accumulate at (or near) the binding site, establishing frequent noncovalent contacts with proflavine and key active-site residues. By contrast, the altered local solvent environment (for instance, in TMAO) favors faster dissociation of the ligand.

In another study, this time of the enzyme formate dehydrogenase of *Candida boidinii* (CbFDH), we investigated, in collaboration with G. Sadowski (BCI) and R. Winter (CCB), the effects of the osmolytes TMAO and sorbitol on enzymatic activity. A key mechanistic distinction emerging from the molecular dynamics simulations was that TMAO is excluded from the protein surface while sorbitol interacts at the protein surface (Figure 2). Sorbitol and TMAO reshaped active-site water organization via differing mechanisms: sorbitol boosts protein flexibility, water trafficking, and formate residence times, whereas TMAO reduces protein dynamics, water exchange, and ligand residence times, with opposite effects on the catalytic reaction.

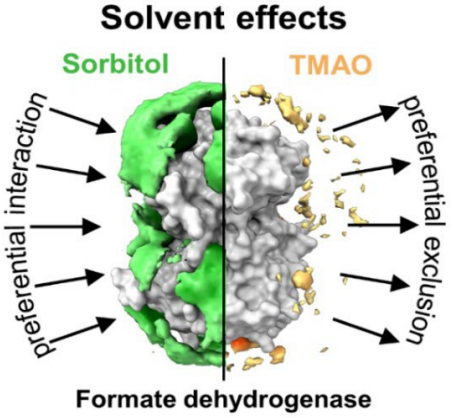

Figure 2. The analysis of our molecular dynamics simulations reveals preferential accumulation of sorbitol at the protein surface (green density) and preferential exclusion of TMAO from the surface (gold density).

Together, these studies show how osmolytes modulate biomolecular function via specific solvation and changes in protein dynamics.

julio.vieyto-nunez@tu-dortmund.de
professors.cbe.bci@tu-dortmund.de

Publications:
Vieyto-Nuñez, J. C.; Campanile, M.; Mieres-Perez, J.; Ostermeier, L.; Agar, C.; Pompea Del Vecchio, L. P.; Oliva, R.; Winter, R.; and Sanchez-Garcia, E. How Osmolytes Regulate Protein–Ligand Interactions: The Case of α-Chymotrypsin and Proflavine. JACS Au 5, (7), 3612-3624, (2025). https://doi.org/10.1021/jacsau.5c00629
Perez-Erviti, J. A., Almeida-Hernández, Y., Mieres-Perez, J., Gajardo-Parra, N., Winter, R., Held, C., Sadowski, G., and Sanchez-Garcia, E. Effect of Trimethylamine-N-Oxide (TMAO) and Sorbitol on the Catalytic Activity of Candida boidinii Formate Dehydrogenase. ChemCatChem 17, (11), e202401961, (2025). https://doi.org/10.1002/cctc.202401961

2025

Peer Reviewed Journal Articles

Silva, A.; Duarte-Silva, S.; Martins, P. M.; Rodrigues, B.; Serrenho, D.; Vilasboas-Campos, D.; Teixeira-Castro, A.; Vieyto-Nuñez, J.; Mieres-Perez, J.; Figueiredo, F.; Podlasiak, M.; Van-der-Kellen, T.; Fraga, J.; Noble, J.; Lantz, C.; Sepanj, N.; Monteiro-Fernandes, D.; Guerreiro, S.; Neves-Carvalho, A.; Pereira-Sousa, J.; Klärner, F.-G.; Schrader, T.; Loo, J. A.; Pastore, A.; Sanchez-Garcia, E.; Bitan, G.; Carvalho, A. L.; Maciel, P.; Macedo-Ribeiro, S.
Allosteric Modulation of Pathological Ataxin-3 Aggregation: A Path to Spinocerebellar Ataxia Type-3 Therapies.
Advanced Science, 13, no. 1, e02216 (2025).
https://doi.org/10.1002/advs.202502216

Sánchez-García, E.; Lütz, S.; Nett, M.
Reaction Engineering of In Vitro Natural Product Biosynthesis: Challenges and Strategies.
ChemBioChem, 26, e202500571 (2025).
https://doi.org/10.1002/cbic.202500571

Liu, Y.; Mieres-Perez, J.; Sanchez-Garcia, E.
Interactions of Carbenes with Coinage Metal Surfaces: An Electrophilic Reactive Carbene vs. a Nucleophilic Stable Carbene.
The Journal of Organic Chemistry, 90, 40, 14066–14073 (2025).
https://doi.org/10.1021/acs.joc.5c01313

Mieres-Perez, J.; Almeida-Hernandez, Y.; Sander, W.; Sanchez-Garcia, E.
A Computational Perspective to Intermolecular Interactions and the Role of the Solvent on Regulating Protein Properties.
Chemical Reviews, 2025, 125, 15, 7023–7056 (2025).
https://doi.org/10.1021/acs.chemrev.4c00807

Vieyto-Nuñez, J. C.; Campanile, M.; Mieres-Perez, J.; Ostermeier, L.; Agar, C.; Petraccone, L.; Del Vecchio, P.; Oliva, R.; Winter, R.; Sanchez-Garcia, E.
How Osmolytes Regulate Protein−Ligand Interactions: The Case of α-Chymotrypsin and Proflavine. *JACS Au, 5, 7, 3612–3624 (2025).* https://doi.org/10.1021/jacsau.5c00629

Brenner, J. C.; Zirden, L. C.; Buzuk, L.; Almeida-Hernandez, Y.; Radzuweit, L.; Diamantino, J.; Kaschani, F.; Kaiser, M.; Sanchez-Garcia, E.; Poepsel, S.; Hellerschmied, D.
Conformational plasticity of a BiP–GRP94 chaperone complex.
Nature Structural & Molecular Biology, 32, 1947–1958 (2025).
https://doi.org/10.1038/s41594-025-01619-0

Albers, D. P. J.; Novikova, S.; Vieyto-Nuñez, J.; Almeida-Hernández, Y.; Pastorio, C.; Klassen, F.; Weiss, D.; von Maltitz, P.; Jaikishan, J.; Datta, M.; Jumaa, H.; Jebaraj, B. M. C.; Stilgenbauer, S.; Kumar, M.; Maity, P. C.; Buske, C.; Stifel, U.; Zinngrebe, J.; Fischer-Posovszky, P.; Chevigné, A.; Kirchhoff, F.; Sanchez-Garcia, E.; Münch, J.; Harms, M. **GPR15LG binds CXCR4 and synergistically modulates CXCL12-induced cell signaling and migration.** *Cell Communication and Signaling, 23, 234 (2025).*
https://doi.org/10.1186/s12964-025-02231-x

Lawrenz, J.; Wettstein, L.; Rodríguez Alfonso, A.; Nchioua, R.; von Maltitz, P.; Albers, D. P. J.; Zech, F.; Vandeput, J.; Naesens, L.; Fois, G.; Neubauer, V.; Preising, N.; Schmierer, E.; Almeida-Hernandez, Y.; Petersen, M.; Ständker, L.; Wiese, S.; Braubach, P.; Frick, M.; Barth, E.; Sauter, D.; Kirchhoff, F.; Sanchez-Garcia, E.; Stevaert, A.; Münch, J.

Trypstatin as a Novel TMPRSS2 Inhibitor with Broad-Spectrum Efficacy against Corona and Influenza Viruses.
Advanced Science, 12, 2506430 (2025).
https://doi.org/10.1002/advs.202506430

Perez-Erviti, J. A.; Almeida-Hernández, Y.; Mieres-Perez, J.; Gajardo-Parra, N.; Winter, R.; Held, C.; Sadowski, G.; Sanchez-Garcia, E.
Effect of Trimethylamine-N-Oxide (TMAO) and Sorbitol on the Catalytic Activity of Candida boidinii Formate Dehydrogenase.
ChemCatChem, e202401961 (2025).
https://doi.org/10.1002/cctc.202401961

2024

Peer Reviewed Journal Articles

Lucht, K., Schweer, P., Cao, Y., Mieres-Perez, J., Ulrich, I., Sanchez-Garcia, E., Sander, W., & Morgenstern, K.
On-surface alcohol formation from a carbene precursor.
The Journal of Physical Chemistry C, 128, 15347–15355 (2024).
https://doi.org/10.1021/acs.jpcc.4c02805

Budean, D., Almeida-Hernández, Y., Pandey, J., Mieres-Perez, J., Sánchez-García, E., & Haglund, E.
Exploring chemokine homodimer stability: Structural insights into CXC and CC interfaces.
Biophysica, 4(4), 561–572 (2024).
https://doi.org/10.3390/biophysica4040037

Harms, M., Haase, A., Rodriguez-Alfonso, A., Löffler, J., Almeida-Hernández, Y., Ruiz-Blanco, Y. B., Albers, D., Gilg, A., von Bank, F., Zech, F., Datta, M., Jaikishan, J., Draphoen, B., Habib, M., Ständker, L., Wiese, S., Lindén, M., Winter, G., Rasche, V., Beer, A. J., Jumaa, H., Abadim, A. H., Kirchhoff, F., Busch, M., Dünker, N., Sanchez-Garcia, E., & Münch, J.
Fatty acid conjugated EPI-X4 derivatives with increased activity and in vivo stability.
Journal of Controlled Release, 373, 583–598 (2024).
https://doi.org/10.1016/j.jconrel.2024.07.04 9

Beaufort, N., Ingendahl, L., Merdanovic, M., Schmidt, A., Podlesainski, D., Richter, T., Neumann, T., Kuszner, M., Vetter, I. R., Stege, P., Burston, S. G., Filipovic, A., Ruiz-Blanco, Y. B., Bravo-Rodriguez, K., Mieres-Perez, J., Beuck, C., Uebel, S., Zobawa, M., Schillinger, J., Malik, R., Todorov-Völgyi, K., Rey, J., Roberti, A., Hagemeier, B., Wefers, B., Müller, S. A., Wurst, W., Sanchez-Garcia, E., Zimmermann, A., Hu, X.-Y., Clausen, T., Huber, R., Lichtenthaler, S. F., Schmuck, C., Giese, M., Kaiser, M., Ehrmann, M., & Dichgans, M. .
Rational correction of pathogenic conformational defects in HTRA1. *Nature Communications, 15, 5944 (2024).* https://doi.org/10.1038/s41467-024-49982-8

Day, M., Tetik, B., Parlak, M., Almeida-Hernandez, Y., Räschle, M., Kaschani, F., Siegert, H., Marko, A., Sanchez-Garcia, E., Kaiser, M., Barker, I. A., Pearl, L. H., Oliver, A. W., & Boos, D.
TopBP1 utilises a bipartite GINS binding mode to activate the replicative helicase.
Nature Communications, 15, 1797 (2024).
https://doi.org/10.1038/s41467-024-45946-0

2023

Peer Reviewed Journal Articles

Harms, M.; Hansson, R. F.; Gilg, A.; Almeida-Hernández, Y.; Löffler, J.; Rodríguez-Alfonso, A.; Habib, M. M. W.; Albers, D.; Ahmed, N. S.; Abadi, A. H.; Winter, G.; Rasche, V.; Beer, A. J.;

Weidinger, G.; Preising, N.; Ständker, L.; Wiese, S.; Sanchez-Garcia, E.; Zelikin, A. N.; Münch, J.
Development of N-Terminally Modified Variants of the CXCR4-Antagonistic Peptide EPI-X4 for Enhanced Plasma Stability.
Journal of Medicinal Chemistry, 66, 22, 15189–15204 (2023).
https://doi.org/10.1021/acs.jmedchem.3c01128

Cao, Y.; Mieres-Perez, J.; Lucht, K.; Ulrich, I.; Schweer, P.; Sanchez-Garcia, E.; Morgenstern, K.; Sander, W.
C-C coupling of carbene molecules on a metal surface in the presence of water.
Journal of the American Chemical Society, 145, 21, 11544–11552 (2023).
https://doi.org/10.1021/jacs.2c12274

Kling, C.; Sommer, A.; Almeida-Hernandez, Y.; Rodríguez, A.; Perez-Erviti, J. A.; Bhadane, R.; Ständker, L.; Wiese, S.; Barth, H.; Pupo-Meriño, M.; Pulliainen, A. T.; Sánchez-García, E.; Ernst, K.
Inhibition of pertussis toxin by human α-defensins-1 and-5: Differential mechanisms of action.
International Journal of Molecular Sciences, 24, 13, 10557 (2023).
https://doi.org/10.3390/ijms241310557

Harms, M.; Smith, N.; Han, M.; Groß, R.; von Maltitz, P.; Stürzel, C.; Ruiz-Blanco, Y. B.; Almeida-Hernández, Y.; Rodriguez-Alfonso, A.; Cathelin, D.; Caspar, B.; Tahar, B.; Sayettat, S.; Bekaddour, N.; Vanshylla, K.; Kleipass, F.; Wiese, S.; Ständker, L.; Klein, F.; Lagane, B.; Boonen, A.; Schols, D.; Benichou, S.; Sanchez-Garcia, E.; Herbeuval, J.-P.; Münch, J.
Spermine and spermidine bind CXCR4 and inhibit CXCR4- but not CCR5-tropic HIV-1 infection.
Science Advances, 9, eadf8251 (2023).
https://doi.org/10.1126/sciadv.adf8251

Cao, Y.; Mieres-Perez, J.; Rowen, J. F.; Sanchez-Garcia, E.; Sander, W.; Morgenstern, K.
Chirality control of a single carbene molecule by tip-induced van der Waals interactions.
Nature Communications, 14, 4500 (2023). https://doi.org/10.1038/s41467-023-39870-y

Neblik, J.; Kirupakaran, A.; Beuck, C.; Mieres-Perez, J.; Carlsson Niemeyer, F.; Le, M.-H.; Telgheder, U.; Schmuck, J. F.; Dudziak, A.; Bayer, P.; Sanchez-Garcia, E.; Westermann, S.; Schrader, T. **Multivalent molecular tweezers disrupt the essential NDC80 interaction with microtubules.** *Journal of the American Chemical Society, 145, 28, 15251–15264 (2023).*
https://doi.org/10.1021/jacs.3c02186

Gaonkar, R. H.; Schmidt, Y. T.; Mansi, R.; Almeida-Hernandez, Y.; Sanchez-Garcia, E.; Harms, M.; Münch, J.; Fani, M. **Development of a new class of CXCR4 targeting radioligands based on the endogenous antagonist EPI-X4 for oncological applications.**
Journal of Medicinal Chemistry, 66, 13, 8484–8497 (2023).
https://doi.org/10.1021/acs.jmedchem.3c0 0131

Olari, L.-R.; Bauer, R.; Gil Miró, M.; Vogel, V.; Cortez Rayas, L.; Groß, R.; Gilg, A.; Klevesath, R.; Rodríguez Alfonso, A. A.; Kaygisiz, K.; Rupp, U.; Pant, P.; Mieres-Perez, J.; Steppe, L.; Schäffer, R.; Rauch-Wirth, L.; Conzelmann, C.; Müller, J. A.; Zech, F.; Gerbl, F.; Bleher, J.; Preising, N.; Ständker, L.; Wiese, S.; Thal, D. R.; Haupt, C.; Jonker, H. R. A.; Wagner, M.; Sanchez-Garcia, E.; Weil, T.; Stenger, S.; Fändrich, M.; von Einem, J.; Read, C.; Walther, P.; Kirchhoff, F.; Spellerberg, B.; Münch, J. **The C-terminal 32-mer fragment of hemoglobin alpha is an amyloidogenic peptide with antimicrobial properties.**

Cellular and Molecular Life Sciences, 80, 151 (2023)

https://doi.org/10.1007/s00018-023-04795-8

Shahpasand-Kroner, H.; Siddique, I.; Malik, R.; Linares, G.; Ivanova, M.; Ichida, J.; Weil, T.; Münch, J.; Sanchez-Garcia, E.; Klärner, F.-G.; Schrader, T.; Bitan, G. **Molecular tweezers – supramolecular hosts with broad-spectrum biological applications.** *Pharmacological Reviews, 75, 2, 263–308 (2023).* https://doi.org/10.1124/pharmrev.122.000654

Wettstein, L.; Immenschuh, P.; Weil, T.; Conzelmann, C.; Almeida-Hernández, Y.; Hoffmann, M.; Kempf, A.; Nehlmeier, I.; Lotke, R.; Petersen, M.; Stenger, S.; Kirchhoff, F.; Sauter, D.; Pöhlmann, S.; Sanchez-Garcia, E.; Münch, J. **Native and activated antithrombin inhibits TMPRSS2 activity and SARS-CoV-2 infection.** *Journal of Medical Virology, 95, 1, e28124 (2023).* https://doi.org/10.1002/jmv.28124

Computational Systems Biology (CSB)

SwarmGenomics: A Unified Pipeline for Individual-Based Whole-Genome Analyses.

A scalable and user-friendly workflow for whole-genome data analysis.

Aure Kylmänen, Yu-Chi Chen, Sahar Javaheri Tehrani, Nikolas Vellnow, Justin J. S. Wilcox, & Toni I. Gossmann

Advances in sequencing technologies have made whole-genome data widely accessible, enabling research in population genetics, evolutionary biology, and conservation. However, the increasing volume and complexity of genomic data pose substantial challenges for reproducibility, scalability, and integration of analytical steps. Here, we present SwarmGenomics, a unified, modular, and scalable pipeline designed to streamline reference-based genome assembly and genomic analyses from raw sequencing reads to population genomic inference.

SwarmGenomics is a modular, user-friendly bioinformatics pipeline for whole-genome sequencing (WGS) analysis. It integrates tools for estimating heterozygosity and runs of homozygosity to assess genetic diversity and inbreeding, reconstructing population history, detecting DNA contamination, analyzing repetitive sequences, assembling mitochondrial genomes, and identifying nuclear mitochondrial DNA segments (NUMTs). Its modular design allows users to run only the analyses relevant to their research questions, providing flexibility without sacrificing reproducibility. An overview of the workflow is shown in Figure 1, with planned future modules indicated in grey. Complete documentation, installation instructions, and the pipeline are freely available on GitHub:
https://github.com/AureKylmanen/Swarmgenomics

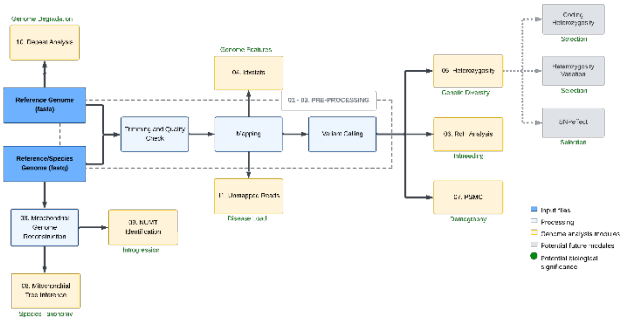

Figure 1. SwarmGenomics pipeline overview starting with reference and species genomes in FASTA and FASTQ format, followed by processing steps (in light blue) and modules for different genomic analyses (in yellow), with possible future modules in grey. Each module is numbered according to the corresponding page in the SwarmGenomics GitHub repository.

By combining a reproducible workflow with a growing dataset of analyzed genomes, SwarmGenomics enables direct comparisons of key population genetics metrics across species. For example, Figure 2 shows the distribution of runs of homozygosity (RoHs) in giant panda and lion genomes. The lion exhibits more long RoHs than the giant panda, suggesting more recent inbreeding in its population.

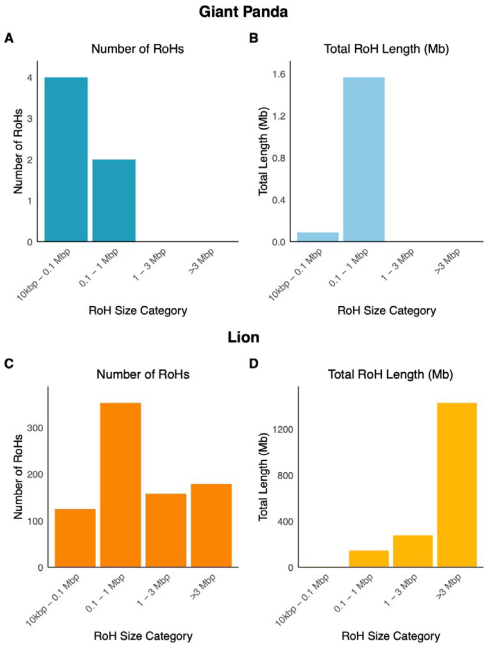

Figure 2. Distribution of runs of homozygosity (RoHs), an indicator of inbreeding, in giant panda and lion genome. The lion exhibits a large amount of long RoHs in comparison to the giant panda, suggesting a more recent inbreeding in the lion population.

Looking forward, SwarmGenomics aims to serve both as a bioinformatics teaching platform and a collaborative research resource. Its GitHub repository provides everything needed to run analyses, with user-friendly documentation supporting students and researchers new to genomics. The pipeline is freely available for university courses and self-guided learning, and a dedicated website is in development to centralize user-generated results.

toni.gossmann@tu-dortmund.de

Publications:
Kylmänen, A., Chen, Y. C., Javaheri Tehrani, S., Vellnow, N., Wilcox, J. J. S., & Gossmann, T. I. (2026).
SwarmGenomics: A Unified Pipeline for Individual-Based Whole-Genome Analyses.
Molecular ecology resources, 26(3), e70119.
https://doi.org/10.1111/1755-0998.70119

2025

Peer Reviewed Journal Articles and preprints

- Lemke, O., Heineike, B. M., Viknander, S., Cohen, N., Li, F., Steenwyk, J. L., Spranger, L., Agostini, F., Lee, C. T., Aulakh, S. K., Berman, J., Rokas, A., Nielsen, J., Gossmann, T. I., Zelezniak, A., & Ralser, M.
  The role of metabolism in shaping enzyme structures over 400 million years.
  Nature, 644(8075), 280–289 (2025)
  https://doi.org/10.1038/s41586-025-09205-6

- Chen, Y.-C., Vendrami, D.L.J., Huber, M.L., Handel, L.E.Y., Cooney, C.R., Hoffman, J.I., Gossmann, T.I.
  Diverse evolutionary trajectories of mitocoding DNA in mammalian and avian nuclear genomes.
  Genome Research, 35, 1313–1324 (2025)
  https://doi.org/10.1101/gr.279428.124

- Chen, Y.-C., Chen, Y.-C., Vellnow, N., Wilcox, J. J. S., Javaheri Tehrani, S., & Gossmann, T. I.
  Opinion: Why Sex-Based Genomic Differentiation Should Not Be Overlooked in Population Genetics.
  Molecular Ecology, 34(18), e70061 (2025)
  https://doi.org/10.1111/mec.70061

- Wilcox, J.J.S., Ord, J., Kappei, D. and Gossmann, T.I.
  The CpG Landscape of Protein Coding DNA in Vertebrates.
  Evolutionary Applications, 18: e70101 (2025)
  https://doi.org/10.1111/eva.70101

- Javaheri Tehrani, S., Rezazadeh, E., Alaei Kakhki, N., Nourani, L., Ebadi, V., Karimi, S., Karami, M., Ashouri, F., Sarshar, A., Gossmann, T. I., & Aliabadian, M.
  DNA barcoding of passerine birds in Iran.
  ZooKeys, 1236, 19–39 (2025)
  https://doi.org/10.3897/zookeys.1236.143336

- Brasó-Vives, M., Hartasánchez, D.A., Ayroles, J.F., Bucao, C.F., Furlan-Magaril, M., Majic, P., Pallares, L.F., Phipps-Tan, J., Rogers, T.F., Ruiz-Herrera, A., Santos-Rodriguez, G., Vellnow, N., Wilcox, J.J.S., Rodríguez, J.A.
  The Genomic Kaleidoscope: On the Hidden Dimensions of Within-Species Genomic Diversity.
  Genome Biology and Evolution 17, evaf204 (2025)
  https://doi.org/10.1093/gbe/evaf204

- Chen, Y.-C., Wilcox, J. J. S., & Gossmann, T. I.
  Linked selection of insertions and deletions in coding regions of the great tit genome
  BioRxiv (2025)
  https://doi.org/10.1101/2025.09.26.678803

- Gautrey, S. L., Dunning, L. T., Gossmann, T. I., & Simons, M. J. P.
  Dietary restriction is evolutionary conserved on the phenotypic and mechanistic level.
  BioRxiv (2025)
  https://doi.org/10.1101/2025.03.26.645451

- Kylmänen, A., Chen, Y.-C., Tehrani, S. J., Vellnow, N., Wilcox, J. J. S., & Gossmann, T. I.
  SwarmGenomics: A Unified Pipeline for Individual-Based Whole-Genome Analyses.
  BioRxiv (2025)
  https://doi.org/10.1101/2025.08.13.670070

- Meuthen, D., Hoffman, J. I., Kurtz, J., Berthelsen, A. L., Chakarov, N., Chen, R. S., Coculla, A., Gadau, J., Gossmann, T. I., Mühlenhaupt, M., Chavarria-Pizarro, T., Rapp, T., Sepers, B., Vellnow, N., Xu, S., & Vendrami, D.
  Exploring the interplay of epigenetics and individualization
  EcoEvoRxiv (2025)
  https://ecoevorxiv.org/repository/view/8694/

2024

Peer Reviewed Journal Articles and preprints

- Kaiser, M. I.; Killin, A.; Abendroth, A.-K.; Back, M. D.; Baune, B. T .; Bilstein, N.; Breitmoser, Y .; Caspers, B. A.; Gadau, J.; Gossmann, T . I.; Kaiser, S.; Krüger, O.; Kurtz, J.; Lengersdorf, D.; Malsch, A. K. F .; Müller, C.; Rauthmann, J. F .; Reinhold, K.; Richter, S. H.; Stummer, C.; Trappes, R.; Voelcker-Rehage, C.; Wittmann, M. J.
  Individualisation and individualised science across disciplinary perspectives.
  European Journal for Philosophy of Science 2024, 14(3)
  https:/ /doi.org/10.1007/s13194-024-00602-8

- Muenzner, J.; Trébulle, P .; Agostini, F .; Zauber, H.; Messner, C. B.; Steger, M.; Kilian, C.; Lau, K.; Barthel, N.; Lehmann, A.; Textoris-Taube, K.; Caudal, E.; Egger, A.-S.; Amari, F .; De Chiara, M.; Demichev, V .; Gossmann, T . I.; Mülleder, M.; Liti, G.; Schacherer, J.; Selbach, M.; Berman, J.; Ralser, M.
  Natural proteome diversity links aneuploidy tolerance to protein turnover.
  Nature 2024, 630(8015), 149–157
  https:/ /doi.org/10.1038/s41586-024-07442-9

- Vellnow, N.; Gossmann, Toni I.; Waxman, D.
  The pseudoentropy of allele frequency trajectories, the persistence of variation, and the effective population size.
  BioSystems 2024, 238, 105176
  https:/ /doi.org/10.1016/j.biosystems.2024.105176

- Vellnow, N.; Gossmann, T . I.; Waxman, D.
  A comprehensive representation of selection at loci with multiple alleles that allows complex forms of genotypic fitness.
  BioRxiv 2024
  https:/ /doi.org/10.1101/2024.11.08.622587

- Wilcox, J. J. S.; Foucault, Q. J. R.; Gossmann, T . I.
  Identification of 5mC within heterogenous tissue using de-novo somatic mutations
  BioRxiv 2024
  https:/ /doi.org/10.1101/2024.06.05.597613

2023

Peer Reviewed Journal Articles

- Ord, J.; Toni I Gossmann; Adrian-Kalchhauser, I.
  High nucleotide diversity accompanies differential DNA methylation in naturally diverging populations
  Molecular Biology and Evolution 2023
  https:/ /doi.org/10.1093/molbev/msad068

Solids Process Engineering (FSV)

Formulating Cannabidiol by Spray Drying.

Exploring potential production routes for solid dosage forms containing Cannabidiol.

Enrico Ercolin, Fabian Schulte, Gerhard Schaldach, Oliver Kayser, Markus Thommes

Cannabidiol (CBD) shows various pharmacological effects for the treatment of medical conditions. Nevertheless, the poor water-solubility and lipophilia result in a low oral bioavailability. To maximize its therapeutic potential, strategies must be explored to enhance oral bioavailability. Therefore, this study aims to present and evaluate two solid Cannabidiol formulations produced by spray drying.

This study investigates two strategies for the continuous production of CBD formulations by spray drying that exhibit high dissolution rates for immediate drug release. The first strategy involves the reduction of the particle size of the drug, which is done by obtaining a second phase in an emulsion containing most of the drug prior to the spray drying process. This emulsification is continuous via a self-developed Swirl-Mixer and produces small drug loaded droplets. In Figure 1, the flow within the Swirl Mixer is color-visualized according to the mass fraction of isopropanol in water in each stream (isopropanol inlet (red) and a water inlet (blue)). The Swirl-Mixer adds a swirl flow regime to the mixing process, which intensifies the mixing and results in a rather homogeneous concentration across the cross-section plane at the outlet.

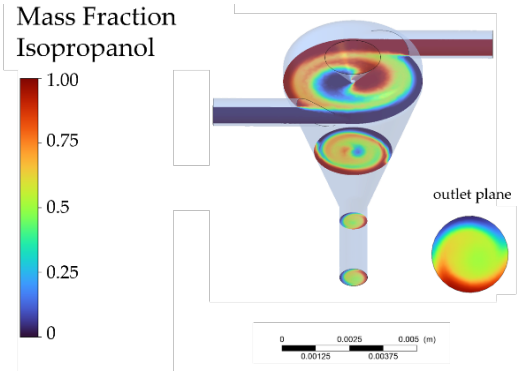

Figure 1. CFD simulation of the Swirl-Mixer in regard of the mixing quality via mass fraction distribution over various cross-sectional planes. The color coding indicates the mass fraction of isopropanol in each stream.

The produced droplets are embedded into a water-soluble carrier via the spray dryer Mobile Minor by GEA, Søborg, Denmark (see Fig. 2, left). The results are composite particles (CP), which combine the advantages of both small particles (i.e. their ability to dissolve rapidly) and larger particles (i.e. their improved handleability for further processing).

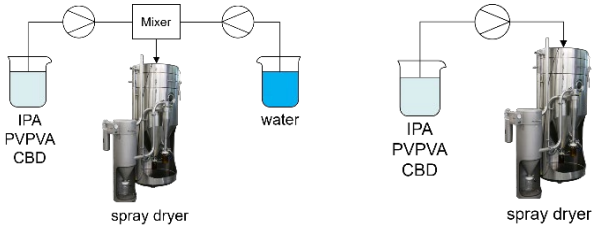

Figure 2. Production route via CP (left) and via ASD (right).

The second strategy under consideration is the production of amorphous solid dispersions (ASD). The drug is distributed molecularly in an amorphous carrier through the process of spray drying (see Fig. 2, right).

Pure CBD shows a comparatively slow and incomplete release within the investigated time frame, the physical mixture enhances the release rate (see Fig.3). Notably, the ASD with 1 wt.% CBD exhibits a faster release profile, reaching 50% release within only 16 minutes. The CP exhibits the most pronounced effect, characterized by a clear change in release kinetics after the initial phase. The rate of release of CBD is accelerated significantly up to 20 minutes, with the result that more than 75% of the substance is released. By 85 minutes, the release of CBD from the CP is complete.

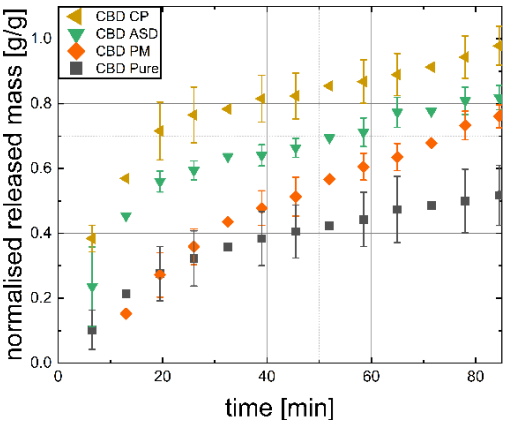

Figure 3. Normalized released mass over time of composite particles (CP), amorphous solid dispersion (ASD), physical mixture (PM) and pure CBD (various weight fractions, n=3, av±s).

In conclusion, this study provides two production routes via spray drying for solid formulations containing cannabidiol. Especially, the route to composite particles through the “Oiling-Out” phenomenon could be applicable to other systems. The two presented production routes via spray drying will help to produce solid dosage forms of cannabidiol.

enrico.ercolin@tu-dortmund.de
fabian3.schulte@tu-dortmund.de
gerhard.schaldach@tu-dortmund.de
oliver.kayser@tu-dortmund.de
markus.thommes@tu-dortmund.de

Publications:
Ercolin, E.M.A; Schulte, F.; Schaldach, G.; Kayser, O.; Thommes, M., Advanced Cannabidiol Formulations Produced by Spray Drying. (submitted)

Towards an autonomous powder compaction process.

In-situ monitoring of critical quality attributes of tablets via UV-Vis spectroscopy.

René Brands, Jens Bartsch, Markus Thommes

Powder compaction on a rotary tablet press is a dry granulation method to transfer powder materials consisting of several components into compacts (tablets). Quality attributes (weight fraction, mass, porosity, lubrication) are maintained by adapting the internal process chain resulting in a complex control task. In this respect, the overall aim is to develop an adaptive, data-driven predictive system replacing human intervention to reduce quality fluctuations.

The objective of the current study is to implement a monitoring system for the in-situ determination of product specifications enabling a real-time control via critical process parameters as input variables (Fig. 1).

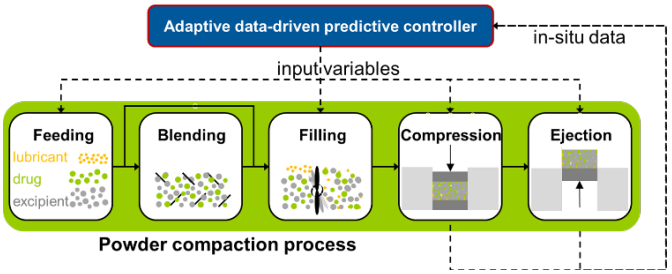

Figure 1. Schematic of an adaptive, data-driven predictive system for autonomous control on powder compaction with a rotary tablet press.

The developed monitoring system is based on provided machine data (ejection force as surrogate for lubrication, pre-compression force as surrogate for mass) as well as on UV-Vis spectroscopy (InSpectroX, ColVisTec, Berlin, Germany). The probe was implemented in a rotary tablet press (Fette 102i, Fette Compacting, Schwarzenbek, Germany) in the ejection position (Fig. 2, left and middle) aligned horizontally with the compacts at a distance of 4 mm. A number of 35 light flashes at 2 ms each were emitted per measurement resulting in a sample rate of 1.5 Hz including the integration time. The set-up also considered a gas jet to prevent particle deposition on the glass fiber surface.

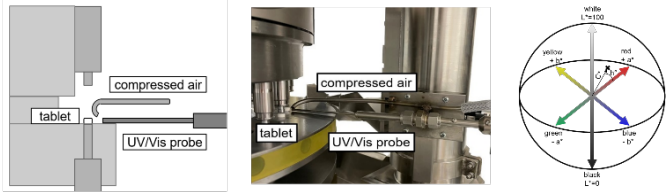

Figure 1. Schematic (left) and photo (middle) of developed set-up for in-line UV-Vis monitoring. Representation of the VIS spectral data in form of the CIELAB color space (right).

For the full determined UV-Vis spectra (224 – 820 nm), the reflectance value as ratio of emitted light intensity to reflected light intensity was utilized as surrogate for the weight fraction of the active pharmaceutical ingredient (API) on the one hand. On the other hand, the visible range was utilized to calculate the coordinates of the CIELAB-color room (Fig.1, right). The chroma value C* representing the relative saturation of the sample color was used for process monitoring of the porosity.

The developed set-up was applied in a systematic study to identify the process parameter impact (compression force, filling system speed) on the ejection force and porosity for formulation pre-mixes with varying weight fractions. The filling system is referred to as FOM.

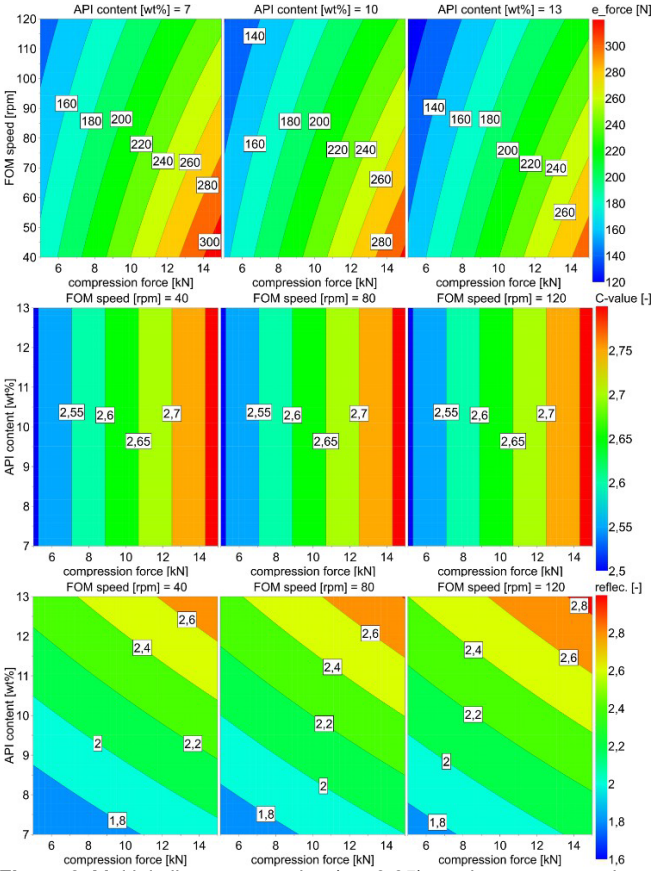

Figure 3. Multiple linear regression (α = 0.05) results as contour plots for ejection force (e_force, top), chroma value (C-value, middle), and reflectance value (reflec., bottom).

The results highlighted the capability of the developed in-situ monitoring system to capture the product quality in real-time and revealed the individual process parameter impact. Also, the acquired data was suitable for process model development in a follow-up study.

rene.brands@tu-dortmund.de
jens.bartsch@tu-dortmund.de
markus.thommes@tu-dortmund.de

Publications:
Brands, R.; Le, T.N.; Bartsch, J.; Thommes, M., A Step Towards Real-Time Release Testing of Pharmaceutical Tablets: Utilization of CIELAB Color Space. Pharmaceutics 2025 (311). https://doi.org/10.3390/pharmaceutics170 https://doi.org/30311
Brands, R.; Tebart, N.; Thommes, M.; Bartsch, J., UV/Vis spectroscopy as an in-line monitoring tool for tablet content uniformity. J Pharmaceut Biomed 2023 (226). https://doi.org/10.1016/j.jpba.2023.115721

Hot Melt Extrusion of Amorphous Solid Dispersions.

Mechanistic Insights into Formulation and Process Design.

Marvin Daalmann, Jana Klüppelberg, Markus Thommes, Judith Winck

The formulation of amorphous solid dispersions (ASDs) remains a key strategy to enhance the bioavailability of poorly soluble drugs by molecularly dispersing them in amorphous carrier polymers. In hot melt extrusion, processing time and temperature are critical parameters regarding the dissolution of the crystalline drug in the polymer. A comprehensive understanding is essential for process design and thus for fully exploiting the potential of ASD formulations in pharmaceutical applications.

An experimental setup was designed to implement inline UV-Vis spectroscopy in small scale hot melt extrusion to assess the drug dissolution behavior in a polymer at early stages of formulation development with minimal material quantities (Figure 1). The DSM Xplore micro compounder is characterized by its small dimensions, enabling the processing of 2.5 g of material. Furthermore, specific processing times can be adjusted via the recirculation mode.

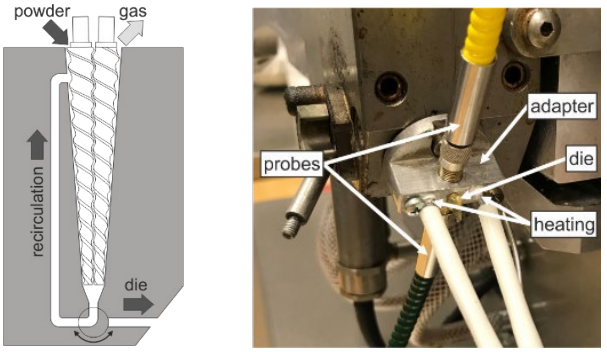

Figure 1. Experimental setup with small scale compounder (left) and alignment of UV-Vis spectroscopy at the die (right).

Two ASD formulations with different drug loads were processed at varying processing times and temperatures (exemplarily shown in Figure 2). Griseofulvin (GRI) and Itraconazole (ITR) were used as model drugs, whereas Copovidone (PVPVA) was applied as polymeric carrier.

The extent of drug dissolution in the polymer for ASD formation during hot melt extrusion was quantified based on light scattering (lightness of CIELAB color system) at the interphases of remaining drug crystals, measured with an Inspectro X UV-Vis spectrophotometer.

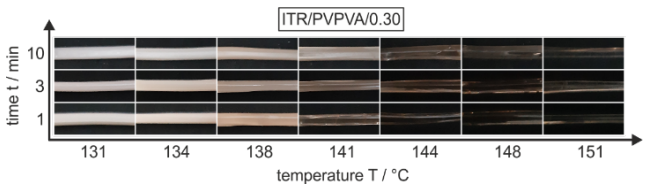

Figure 2. Extrudates of ITR/PVPVA solid dispersions at 30 wt% drug depending on processing time and temperature.

The processing temperature has a significant impact on drug dissolution within the polymer matrix. Moreover, complete drug dissolution shifted to lower temperatures when longer residence times were applied (Figure 3, left). Based on the courses of lightness over processing times and temperatures, regime maps were modeled that define the process conditions under which ASDs can be successfully manufactured (Figure 3, right). Depending on drug-polymer interactions and molecular mobilities, the required processing time at the solubility limit of the crystalline drug in the polymer varies for the different formulations.

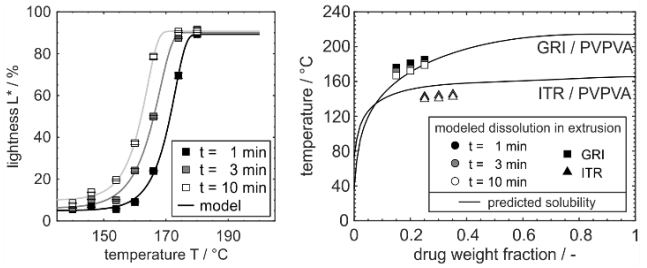

Figure 3. Modeled dissolution profiles of GRI/PVPVA solid dispersions at 15 wt% drug depending on processing time and temperature (left) and dissolution regimes depending on processing time and temperature in comparison to predicted phase diagrams according to a proposed extended Flory-Huggins model (right).

These insights enable a mechanistic understanding of process-structure-property relationships in ASD manufacturing and support predictive design strategies within pharmaceutical hot melt extrusion.

judith.winck@tu-dortmund.de

Publications:
Daalmann, M.; Kimmel, V.; Muehlenfeld, C.; Thommes, M.; Winck, J., Characterization of Different Copovidone Grades as Carrier Materials in Hot Melt Extrusion of Amorphous Solid Dispersions. Pharmaceutics 17:1138, 2025.
https://doi.org/10.3390/pharmaceutics17091138
Klueppelberg, J.; Handge, U.A.; Thommes, M.; Winck, J., Composition Dependency of the Flory–Huggins Interaction Parameter in Drug–Polymer Phase Behavior. Pharmaceutics, 15:2650, 2023.
https://doi.org/10.3390/pharmaceutics15122650
Winck, J.; Daalmann, M.; Berghaus, A.; Thommes, M., In-line Monitoring of Solid Dispersion Preparation in Small Scale Extrusion based on UV-Vis Spectroscopy. Pharmaceutical Development and Technology, 27(10), 2022.
https://doi.org/10.1080/10837450.2022.2144887

2025

Peer Reviewed Journal Articles

- Brands, R., Bartsch, J., Thommes, M.
Complemental hard modeling in Raman spectroscopy: A case study on titanium dioxide-free coating in-line monitoring.
Journal of Pharmaceutical Sciences, 114, 577-585 (2025)
https://doi.org/10.1016/j.xphs.2024.10.044

- Brands, R., Fuch, L., Seyffer, J. M., Bajcinca, N., Bartsch, J., Peuker, U., Schmidt, V., Thommes, M.
Penetration depth and effective sample size characterization of UV/Vis radiation into pharmaceutical tablets.
Journal of Pharmaceutical Sciences, 114, 12, 103889 (2025)
https://doi.org/10.1016/j.xphs.2025.103889

- Brands, R., Le, T. N., Bartsch, J., Thommes, M.
A Step Towards Real-Time Release Testing of Pharmaceutical Tablets: Utilization of CIELAB Color Space.
Pharmaceutics 17, 311 (2025)
https://doi.org/10.3390/pharmaceutics17030311

- Daalmann, M., Kimmel, V., Muehlenfeld, Ch., Thommes, M.; Winck, J.
Characterization of Different Copovidone Grades as Carrier Materials in Hot Melt Extrusion of Amorphous Solid Dispersions.
Pharmaceutics 17, 1138 (2025)
https://doi.org/10.3390/pharmaceutics17091138

- Ercolin, E. M. A., Fricke, J., Lehman, D., Schaldach, G., Nestrovic, T., Thommes, M.
Elucidation of Droplet Formation Mechanisms by Vibrating Mesh Atomizers.
Chemical Engineering & Technology 48, 7, e70063 (2025)
https://doi.org/10.1002/ceat.70063

- Kimmel, V., Gräfe, L., Grieser, L., Lips, A., Hennig, R., Winck, J., Thommes, M.
Modeling Shear-Thinning Flow in Twin-Screw Extrusion Processes.
Pharmaceutics, 17, 353 (2025)
https://doi.org/10.3390/pharmaceutics17030353

- Mattusch, A., Meurers, A., Hense, N., Bartsch, J., Thommes, M.
Hydrodynamic Influences on Dissolution Testing Using Flow Channel Apparatuses.
Chemical Engineering & Technology 48, 2, e202400325 (2025)
https://doi.org/10.1002/ceat.202400325

- Mattusch, A. M., Schaldach, G., Bartsch, J., Thommes, M.
Intrinsic Dissolution Modeling: Interdependence Between Dissolution Rate, Solubility, and Boundary Layer Thickness.
Pharmaceutics 17,570 (2025)
https://doi.org/10.3390/pharmaceutics17050570

- Pech, J., Kaminski, Ch., Markus, M., Hoheisel, W., Heumann, R., Winck, J., Thommes, M.
Predictive Modeling of Drug Product Stability in Pharmaceutical Blister Packs.
Pharmaceutics 17, 1233 (2025)
https://doi.org/10.3390/pharmaceutics17091233

- Pennemann, A., Zavalii, K., Schaldach, G., Thommes, M.
Drying Rate Prediction for Droplets under Combined Convection and Infrared Radiation Drying.
Chemical Engineering & Technology, 48, 6, e70033 (2025)
https://doi.org/10.1002/ceat.70033

- Quodbach, J., Preis, E., Karkossa, F., Winck, J., Finke, J. H., Steiner, D.
Novel Strategies for the Formulation of Poorly Water-Soluble Drug Substances by Different Physical Modification Strategies with a Focus on Peroral Applications.
Pharmaceuticals (Basel), 18, 1089 (2025)
https://doi.org/10.3390/ph18081089

- Sleziona, D, Ely, D. R., Thommes, M.
Mechanisms of drug release from a melt-milled, poorly soluble drug substance.
Journal of Pharmaceutical Sciences, 114, 394-401 (2025)
https://doi.org/10.1016/j.xphs.2024.10.016

- Klueppelberg, J., Handge, U. A., Thommes, M., Winck, J.
Influence of Carbon Dioxide on the Phase Behavior of Pharmaceutical Drug-Polymer Dispersions.
Macromolecular Chemistry and Physics, 226, 2400359 (2025)
https://doi.org/10.1002/macp.202400359

2024

Peer Reviewed Journal Articles

- Lang, T., Bartsch, J.
Adapting the process conditions and performance in planetary roller melt granulation (PRMG) via the planetary spindle number
Powder Technology 442, 119864 (2024)
https://doi.org/10.1016/j.powtec.2024.119864

- Lang, T., Bartsch, J.
Impact of the spindle number on the material transport and mixing during planetary roller melt granulation.
Particuology 91, 260-267 (2024)
https://doi.org/10.1016/j.partic.2024.02.010

- Mansuri, A., Vora, P., Feuerbach, T., Winck, J., Vermeer, A. W. P., Hoheisel, W., Kierfeld, J., Thommes, M.
A Monte Carlo simulation of tracer diffusion in amorphous polymers.
Journal of Soft Matter, 20, 6204-6214 (2024)
http://dx.doi.org/10.1039/D4SM00782D

- da Igreja, P., Grenda, T., Bartsch, J., Thommes, M.
Design and Characterization of a Continuous Melt Milling Process Tailoring Submicron Drug Particles.
Processes, 12 (7), (2024)
https://doi.org/10.3390/pr12071417

- Düphans, V., Kimmel, V., Messing, L., Schaldach, G., Thommes, M.
Experimental and numerical characterization of screw elements used in twin-screw extrusion.
Pharmaceutical Development and Technology, 29 (7), 675–683 (2024)
https://doi.org/10.1080/10837450.2024.2378323

- Hoppe, K., Giesa, F., Schaldach, G., Thommes, M., Pieloth, D.
Optimization of filter structures by evolutionary strategies.
Materials Today Communications, 38 (2024)
https://doi.org/10.1016/j.mtcomm.2024.108510

- Mattusch, A. M., Schaldach, G., Bartsch, J., Thommes, M.
Intrinsic dissolution rate modeling for the pharmacopoeia apparatus rotating disk compared to flow channel method.
Pharmaceutical Development and Technology, 29 (4), 281–290 (2024)
https://doi.org/10.1080/10837450.2024.2329115

- Justen, A., Schaldach, G., Thommes, M.
Insights into the Mechanism of Enhanced Dissolution in Solid Crystalline Formulations
Pharmaceutics, 16 (4), (2024)
https://doi.org/10.3390/pharmaceutics16040510

- Kimmel, V., Ercolin, E., Zimmer, R., Yörük, M., Winck, J., Thommes, M.
Measuring and Modeling of Melt Viscosity for Drug Polymer Mixtures.
Pharmaceutics, 16 (3), (2024)
https://doi.org/10.3390/pharmaceutics16030301

- Brands, R., Mathias, C., Bartsch, J., Thommes, M.
Advancing tablet lubrication: A systematic comparison of feed frame lubrication and internal lubrication.
Powder Technology, 434 (2024)
https://doi.org/10.1016/j.powtec.2024.119369

- Justen, A., Weltersbach, A. F., Schaldach, G., Thommes, M.
Design and Characterization of a Melt Electrostatic Precipitator for Advanced Drug Formulations.
Processes, 12 (1), (2024)
https://doi.org/10.3390/pr12010100

2023

- Brands, R., Tebart, N.,Thommes, M.
UV/Vis spectroscopy as an in-line monitoring tool for tablet content uniformity.
Journal of Pharmaceutical and Biomedical Analysis, 236 (2023)
https://doi.org/10.1016/j.jpba.2023.115721

- Mansuri, A., Völkel, M., Mihiranga, D., Feuerbach, T., Winck, J., Vermeer, A. W. P., Hoheisel, W., Thommes, M.
Predicting self-diffusion coefficients in semi-crystalline and amorphous solid dispersions using free volume theory.
European Journal of Pharmaceutics and Biopharmaceutica, 190, 107-120 (2023)
https://doi.org/10.1016/j.ejpb.2023.07.001

- Nesges, D., Lang, T., Birr, T., Thommes, M., Bartsch, J.
Planetary roller melt granulation (PRMG) – A new continuous method for powder processing.
Powder Technology, 427 (2023)
https://doi.org/10.1016/j.powtec.2023.118728

- Lang, T., Bramböck, A., Thommes, M., Bartsch, J.
Material Transport Characteristics in Planetary Roller Melt Granulation.
Pharmaceutics, 15, 8 (2023)
https://doi.org/10.3390/pharmaceutics15082039

- Winck, J., Gottschalk, T., Thommes, M.
Predicting Residence Time and Melt Temperature in Pharmaceutical Hot Melt Extrusion.
Pharmaceutics 15 (5), 1417 (2023)
https://doi.org/10.3390/pharmaceutics15051417

- Klüppelberg, J., Handge, U. A., Thommes, M., Winck, J.
Composition Dependency of the Flory–Huggins Interaction Parameter in Drug–Polymer Phase Behavior.
Pharmaceutics 15, 2650 (2023)
https://doi.org/10.3390/pharmaceutics15122650

- Mansuri, A., Völkel, M., Feuerbach, T., Winck, J., Vermeer, A. W. P., Hoheisel, W., Thommes, M.**Modified Free Volume Theory for Self-Diffusion of Small Molecules in Amorphous Polymers.**
Macromolecules, 56 (8), 3224-3237 (2023)
https://doi.org/10.1021/acs.macromol.2c02451

- Mansuri, A., Münzner, P., Heermant, A., Hänsch, S., Feuerbach, T., Fischer, B., Winck, J., Vermeer, A. W.P., Hoheisel, W., Böhmer, R., Gainaru, C., Thommes, M.
Characterizing Phase Separation of Amorphous Solid Dispersions Containing Imidacloprid.
Molecular Pharmaceutics, 20 (4), 2080-2093 (2023)
https://doi.org/10.1021/acs.molpharmaceut.2c01043

- Mansuri, A., Münzner, Ph., Heermant, A., Patzina, F., Feuerbach, T., Winck, J., Vermeer, A. W. P., Hoheisel, W., Böhmer, R., Gainaru, C., Thommes, M.
Molecular Dynamics and Diffusion in Amorphous Solid Dispersions Containing Imidacloprid.
Molecular Pharmaceutics, 20 (4), 2067-2079 (2023)
https://doi.org/10.1021/acs.molpharmaceut.2c01042

- Justen, A., Kurth, C., Schaldach, G., Thommes, M.
Preparation of Micron and Submicron Particles via Spray Drying and Electrostatic Precipitation.
Chemical Engineering and Technology, 46 (2), 343–349 (2023)
https://doi.org/10.1002/ceat.202200357

- Zimmermann, M., Michel, F.; Bartsch, J., Thommes, M.
A novel approach of external lubrication in a rotary tablet press using electrostatics.
Drug Development and Industrial Pharmacy, 48, 737-744 (2023)
https://doi.org/10.1080/03639045.2023.2165662

- Pieloth, D., Rodeck, M., Schaldach, G., Thommes, M.
Categorization of Sprays by Image Analysis with Convolutional Neuronal Networks.
Chemical Engineering Technology, 46 (2), 264-269 (2023)
https://doi.org/10.1002/ceat.202200356

- Hoppe, K., Wischemann, L., Schaldach, G., Zielke, R., Tillmann, W., Thommes, M., Pieloth, D.
Filtration Kinetrics of Depth Filters-Modeling and Comparison with Tomographic Data of Particle Depositions.
Atmosphere, 14 (4), 640 (2023)
https://doi.org/10.3390/atmos14040640

- Lauscher, C., Licau, A., Schaldach, G., Thommes, M.
Characterization of Sprays Generated by the Expansion of Emulsions with Liquid Carbon Dioxide
Chemical Engineering and Technology online (2023); 47 (2), 262-267 (2024)
https://doi.org/10.1002/ceat.202300261

Fluid Separations (FVT)

Co-Oriented Fluid Functional Equation for Electrostatic interactions (COFFEE).

Julia Amplatz, Joshua Marx, Kai Langenbach

Equation of States (EoS) are an established method in industry to predict the phase behavior of mixtures. The prediction of mixtures of polar and nonpolar components is still challenging for classic EoS, since they do not consider the orientation of the molecules. The Co-Orientated Fluid Functional Equation for Electrostatic interactions (COFFEE) is an EoS, that explicitly considers the orientation of the molecules in terms of an Orientation Distribution Function (ODF). In mixtures of differently polar components, the molecules compete for the energetically more favorable spots. This leads to so-called multi-body repulsive effects that need to be considered in COFFEE.

In the perturbation theory, COFFEE, the perturbation free energy is split into a near field and a far field free energy. The structural effects due to preferential orientations of polar molecules are considered in the near field free energy, which is a functional of the ODF. The ODF depends on three angles between two dipolar molecules, as shown in Figure 1, and enables the calculation of the probability of specific orientation. The dipole moment in Figure 1 is depicted in center of mass of the molecules, but it can be also shifted out of the center of mass.

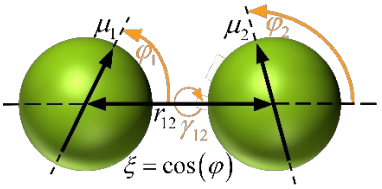

Figure 1. Vectors and angles between two dipolar molecules.

In Figure 2, a three-dimensional plot of the ODF is shown. The colors are iso-surfaces for probabilities equal to (green), 40% higher (red), and 40% lower (blue) than the value corresponding to random orientation. The surface areas represent the result of molecular dynamic (MD) simulations and the gridlines represent the result of COFFEE. In a binary mixture, four ODF exist due to the different consideration as central and neighboring molecule.

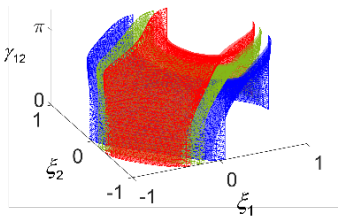

Figure 2. Orientation Distribution Function (ODF). Surface area: MD simulation, gridlines: COFFEE, green: random orientation (100%), red (140%), blue (60%).

A reduced, one-dimensional form of the ODF is the angular distribution function (ADF). In mixtures with differently polar components, the molecules compete for the energetically more favorable spots. The molecules with the higher dipole moment get the more favorable places due to their higher electrostatic interactions, while the molecules with the lower dipole moment are displaced to the energetically less favorable spots. This effect is called multi-body repulsive effects (MBRE) and leads to a qualitatively wrong result in the ADF, if the molecule with the lower dipole moment is considered as the neighboring molecule. Even without MBRE, COFFEE is shown to be better to predict mixtures of differently polar components than common EoS.

To consider MBRE in COFFEE, a repulsive van der Waals free energy functional can be added in the perturbation theory. A local and non-local density approach are tested within the theory. Both approaches achieve qualitatively correct results. The result of an ADF of a Lennard-Jones (LJ) Stockmayer (LJ + dipole moment) mixture with the local density approach is shown in Figure 3 compared to molecular simulation results. The LJ molecule is considered as neighboring molecule, which leads to strong MBRE. Since LJ molecules have no dipole moment, COFFEE without MBRE predicts their preferential orientation is the same at every point. However, since the LJ molecules are displaced to energetically less favorable places for the Stockmayer molecule, the ADF takes on the shape shown, which can be accurately predicted using the extended version of COFFEE. With the new COFFEE version, it becomes possible for the first time to consider preferential orientations in an EoS in polar-nonpolar mixtures.

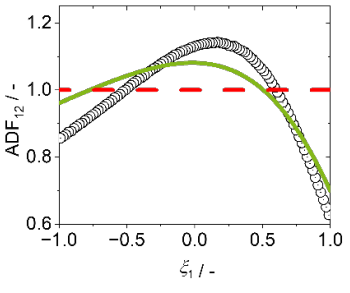

Figure 3. Angular Distribution Function (ADF). $\mu_1^* = 2$, $\mu_2^* = 0$, $\rho^* = 0.66$, $T^* = 1.9$; $x_1 = 0.9$, $d_1 = 0.1$; circles: MD simulation, red dashes line: COFFEE without MBRE, green line: COFFEE with MBRE.

julia.amplatz@tu-dortmund.de
kai.langenbach@tu-dortmund.de

Publications:
J. Marx, K. Langenbach, Co-Oriented Fluid Functional Equation for Electrostatic interactions (COFFEE) for Mixtures: Phase Equilibria, Fluid Phase Equilibria 597 (2025) 114453. https://doi.org/10.1016/j.fluid.2025.114453.

2025

Peer-reviewed Journal Articles

- Marx, J., Langenbach, K.,
Co-Oriented Fluid Functional Equation for Electrostatic interactions (COFFEE) for Mixtures: Phase Equilibria.
Fluid Phase Equilibria, 597, 114453 (2025)
https://doi.org/10.1016/j.fluid.2025.114453

2024

Peer-reviewed Journal Articles

- Maidl, P., Langenbach, K., & Frank, F.
Achieving Convergence in Multiphase Multicomponent Density Gradient Theory Calculations through Regularization.
Industrial & Engineering Chemistry Research, 63 (32), 14367-14380 (2024)
https://doi.org/10.1021/acs.iecr.4c01669

- Marx, J., Langenbach, K., & Kohns, M.
Assessment of Approaches towards the Relative Permittivity of Mixtures.
Journal of Chemical & Engineering Data, 69 (10), 3265-3274 (2024)
https://doi.org/10.1021/acs.jced.3c00765

- Großmann, O., Stephan, S., Langenbach, K., & Hasse, H.
Vapor-liquid interfacial properties of binary mixtures from molecular simulation and density gradient theory.
AIChE Journal, 70(10), e18503 (2024)
https://doi.org/10.1002/aic.18503

2023

Peer Reviewed Journal Articles

- Schaefer, D., Stephan, S., Langenbach, K., Horsch, M. T., & Hasse, H.
Mass transfer through vapor–liquid interfaces studied by non-stationary molecular dynamics simulations.
The Journal of Physical Chemistry B, 127 (11), 2521-2533 (2023)
https://doi.org/10.1021/acs.jpcb.2c08752

- Mühlegger, E., & Langenbach, K.
Investigation of the density dependence of the influence parameter.
International Journal of Thermophysics, 44 (12), 173 (2023)
https://doi.org/10.1007/s10765-023-03281-4

- Marx, J., Kohns, M., & Langenbach, K.
Vapor-liquid equilibria of binary mixtures containing Stockmayer-type model fluids from Monte-Carlo simulations.
Fluid Phase Equilibria, 568, 113742 (2023)
https://doi.org/10.1016/j.fluid.2023.113742

- Marx, J., Kohns, M., & Langenbach, K.
Co-Oriented Fluid Functional Equation for Electrostatic interactions (COFFEE) for Mixtures: Molecular Orientations.
Journal of Chemical & Engineering Data, 69 (2), 400-413 (2023)
https://doi.org/10.1021/acs.jced.3c00328

- Hasse, H., Horsch, M. T., Kopnarski, M., Langenbach, K., Müller, R., Stephan, S., & Urbassek, H. M.
Adsorption and Wetting of Component Surfaces
In Component Surfaces: Manufacturing-Morphology-Property Relationships.
Cham: Springer International Publishing (pp. 203-229) (2023)
https://doi.org/10.1007/978-3-031-35575-2_9

Process Automation Systems (PAS)

Strategic Network Design for the Chemical Recycling of Polyurethane Rigid Foam Waste in Germany.

A MILP-Based Optimization Framework to Assess Economic Viability and Optimal System Layout.

Dalga Merve Özkan, Sergio Lucia, Sebastian Engell

Transitioning to a circular economy is essential for sustainable resource management, yet many industries face significant technical and economic barriers. This is particularly true for the plastics sector, where thermoset materials such as polyurethane (PUR) rigid foams are still predominantly incinerated. While chemical recycling technologies for PUR have advanced, their large-scale deployment requires careful planning of the entire reverse supply chain. Here, we present an optimization framework that supports such planning, helping to identify economically viable pathways for the chemical recycling of PUR rigid foam waste.

A multi-product, multi-echelon, multi-period mixed-integer linear programming (MILP) model was developed to design a reverse supply chain network that maximizes annual gross profit. The framework determines the optimal number, locations, and capacities of collection, recovery, chemical and downstream processing facilities, as well as the material flows between them. Two waste sources are considered: end-of-life (EoL) construction materials and EoL cooling appliances. The applicability of the framework is demonstrated through a case study on PUR waste management in Germany, comparing catalytic pyrolysis with conventional incineration.

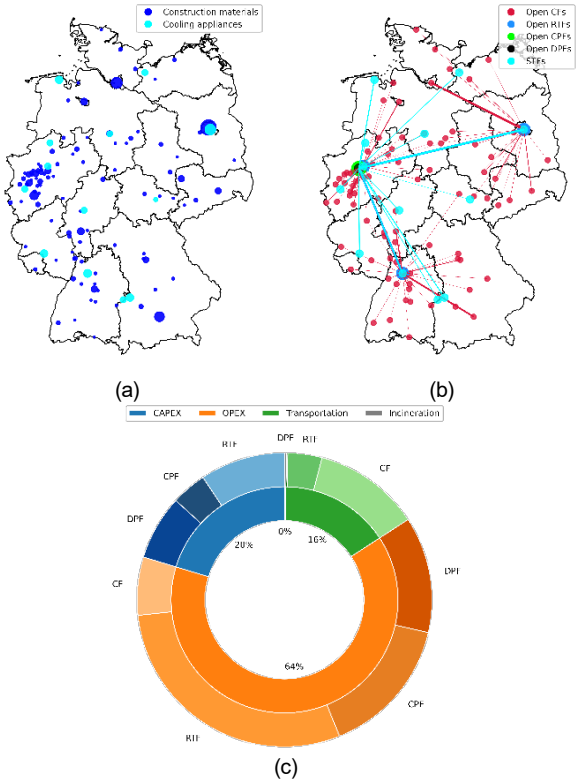

Figure 1. (a) Geographical distribution of PUR rigid foam waste in Germany, with marker size indicating the relative amount of waste at each point source. (b) Optimal material flows for the layout in which both PUR and PIR are chemically recycled, from collection facilities to recovery and treatment facilities (red), from there to the chemical processing facility (blue), and from the second treatment facilities to the chemical processing facility (cyan). (c) Total annual cost breakdown for the same layout, decomposed into capital, operating, transportation and incineration costs, and split by facility type.

In the baseline scenario, where only PUR is chemically recycled, the system shows a negative annual profit, by an amount equivalent to 29% of the annual revenue. The optimal layout features a decentralized network of collection facilities placed near the waste sources, while capital-intensive recovery, chemical and downstream processing facilities are centralized to benefit from economies of scale (Figure 1). When polyisocyanurate (PIR) waste is also redirected to chemical recycling, the collection rate of construction-derived waste rises from 65% to 99% and the net loss drops to only 5.4% of the annual revenue, highlighting the strong value-adding potential of co-processing PIR alongside PUR.

A sensitivity analysis was carried out to test the robustness of the system under changing market conditions and policy parameters. Catalytic pyrolysis consistently outperforms incineration in both scenarios across the explored range of product prices and gate fees. Incineration is only preferred in two narrow cases: when product prices fall below 60% of their current value in either scenario, or, when the gate fee for incineration is reduced to 60% of its current value in the baseline scenario. The PIR-inclusive scenario remains robust against such gate-fee reductions, with waste being directed to incineration only in remote areas where collection costs would outweigh the recycling benefits. The break-even point lies at a price increase of about 50% when only PUR is recycled, but drops to roughly 10% once PIR is included, bringing the system within reach of current market conditions.

The framework provides strategic insights into the economic and logistical trade-offs of plastic waste recycling, and can serve as a decision-support tool for policy-makers and industry stakeholders aiming to establish sustainable waste valorization networks for thermoset plastics.

merve.oezkan@tu-dortmund.de
sergio.lucia@tu-dortmund.de
sebastian.engell@tu-dortmund.de

Publications:
Özkan, D.M.; Lucia, S.; Engell, S., Strategic network design for the chemical recycling of polyurethane rigid foam waste in Germany. Computers and Chemical Engineering 202 (2025) 109273. https://doi.org/10.1016/j.compchemeng.2025.109273

2025

Peer Reviewed Journal Articles

- M Heinlein, S Subramanian, S Lucia
  Robust model predictive control exploiting monotonicity properties.
  IEEE Transactions on Automatic Control, Volume 70, 6260 -6267, 2025
  https://doi.org/10.1109/TAC.2025.3558137

- CR Johnson, S de Vries, K Wohlgemuth, S Lucia
  Multi-stage model predictive control for slug flow crystallizers using uncertainty-aware surrogate models.
  Computers & Chemical Engineering, 109456, 2025
  https://doi.org/10.1016/j.compchemeng.2025.109456

- DM Özkan, S Lucia, S Engell
  Strategic network design for the chemical recycling of polyurethane rigid foam waste in Germany.
  Computers & Chemical Engineering, Volume 202, 109273, 2025
  https://doi.org/10.1016/j.compchemeng.2025.109273

- JJ Rico, A Dernbecher, JM de la Rosa, L Hilfert, H Almuina-Villar, N Kulak, S Lucia, A. Dieguez-Alonso
  Investigation on the impact of potassium and mild transport limitations on the pyrolysis behavior of beech wood and its macrocomponents.
  Journal of Analytical and Applied Pyrolysis, Volume 192, 107201, 2025
  https://doi.org/10.1016/j.jaap.2025.107201

2024

Peer Reviewed Journal Articles

- T Faulwasser, EC Kerrigan, F Logist, S Lucia, M Mönnigmann, A Parisio
  Teaching Model Predictive Control: What, When, Where, Why, Who, and How?
  IEEE Control Systems Magazine 44 (4), 47-65, 2024
  https://doi.org/10.1109/MCS.2024.3402908

- J Adamek, M Heinlein, L Lüken, S Lucia
  Deterministic safety guarantees for learning-based control of monotone nonlinear systems under uncertainty.
  IEEE Control Systems Letters 8, 1030-1035, 2024
  https://doi.org/10.1109/LCSYS.2024.3407635

- F Messerer, K Baumgärtner, S Lucia, M Diehl
  Fourth-order suboptimality of nominal model predictive control in the presence of uncertainty
  IEEE Control Systems Letters 8, 508-2013, 2024
  https://doi.org/10.1109/LCSYS.2024.3396611

2023

Peer Reviewed Journal Articles

- Fiedler, F.; Lucia.S.
  Improved uncertainty quantification for neural networks with Bayesian last layer.
  IEEE Access, Volume 11, 123149, 2023
  https://doi.org/10.1109/ACCESS.2023.3329685

- JW Kim, N Krausch, J Aizpuru, T Barz, S Lucia, P Neubauer, MNC Bournazou
  Model predictive control and moving horizon estimation for adaptive optimal bolus feeding in high-throughput cultivation of E. coli.
  Computers & Chemical Engineering Volume 172, 108158 2023 https://doi.org/10.1016/j.compchemeng.2023.108158

- AD Carnerero, DR Ramirez, S Lucia, T Alamo
  Prediction regions based on dissimilarity functions
  ISA transactions, Volume 139, 49-59 (2023)
  https://doi.org/10.1016/j.isatra.2023.03.048

- A Castelletti, A Ficchì, A Cominola, P Segovia, M Giuliani, W Wu, S Lucia, C Ocampo-Martinez, B De Schutter, JM Maestre
  Model Predictive Control of water resources systems: A review and research agenda
  Annual Reviews in Control, Volume 55, 442-465 (2023)
  https://doi.org/10.1016/j.arcontrol.2023.03.013

- F Fiedler, B Karg, L Lüken, D Brandner, M Heinlein, F Brabender, S Lucia
  do-mpc: Towards FAIR nonlinear and robust model predictive control
  Control Engineering Practice Volume 140, 105676 (2023)
  https://doi.org/10.1016/j.conengprac.2023.105676

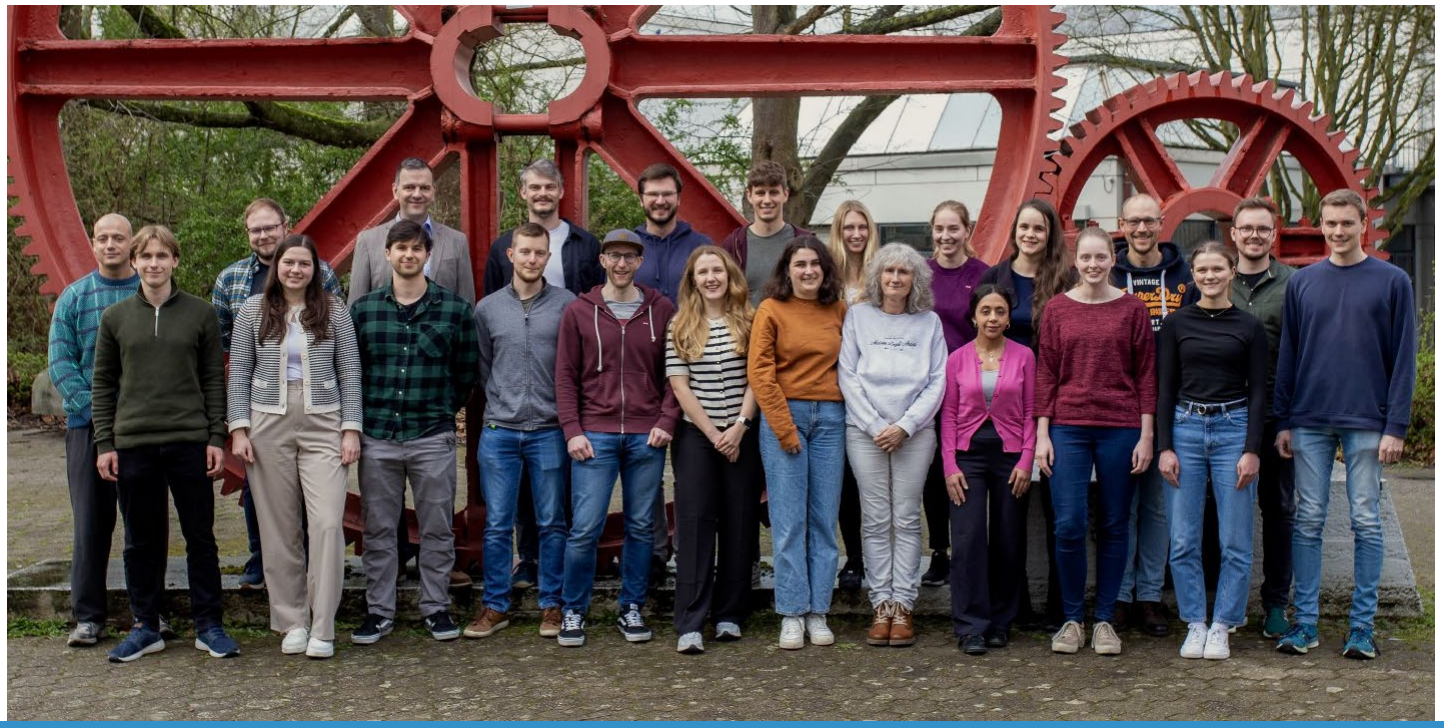

Reaction Engineering and Catalysis (REC)

Combined Deactivation and Reaction Kinetics for CO_2 Methanation.

A Holistic Kinetic Model for Catalyst Lifetime Prediction under Dynamic Conditions.

Mathias Waldner, Moritz Langer, Hannsjörg Freund

Power-to-X technologies like CO_2 methanation play a crucial role in the energy transition by converting green hydrogen into synthetic natural gas. However, catalyst deactivation under dynamic operation conditions poses significant challenges for process design and economic viability. A holistic mathematical description of both deactivation and reaction kinetics enables optimization of reactor design and operation over the entire catalyst lifetime - yet such models remain scarce in literature.

In this work, we systematically investigated the deactivation behavior of an industrial Ni/Al_2O_3 catalyst for CO_2 methanation across a broad range of operating conditions (350 - 450 °C, 3 - 8 bar) using a Berty-type reactor. This reactor type ensures gradient-less reaction conditions, making it ideally suited for deactivation studies. The experiments consist of a deactivation period at constant temperature and pressure and a kinetic period, conducting a temperature variation (cf. Figure 1).

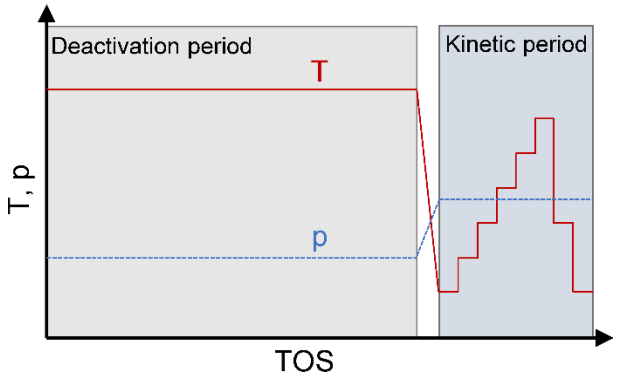

Figure 1. The deactivation experiments consist of a deactivation period at constant total pressure and temperature, and a kinetic period. During the kinetic period, temperature is varied to obtain information on temperature dependency.

From the kinetic measurements and additional post-mortem catalyst characterization (physisorption, chemisorption, TGA), we identified two distinct deactivation mechanisms: 1) Hydrothermal sintering: loss of active nickel surface through sintering of the carrier and/or nickel nanoparticles, accelerated by water presence at elevated temperatures. 2) CO-induced restructuring: structural changes of nickel nanoparticles at elevated CO partial pressures, likely through formation of mobile nickel (sub)carbonyl species. Importantly, we found that the reverse water-gas shift (RWGS) reaction exhibits non-separable kinetics. Its activation energy changes from 148 kJ mol^{-1} for a fresh catalyst to 83 kJ mol^{-1} for a deactivated catalyst. In contrast, CO methanation shows separable kinetics with constant activation energy throughout deactivation.

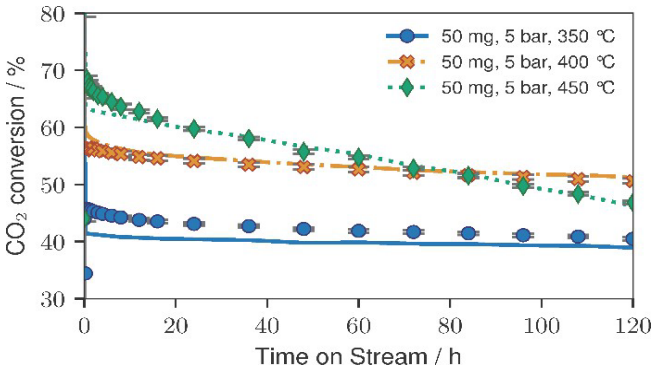

Figure 2. Observed and predicted CO_2 conversion over time on stream during deactivation. Experiments are conducted at temperatures of 350, 400, and 450 °C using 50 mg of catalyst at 5 bar reaction pressure (GHSV = 8 mL_{STP} min^{-1} mg_{cat}^{-1}, feed composition: H_2:CO_2 = 4:1 in 50% N_2).

Based on this insight, we developed a combined deactivation and reaction kinetic model using general power-law approaches including composition influence terms. The model incorporates our previously published quasi-steady-state reaction kinetics and is extended by two additional variables, each describing one of the two deactivation mechanisms. The complex time course of these variables is described by 15 only weakly correlated parameters. The model accurately predicts both evolution of the reaction rates (cf. Figure 2) over time as well as the kinetics of the deactivated catalysts.

The model enables prediction of reactor behavior under various conditions - from low to high conversions and therefore different compositions. This capability is particularly valuable for designing load-flexible Power-to-X reactors, accommodating fluctuating hydrogen supply from renewable sources, which can lead to potentially deactivating conditions. By integrating catalyst lifetime considerations into reactor simulations, the model paves the way for economic optimization of process design and operation strategies that minimize deactivation while maintaining high productivity.

mathias.waldner@tu-dortmund.de
hannsjoerg.freund@tu-dortmund.de

Publications:
Langer, M.; Waldner, M.; Freund, H., Modeling of the combined deactivation and reaction kinetic behavior of an impregnated Ni/Al_2O_3 catalyst in the CO_2 methanation reaction. Chemical Engineering Journal 2025.
https://doi.org/10.1016/j.cej.2025.169363

Process Intensification in Falling Film Reactors.

How Structure-Induced Resonance Waves Intensify Mass Transfer in CO_2 Capture Applications

Marion Börnhorst

(In cooperation with Andrea Düll, Thomas Häber, Olaf Deutschmann, Karlsruher Institut für Technologie)

Efficient solvent utilization is critical in energy-intensive processes such as solvent-based carbon capture, where regeneration costs dominate operational expenses. Falling film absorbers offer advantages including thin liquid layers, large interfacial areas, and low pressure drop, making them attractive for CO_2 capture applications. Surface structuring has emerged as a promising process intensification strategy, yet the fundamental mechanisms linking hydrodynamics and mass transfer enhancement remain poorly understood.

This work investigates how rectangular surface corrugations intensify liquid-side mass transfer in falling film CO_2 absorbers through structure-induced wave resonance effects. Using combined experimental and numerical approaches, we demonstrate that carefully tailored surface structures can increase the volumetric mass transfer coefficient by up to a factor of four compared to smooth reference surfaces.

High-speed imaging with an internally referenced light absorption technique reveals that transient film instabilities evolve from initially steady flow (Fig. 1), with inertia-controlled liquid overshoot at structure element edges playing a crucial role in flow destabilization. The developed flow can be decomposed into steady and time-oscillatory contributions exhibiting distinct spatial characteristics.

CO_2 absorption experiments across varying structure dimensions and Reynolds numbers demonstrate that an optimum exists where resonance-like conditions maximize interfacial oscillations and mass transfer enhancement. The observed structure-induced mass transfer intensification correlates directly with film waviness, quantified through standard deviation of local film thickness measurements.

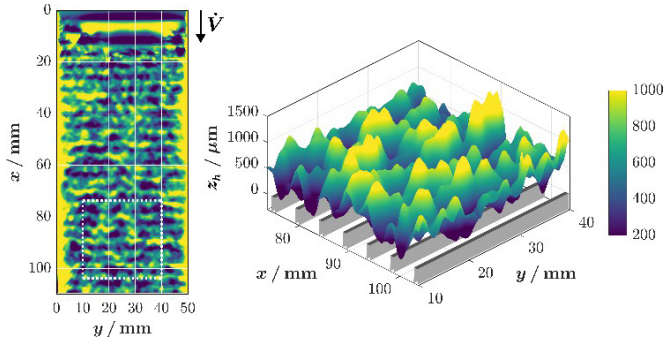

Figure 1. Experimentally determined spatial distribution of the interface elevation over the entire measurement domain (left) and in a zoomed-in region of interest (right) for a film flow with Re = 382 and rectangular structures of dimensions D_s = 4 mm and H_s = 0.45 mm.

Complementary volume-of-fluid simulations including species transport provide mechanistic insights: while structure-induced interfacial area increases contribute marginally, enhanced internal mixing dominates mass transfer intensification. Convective mixing patterns in steep wave humps transport CO_2-saturated liquid from the interface toward less saturated bulk regions (Fig. 2).

The highly dynamic interface reconfiguration, combined with interplay between large-scale and small-scale mixing patterns, continuously disrupts the concentration boundary layer, enabling substantially larger liquid phase fractions to participate in absorption. However, tracer simulations reveal broadened residence time distributions, indicating potential limitations where short contact times are required.

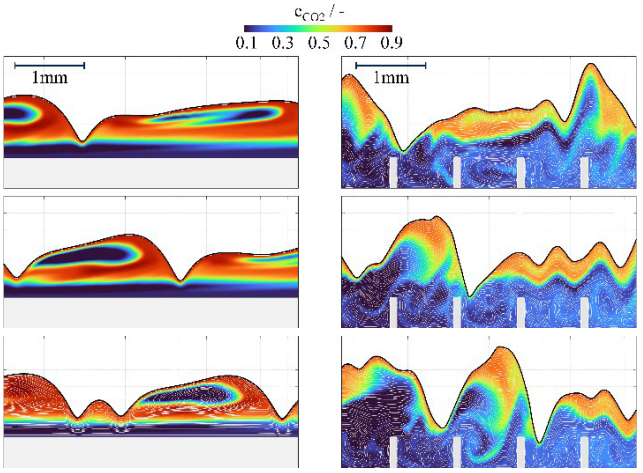

Figure 2. Spatial CO_2 concentration distribution reveals distinct transport mechanisms. Left: Solitary waves on smooth surfaces transport CO_2 in isolated clusters. Right: Structured surfaces (D_s = 4 mm, H_s = 0.45 mm) generate convective mixing zones that transport saturated liquid toward bulk while wave humps continuously merge, disrupting the concentration boundary layer. Re = 342.

These findings establish fundamental understanding of structure-induced resonance wave effects in falling film reactors, providing design guidelines for surface structure optimization, e.g., in CO_2 capture and related mass transfer applications. The approach demonstrates significant potential for process intensification through passive flow manipulation without requiring external energy input.

marion.boernhorst@tu-dortmund.de

Publications:
Düll, A.; Happ, A.; Buchmüller, J.; Ates, C.; Börnhorst, M.; Häber, T.; Deutschmann, O., How structure-induced resonance waves intensify mass transfer in a falling film absorber for CO_2 capture. Chemical Engineering Journal 2025. https://doi.org/10.1016/j.cej.2025.168228
Düll, A.; Lehmann, J.; Börnhorst, M.; Ates, C.; Häber, T.; Deutschmann, O., Spatio-temporal characterization of the three-dimensional wave dynamics in falling film flows over rectangular corrugations. Experiments in Fluids 2025. https://doi.org/10.1007/s00348-025-03978-2

2025

Peer Reviewed Journal Articles

- Sofialidis, D., Mutyal, J.; Faltsi, R., Braun, M.; Börnhorst, M., Esch, T.
Efficient Modeling of SCR Urea Deposits Formation Using ANSYS Fluent.
SAE Technical Paper, 2025-01-8485 (2025)
https://doi.org/10.4271/2025-01-8485

- Düll, A., Lehmann, J., Börnhorst, M., Ateş, C., Häber, T., Deutschmann, O.
Spatio-temporal characterization of the three-dimensional wave dynamics in falling film flows over rectangular corrugations.
Experiments in Fluids, 66, 71 (2025)
https://doi.org/10.1007/s00348-025-03978-2

- Warnecke, F., Lin, L., Haag S., Freund, H.
Mechanistic Investigations and Kinetic Modeling of Hydrogen Transfer Reactions in Olefin Cracking Processes over H-ZSM-5.
Industrial & Engineering Chemistry Research, 64 (12), 6321-6340 (2025)
https://doi.org/10.1021/acs.iecr.4c04140

- Düll, A., Happ, A., Buchmüller, J., Ateş, C., Börnhorst, M., Häber, T., Deutschmann, O.
How structure-induced resonance waves intensify mass transfer in a falling film absorber for CO2 capture.
Chemical Engineering Journal, 523, 168228 (2025)
https://doi.org/10.1016/j.cej.2025.168228

- Langer, M., Waldner, M., Freund, H.
Modeling of the combined deactivation and reaction kinetic behavior of an impregnated Ni/Al2O3 catalyst in the CO2 methanation reaction.
Chemical Engineering Journal, 524, 169363 (2025)
https://doi.org/10.1016/j.cej.2025.169363

Essays

- Kurig, N., Kreitz, B.; Moioli, E., Börnhorst, M., Friedland, J.
NaWuReT Colloquium: Veni, Vidi, Vici? Visionary Leaders in Chemical Reaction Engineering.
Chemie Ingenieur Technik, 97 (5), 374–377 (2025)
https://doi.org/10.1002/cite.202500029

Editorials

- Freund, H., Sauer, J., Ehrhardt, K.
Elektrifizierung der chemischen Industrie: Eine spannende Herausforderung entlang Skalen und Prozessketten.
Chemie Ingenieur Technik, 97 (5), 363 (2025)
https://doi.org/10.1002/cite.202500048

2024

Peer Reviewed Journal Articles

- Ferroni, C.; Bracconi, M.; Ambrosetti, M.; Groppi, G.; Maestri, M.; Freund, H.; Tronconi, E.
Process Intensification in Mass-Transfer Limited Catalytic Reactors Through Anisotropic Periodic Open Cellular Structures.
Chem. Eng. Process. 195, 109613 (2024)
https://doi.org/10.1016/j.cej.2023.109613

- Trunk, S.; Freund, H.
Detailed numerical investigations of the in operando adjustable flow field in a diamond unit cell-based interpenetrating periodic open cellular structure (interPOCS).
Chemical Engineering & Processing: Process Intensification 195, 109617 (2024)
https://doi.org/10.1016/j.cep.2023.109617

- Held, H.; Freund, H.
Identification of Mass Transfer Limitations by Kinetic Modelling of a Technical-Scale Trickle Bed Reactor for the Hydrogenation of Viscous Aromatics.
Industrial & Engineering Chemistry Research, 63(1), 147-162 (2024)
https://doi.org/10.1021/acs.iecr.3c03273

- Sadeghi, M.; Brix, A.; Trunk, S.; Pesch, G.; Freund, H.; Thöming, J.
Complementary Mass Transport Investigations in Open-Cell Foams: Full-Field Computational Fluid Dynamics Simulation with Random-Walk Microscopic Particle Tracking and Methane Nuclear Magnetic Resonance Displacement Measurements.
Transport in Porous Media, 151:645-664 (2024)
https://doi.org/10.1007/s11242-023-02045-w

- Eckendörfer, L.; Rudolf, D.; Brix, A.; Börnhorst, M.; Freund, H.
Periodic Open Cellular Structures in Chemical Engineering: Application in Catalysis and Separation Processes.
Annu. Rev. Chem. Biomol. Eng., 15:163-86 (2024)
https://doi.org/10.1146/annurev-chembioeng-101121-085630

- Busse, C.; Freund, H.; Schwieger, W.
Periodic open cellular structures (POCS) as catalyst support for intensified heat transport in the partial oxidation of methanol to formaldehyde.
Chemical Engineering Journal, 489, 151139 (2024)
https://doi.org/10.1016/j.cej.2024.151139

- Langer, M.; Freund, H.
Reaction Kinetic Modeling of the Cox Methanation over a Broad Range of Operation Conditions on an Impregnated Ni/Al2O3 Catalyst.
Ind. Eng. Chem. Res., 63, 10981-10996 (2024)
https://doi.org/10.1021/acs.iecr.4c00819

- Düll, A.; Cros-Le Lagadec, A.; Buchmüller, J.; Häber, T.; Ates, C.; Börnhorst, M.
Intensifying interfacial oscillations in falling film flows over rectangular corrugations.
Physics of Fluids, 36, 092107 (2024)
https://doi.org/10.1063/5.0222760

- Held, H.; Freund, H.
Conceptual study on the intensification of gas-liquid mass transfer in trickle bed reactors by the application of strut-based and novel sheet-based periodic open cellular structures (POCS).
Chemical Engineering & Processing: Process Intensification 204, 109930, (2024)
https://doi.org/10.1016/j.cep.109930

- Rudolf, D.; Fink, A; Körner, C.; Freund, H.
Thermo-Mechanical Study on Auxetic Shape Memory Periodic Cellular Structures – Part I: Characterization of Reentrant Geometry and Effective Heat Conductivity.
Advanced Engineering Materials, 26, 2401717 (2024)
https://doi.org/10.1002/adem.202401717

- Fink, A; Rudolf, D.; Wahlmann, B.; Freund, H.; Körner, C.
Thermo-Mechanical Study on Auxetic Shape Memory Periodic Cellular Structures – Part II: Mechanical and Shape Memory Properties.
Advanced Engineering Materials, 26, 2401310 (2024)
https://doi.org/10.1002/adem.202401310

Essays

- Kreitz, B.; Börnhorst, M.; Friedland, J.; Moioli, E.
NaWuReT Colloquium: Career Pathways and Oppertunities for Reaction Engineers in Industry.
Chemie Ingenieur Technik, 00, No. 0, 1-5 (2024)
https://doi.org/10.1002/cite.202300182

Books & Book chapters

- Emig, G.; Klemm, E.; Freund, H.
Chemische Reaktionstechnik
Springer, Berlin 7.Auflage (2024)
https://doi.org/10.1007/978-3-662-68826-7

2023

Peer Reviewed Journal Articles

- Schumacher, O.; Ates, C; Börnhorst, M.; Koch, R.; Stephan, P.
Deposit formation from evaporating urea-water droplets on substrates of different wettability.
Journal of Colloid and Interface Science, 634, 1-13 (2023)
https://doi.org/10.1016/j.jcis.2022.12.021

- Engl, T.; Langer, M.; Freund, H.; Rubin, M.; Dittmeyer, R.
Tap Reactor for Temporally and Spatially Resolved Analysis of the CO2 Methanation Reaction.
Chem.-Ing.-Tech. 95(5), 658-667 (2023)
https://doi.org/10.1002/cite.202200204

- Langer, M.; Kellermann, D.; Freund, H.
Kinetic modeling of dynamically operated heterogeneously catalyzed reactions: Microkinetic model reduction and semi-mechanistisc approach on the example of the CO2 methanation.
Chemical Engineering Journal 467, 143217 (2023)
https://doi.org/10.1016/j.cej.2023.143217

Essays

- Naliwajko, P.; Friedland, J.; Börnhorst, M.
NaWuReT and YounGeCatS Joint Summer School – Shaping a Green Future by Reaction Engineering and Catalysis.
ChemCatChem, e202201548 (2023)
https://doi.org/10.1002/cctc.202201548

Editorials

- Freund, H.; Sauer, J.; Wachsen, O.
„Digitalisierung der Reaktionstechnik“: Ein Themenfeld mit vielen Facetten!
Editorial, Chem.-Ing.-Tech. 95(5), 619 (2023)
https://doi.org/10.1002/cite.202370502

Technical Biochemistry (TB)

Sweetening the Deal: Boosting Cannabinoid Bioavailability through Yeast-Based Glycosylation.

Enzymatic glycosylation of phytocannabinoids utilizing a bioengineered Saccharomyces cerevisiae expression platform.

Christina Schmidt, Astrid Maria Imann, Nikolay Vasilev, Oliver Kayser

Phytocannabinoids like cannabidiol (CBD) and Δ⁹-tetrahydrocannabinol (THC) hold immense pharmaceutical promise, yet the clinical application of these terpenophenolic compounds is frequently hampered by high lipophilicity, which severely limits their bioavailability in the human body. Glycosylation, the enzymatic attachment of sugar moieties, offers a solution by dramatically increasing the water solubility and stability of these molecules, potentially transforming them into more effective prodrugs.

In this study, the group explored the potential of the UDP-glycosyltransferase CrUGT74AN3 from the Madagascar periwinkle (*Catharanthus roseus*). The researchers demonstrated that this enzyme is a versatile biocatalyst, and in its extracted and purified form successfully glycosylates 12 different cannabinoids and two biosynthetic intermediates (Fig. 1). The highest activity was observed with CBD, achieving a remarkable 97% conversion rate and while neutral forms like CBD and cannabigerol (CBG) were easily converted, the enzyme struggled with acidic precursors (e.g., cannabigerolic acid), suggesting that an additional carboxyl group hinders proper binding in the catalytic pocket of the enzyme.

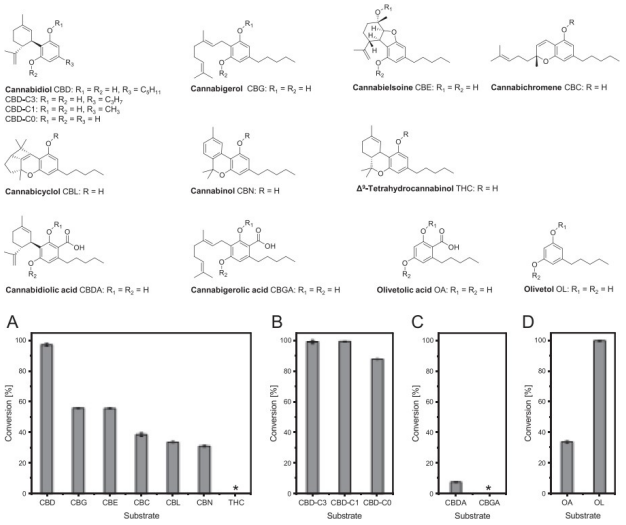

Figure 1. Conversion of different cannabinoids and cannabinoid biosynthesis intermediates by CrUGT74AN3. (A) Cannabinoids, (B) Cannabidiol derivatives with decreasing alkyl chain length, (C) Acidic cannabinoids CBDA and CBGA, (D) Cannabinoid biosynthesis intermediates OA and OL.

The team moved beyond in vitro enzyme assays to develop a whole-cell biotransformation platform using bioengineered *Saccharomyces cerevisiae*. By identifying and overcoming metabolic bottlenecks, significant production milestones were achieved. The study identified the supply of UDP-glucose as the primary limiting factor for in vivo production. This was shown by producing the heterologous strain yGLY13 expressing CrUGT74AN3 with additional modifications, including overexpression of internal UDP-glucose biosynthesis genes (PGM2 and UGP1) and knocking out endogenous glucosidases (EXG1, SPR1, and EGH1). The results showed an overall increase in internal UDP-glucose concentration, a 1.3-fold increase in CBD-diglycoside production, and complete conversion of CBD to glycosylated moieties within 24 hours (Fig. 2).

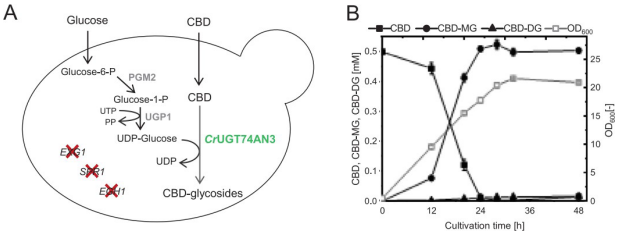

Figure 2. Biotransformation of CBD to CBD-monoglycoside (CBD-MG) and CBD-diglycoside (CBD-DG) using *S. cerevisiae* cells expressing CrUGT74AN3. (A) Schematic overview of the bioengineered yGLY13 strain. (B) Biotransformation experiment using strain yGLY13.

Perhaps the most striking breakthrough of this study was the co-expression of CrUGT74AN3 with a cyclodextrin glycosyltransferase (BICGTase) from *Bacillus licheniformis.* This "tag-team" approach allowed the yeast to build extended sugar chains, producing CBD-glycosides with up to six glucose moieties. This significantly increases the potential for tailored solubility and the development of targeted drug delivery systems.

These findings provide a robust foundation for the industrial-scale production of bioavailable, water-soluble cannabinoids. Future research will focus on selective production strategies and further enzyme engineering to optimize these microscopic factories for a broader range of pharmaceutical aglycones.

christina2.schmidt@tu-dortmund.de
oliver.kayser@tu-dortmund.de

Publications:
Schmidt, C., Imann, A.M., Vasilev, N., Kayser, O. Approaches for cannabinoid glycosylation catalyzed by CrUGT74AN3 and BICGTase. Biotechnology Journal, Volume 20, 5 (2025) https://doi.org/10.1002/biot.70007

2025

Peer Reviewed Journal Articles

- Schäfer, K.J., Chalwatzis, L., Feka, A.M., Aras, M., Boles, E., Kayser, O.
Biochemical and metabolic engineering of *Saccharomyces cerevisiae* for the biosynthesis of olivetolic acid, a key cannabinoid precursor.
Biotechnology Journal, Volume 20, 6 (2025)
https://doi.org/10.1002/biot.70042

- Schmidt, C., Imann, A.M., Vasilev, N., Kayser, O.
Approaches for cannabinoid glycosylation catalyzed by CrUGT74AN3 and BlCGTase.
Biotechnology Journal, Volume 20, 5 (2025)
https://doi.org/10.1002/biot.70007

- Pitakbut, T., Kayser, O.
Anti-infective screening of selected nine cannabinoids against Clostridium perfringens and Influenza A (H5N1) neuraminidases, and SARS-CoV-2 main protease and spike protein interactions.
Curr Issues Mol Biol, Volume 47, 3, 185 (2025)
https://doi.org/10.3390/cimb47030185

2024

Peer Reviewed Journal Articles

- Schäfer, K.J., Aras, M., Boles, E., Kayser, O.
Optimizing hexanoic acid biosynthesis in Saccharomyces cerevisiae for the de novo production of olivetolic acid.
Biotechnol Biofuels, Volume 17, 141 (2024)
https://doi.org/10.1186/s13068-024-02586-2

- Spitzer, S., Aras, M., Kayser, O.
Improving CsOAC activity in Saccharomyces cerevisiae for directed production of olivetolic acid through rational design.
ChemBioChem e202400651 (2024)
https://doi.org/10.1002/cbic.202400651

- Classen, N., Pitakbut, T., Schöfbänker, M., Kühn, J., Hrincius, E.R., Ludwig, S., Hensel, A., Kayser, O.
Cannabigerol and cannabicyclol block SARS-CoV-2 cell fusion.
Planta Medica, Volume 90, 217-725 (2024)
https://doi.org/10.1055/a-2320-8822

- Jordan, E.N., Shirali Hossein Zade, R., Pillay, S., van Lent, P., Abeel, T., Kayser, O. Integrated omics of
Saccharomyces cerevisiae CENPK2-1C reveals pleiotropic drug resistance and lipidomic adaptations to cannabidiol.
npj Syst Biol Appl, Volume 10, 63 (2024)
https://doi.org/10.1038/s41540-024-00382-0

- Schmidt, C., Aras, M., Kayser, O.
Engineering cannabinoid production in Saccharomyces cerevisiae.
Biotechnology Journal, Volume 19, 2 (2024)
https://doi.org/10.1002/biot.202300507

- Jordan, E.N., Schmidt, C., Kayser, O.
Foldseek reveals a CBGA prenylating enzyme GlyMa_02G168000 from Glycine max.
Biochem Biophys Res Com, Volume 696, 149471 (2024)
https://doi.org/10.1016/j.bbrc.2024.149471

- Jordan, E.N., Nguyen, G.-N., Reynoso-Moreno, I., Gertsch, J., Kayser, O.
Synthesis of stilbenyl and bibenzyl cannabinoids and analysis of their cannabimimetic potential.
Synthesis, Volume 56 (2024)
https://doi.org/10.1055/s-0042-1751539

2023

- Spitzer, S., Wloka, J, Pietruszka, J., Kayser, O.
Generation of cannabigerolic acid derivatives and their precursors using the promiscuity of the aromatic prenyltransferase NphB.
ChemBioChem, Volume 24, 22 (2023)
https://doi.org/10.1002/cbic.202300441

- Thomas, F., Kayser, O.
Improving CBCA synthase activity through rational protein design.
Journal of Biotechnology, Volume 363 (2023)
https://doi.org/10.1016/j.jbiotec.2023.01.004

Technical Biology (TBL)

Genome reduction of *Myxococcus xanthus.*

Toward the development of a versatile host for heterologous natural product biosynthesis

Dustin Joshua Vollmann, Lucia Lernoud, Markus Nett

The myxobacterium Myxococcus xanthus *is an attractive host for the recombinant generation of bioactive small molecules, including the new antibiotic corallopyronin A and the cholinesterase inhibitor physostigmine. Since the selection of the correct host strain is of utmost importance to achieve high product titers in heterologous systems, we previously analyzed different strains of* M. xanthus *with regard to their growth characteristics and genetic amenability. A non-motile derivative of the type strain FB was found to exhibit particularly short generation times and to be highly susceptible to transformation procedures. This strain, NM, was now selected as a starting point for the development of a genome reduced platform organism.*

M. xanthus NM possesses a comparatively large genome of about 9.3 Mb. Bioinformatic analyses revealed the presence of 31 biosynthetic gene clusters (BGCs), of which 11 could be associated with the production of known natural products (Figure 1). We hypothesized that the deletion of these loci could improve the biotechnological performance of *M. xanthus* by economizing the cellular metabolite flux and liberating biosynthetic resources. Moreover, we anticipated that the abolishment of the natural secondary metabolome in *M. xanthus* would facilitate the recovery and purification of recombinantly generated natural products.

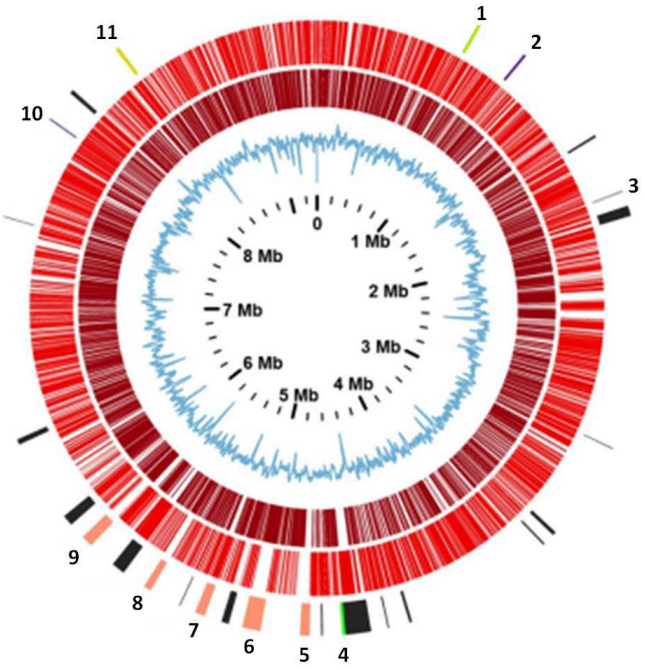

Figure 1. Graphical display of the *M. xanthus* NM chromosome. The inner ring shows a normalized plot of G+C content (blue). The outer two rings show predicted open reading frames on the reverse (dark red) and forward strands (light red), respectively. Boxes indicate the location of biosynthetic loci.

To test our hypothesis, we focused our efforts on the characterized BGCs **1-11**, all of which were individually deleted from the *M. xanthus* chromosome. Since all single deletion strains were viable, the next step was to construct a genome-reduced strain by successive BGC removal. Unexpectedly, the combined deletion of certain BGCs was not tolerated by *M. xanthus.* Despite these difficulties, we eventually generated a strain, which lacks seven BGCs of the parental NM strain corresponding to 230 kb or 2.5% of the original genome. To explore the biotechnological performance of the genome-reduced strains, they were individually transformed with a previously constructed expression plasmid, which enabled them to synthesize a caboxamycin-type benzoxazole. A comparative analysis of all generated strains showed that the accumulation of BGC deletions was initially accompanied by increasing titers of the recombinantly produced benzoxazole (Figure 2).

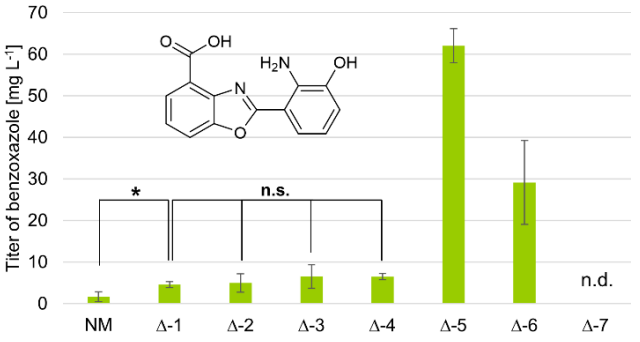

Figure 2. Production titer of the heterologously produced benzoxazole in *M. xanthus* NM and genome-reduced strains Δ-1 to Δ-7. The bars represent the mean value ± standard deviation (n = 3); n.d. = not determined. Independent t test: *, $p < 0.025$. n.s., no significant difference ($p > 0.2$).

The biotechnological capacity of the *M. xanthus* deletion mutants peaked at the Δ-5 strain. Here about 1.7% of the genome were removed. The considerable titer increase that was achieved with the genome-reduced Δ-5 strain, together with its robust growth profile, should make it a promising host for the heterologous production of bioactive small molecules.

markus.nett@tu-dortmund.de

Publications:
Vollmann, D.J.; Lernoud, L.; Nett, M., Genome Reduction Improves Recombinant Benzoxazole Production in *Myxococcus xanthus. ACS Synthetic Biology, 14*, 1756-1765 (2025)
https://doi.org/10.1021/acssynbio.5c00114

2025

Peer Reviewed Journal Articles

- Lernoud, L.; Jakob, R.; Warnick, L.; Marx, M. L.; Winand, L.
Discovery and In Vitro Reconstitution of Closoxazole Biosynthesis from *Pyxidicoccus fallax*
ChemBioChem, 26, e202500126 (2025)
https://doi.org/10.1002/cbic.202500126

- Sánchez-García, E.; Lütz, S.; Nett, M.
Reaction Engineering of In Vitro Natural Product Biosynthesis: Challenges and Strategies
ChemBioChem, 26, e202500571 (2025)
https://doi.org/10.1002/cbic.202500571

- Vollmann, D. J.; Lernoud, L.; Nett, M.
Genome Reduction Improves Recombinant Benzoxazole Production in *Myxococcus xanthus*
ACS Synthetic Biology, 14, 1756-1765 (2025)
https://doi.org/10.1021/acssynbio.5c00114

- Winand, L.; Nett, M.
Whole-Cell Biocatalysis with *Myxococcus xanthus*
Methods in Enzymology, 14, 219-237 (2025)
https://doi.org/10.1016/bs.mie.2025.01.005

2024

Peer Reviewed Journal Articles

- Steinmetz, T.; Lindig, A.; Lütz, S.; Nett, M.
Molecular Networking-Guided Discovery of Kyonggic Acids in *Massilia* spp.
European Journal of Organic Chemistry, 27, e202400017 (2024)
https://doi.org/10.1002/ejoc.202400017

2023

- Kruth, S.; Nett, M.
Aurachins, Bacterial Antibiotics Interfering with Electron Transport Processes
Antibiotics, 12, 1067 (2023)
https://doi.org/10.3390/antibiotics12061067

- Kruth, S.; Zimmermann, C. J.-M.; Kuhr, K.; Hiller, W.; Lütz, S.; Pietruszka, J.; Kaiser, M.; Nett, M.
Generation of Aurachin Derivatives by Whole-Cell Biotransformation and Evaluation of Their Antiprotozoal Properties
Molecules, 28, 1066 (2023)
https://doi.org/10.3390/molecules28031066

- Steinmetz, T.; Lombe, B. K.; Nett, M.
Intermediates and Shunt Products of Massiliachelin Biosynthesis in *Massilia* sp. NR 4-1
Beilstein Journal of Organic Chemistry, 19, 909-917 (2023)
https://doi.org/10.3762/bjoc.19.69

- Winand, L.; Lernoud, L.; Meyners, S. A.; Kuhr, K.; Hiller, W.; Nett, M.
***Myxococcus xanthus* as Host for the Production of Benzoxazoles**
ChemBioChem, 24, e202200635 (2023)
https://doi.org/10.1002/cbic.202200635

- Winand, L.; Theisen, S.; Lütz, S.; Rosenthal, K.; Nett, M.
Immobilization of the Amidohydrolase MxcM and Its Application for Biocatalytic Flow Synthesis of Pseudochelin A
Catalysts, 13, 229 (2023)
https://doi.org/10.3390/catal13020229

Industrial Chemistry (TC)

Continuous Production of Renewable Platform Chemicals.

Producing ester-aldehydes from Plant Oils by Cyclodextrin-Mediated Hydroformylation in Water

Thomas Friedrich Hubertus Roth, Tobias Averbeck, Marvin Daalmann, Dieter Vogt and Thomas Seidensticker

Renewable "platform" chemicals that can replace fossil-based monomers are in high demand. One promising route starts from plant-oil molecules with a carbon–carbon double bond. Using a rhodium catalyst in a water-and-oil (two-phase) system—assisted by cyclodextrins—a formyl group can be added in a highly selective way (hydroformylation) to make useful ester-aldehydes. These products can then be turned into important building blocks for biobased plastics, such as amino/hydroxy esters and dicarboxylic acids. Because the process must be cost-effective, recycling the catalyst is essential. In this work, methyl 10-undecenoate (from castor oil) and methyl 9-decenoate (from rapeseed oil) are converted into methyl 12-oxododecanoate and methyl 11-oxoundecanoate, respectively, in high yield and with high productivity.

A technically viable route to renewable, bifunctional platform chemicals was established by combining regioselective hydroformylation of plant-oil–derived terminally unsaturated esters with an aqueous biphasic catalyst-recycling concept. Methyl 10-undecenoate (from castor oil) and methyl 9-decenoate (from rapeseed-oil–derived streams) were selected as representative feedstocks, and the corresponding linear ester-aldehydes methyl 12-oxododecanoate and methyl 11-oxoundecanoate were targeted. These products were positioned as versatile intermediates for subsequent conversion into ω-functional building blocks relevant to bio-based aliphatic polycondensates (Figure 1).

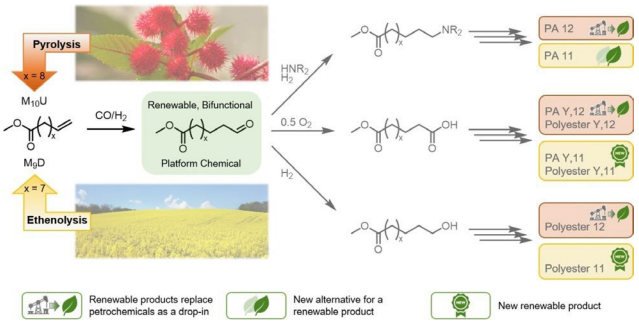

Figure 1: Linear, aliphatic ester-aldehydes as renewable platform chemicals derived from the hydroformylation of unsaturated oleochemicals offer a broad field of application in different polycondensates.

The central limitation addressed was the trade-off between the high performance of homogeneous rhodium catalysis and economically feasible catalyst recovery. A cyclodextrin-mediated aqueous biphasic system was therefore implemented in which a sulfonated Rh–sulfoXantphos catalyst was retained in the polar phase while substrate and products formed a separate organic phase. Randomly methylated β-cyclodextrins were applied as phase-transfer intensifiers; inclusion-complex formation was exploited to enhance the effective availability of hydrophobic substrates in the aqueous catalyst phase without compromising macroscopic phase separation. The mechanistic concept and recycle-oriented flowsheet are summarized in Figure 2.

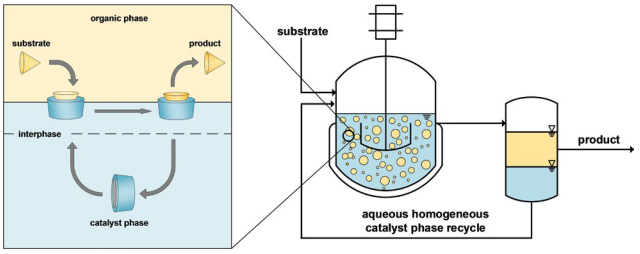

Figure 2. Postulated mechanism in the cyclodextrin-mediated biphasic reaction system (left. A basic flow sheet for the recycling of homogeneous catalysts in aqueous biphasic reaction systems is used in this work (right).

Reaction conditions were optimized using a tailored Design-of-Experiments strategy combined with Gaussian-process regression. A composite objective function integrating selectivity, space–time yield (STY), turnover number (TON), and rhodium leaching was defined to reflect the multi-criteria requirements of continuous processing. A decisive lever was the strong increase of the cyclodextrin-to-rhodium ratio (within viscosity-imposed operability limits), enabling a marked reduction in catalyst concentration together with higher substrate loading and thus higher productivity. When the parameter set was transferred to methyl 9-decenoate, comparable performance was obtained, indicating robustness across relevant substrates.

The optimized conditions were subsequently transferred to continuous miniplant operation. As full conversion could not be reached in continuously stirred tank reactors at practical residence times, the residence time was set to 3 h. In continuous operation, yields of up to 65% were achieved with aldehyde selectivities close to 90%. Overall, competitive continuous productivity and efficient homogeneous catalyst recycling were demonstrated for bio-based ester-aldehydes as renewable platform chemicals.

dieter.vogt@tu-dortmund.de
thomas.seidensticker@tu-dortmund.de

Publications:
Roth, T.F.H.; Averbeck, T.; Daalmann, M.; Vogt, D.; Seidensticker, T.; Continuous Production of Bifunctional Platform Chemicals From Plant Oils in Water by Cyclodextrin-Mediated Hydroformylation. ChemSusChem (published online). https://doi.org/10.1002/cssc.202402421

Waste-Free Isolation of High-Purity Amines.

Selective Ammonium Carbamate Crystallization for Isolating Primary Amines from Amine and Reaction Mixtures.

Bernd Rienhoff, Dilara Mede, Mara Schöler, Dieter Vogt, Thomas Seidensticker

Amines are widely used to produce fine chemicals, dyes, agrochemicals, pharmaceuticals, and polymers. Primary aliphatic amines present especially valuable intermediates, but their high reactivity yields product mixtures with secondary and tertiary amine species that require energy-intensive separation. The utilization of homogeneous catalysis presents a selective alternative, although the challenging separation of product and catalyst arises. In this work, CO2 is used to reversibly form solid ammonium carbamate salts, demonstrating purification of amine mixtures and separation of product and homogeneous catalyst mixtures by crystallization.

Separating primary from secondary and tertiary amines is a persistent bottleneck for sustainable amine production, as many established purification routes are multistep, energy-intensive, or generate substantial waste (Figure 1). Here, we describe selective ammonium carbamate crystallization (SACC), an efficient separation strategy exploiting solubility differences of ammonium carbamate species formed via reversible, waste-free salt formation of amines with CO2. As CO2 addition and release is reversible, it acts as a clean, switchable agent enabling selective crystallization of primary amine species without stoichiometric waste formation (Figure 2).

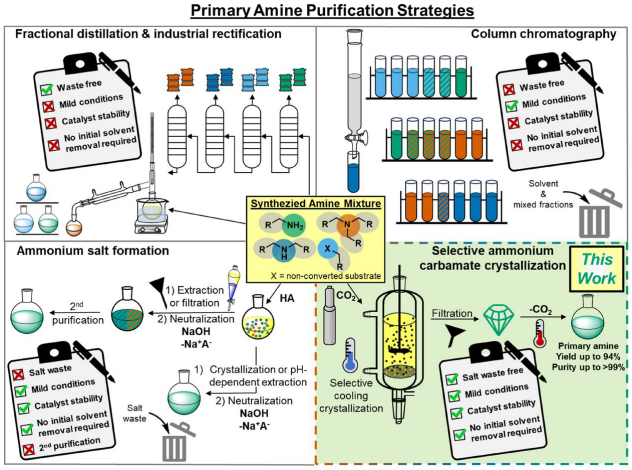

Figure 1. Illustration of standard primary amine purification strategies and selective ammonium carbamate crystallization (SACC, this work).

SACC demonstrated the purification of challenging amine mixtures. Starting from feeds with only 35% primary amine content, it achieved up to 94% isolated yield with >99% purity. Beyond primary amine isolation, it also enables secondary/tertiary separation (up to 86% yield, 91% purity) and fractional crystallization of mixtures containing all three amine classes, producing fractions with 83–94% yields and ~90% to >99% purities. Notably, the method can also enrich unsaturated, cis fatty amines by preferential crystallization of saturated and trans-configured components.

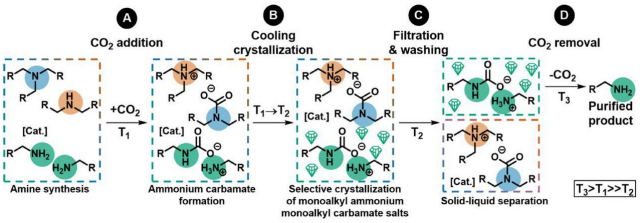

Figure 2. Illustration of the selective ammonium carbamate crystallization (SACC) comprising of the steps (A-D) for primary amine isolation.

Furthermore, SACC was also implemented in the alcohol amination reaction as an isolation strategy from homogeneously catalyzed reaction mixtures. High isolation performances were achieved with primary amine yields up to 84% and purities exceeding 99%. Catalyst losses indicated by the ruthenium and phosphorus contents in the final product are minimal, averaging <1% of initially utilized amounts.

Overall, SACC indicated high potential as a versatile purification and isolation method that improves separations and supports scalable, lower-free primary amine production. Ongoing work will broaden compatible reactions and further assess catalyst stability and recyclability.

bernd.rienhoff@tu-dortmund.de
dieter.vogt@tu-dortmund.de
thomas.seidensticker@tu-dortmund.de

Publications:
Rienhoff, B.; Mede, D.; Schöler, M.; Vogt, D.; Seidensticker, T.; Selective and Waste-Free Isolation of High Purity Primary Amines from Amine and Reaction Mixtures by Selective Ammonium Carbamate Crystallization. ChemEurJ 2025 (published online). https://doi.org/10.1002/chem.202500059

Efficient Product-Catalyst Separation in Homogeneous Catalysis.

Selective Separation of Tertiary Amines via a CO_2-Induced Polarity Switch

Tim Benjamin Riemer, Milan Danilo Kulaš , Ma-Azou Baba, Dieter Vogt, and Thomas Seidensticker

Amines appear in many everyday products, from medicines and crop-protection agents to solvents, plastics, and detergents. They can be made efficiently by homogeneous catalysis, which often gives high selectivity under mild conditions, but catalyst–product separation is difficult. In switchable systems, reactions are run as one phase for high productivity, then shifted to two phases so products and catalyst separate easily. In thermomorphic multiphase systems, the mixture is uniform when hot and splits on cooling into a polar catalyst phase and a nonpolar product phase. One option is reversible binding of amines with CO_2 to form water-soluble ammonium bicarbonates. Usually the amines are part of the solvent system. Here the amines are targeted as the product.

In this article we introduce Switchable Hydrophilicity Amine Product Extraction (SHAPE) as an integrated downstream concept for homogeneously catalyzed tertiary amine synthesis, with the explicit objective of replacing energy-intensive distillation by a phase-switching work-up. The separation principle was based on a reversible CO_2-triggered polarity switch: after catalytic formation in a nonpolar organic phase, the tertiary amine product was converted into a polar ammonium bicarbonate upon CO_2 loading and was thereby transferred selectively into an aqueous phase by reactive extraction. Subsequent CO_2 stripping regenerated the free amine, which then phase-separated from water and was recovered by simple decantation.

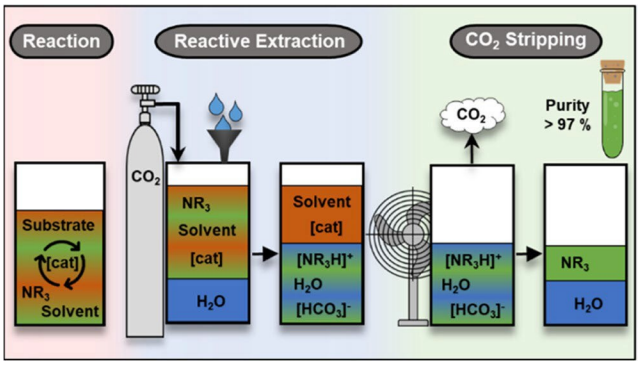

Figure 1. General concept of Switchable Hydrophilicity Amine Product Extraction (SHAPE): consisting of reaction (A), reactive extraction via CO_2 (B) and stripping of CO_2 (C) for pure amine recovery.

A systematic solvent screening, performed with N,N-dimethylbenzylamine (DMBA) as a model product, demonstrated that solvent polarity governed both extraction kinetics and the final phase distribution. More polar solvents accelerated equilibration - consistent with improved CO_2/carbonic-acid availability and mass transfer - but retained larger fractions of protonated amine in the organic phase. Highly nonpolar solvents minimized organic retention of the protonated species but exhibited slower approach to equilibrium. Anisole was identified as the best compromise, providing efficient extraction and favorable partitioning. Beyond technical performance, anisole was also preferred over other nonpolar solvents such as n-heptane and cyclohexane due to their ecotoxicology. Operating parameters were then optimized for both steps of the switchable sequence.

Applicability to catalytic systems was assessed thereafter. Reductive amination was reported to be poorly compatible with nonpolar aprotic solvents, whereas alcohol amination provided a better match to the solvent environment preferred for SHAPE. Consequently, Ru-catalyzed alcohol amination of benzyl alcohol in anisole was used as the model synthesis route (Figure 2).

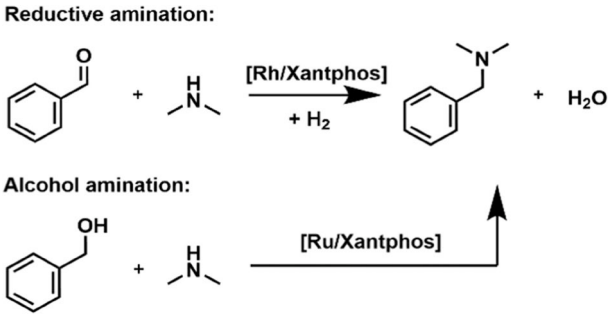

Figure 2. Main reaction paths in reductive amination and alcohol amination for the production of N,N-dimethylbenzylamine (DMBA).

After reaction and SHAPE work-up, DMBA was isolated in 84.9% yield at 91.8 wt% purity, with residual impurities dominated by water and minor anisole. Catalyst retention was high, as only 0.09 wt% of Ru was detected in the product phase. Finally, SHAPE was combined with thermomorphic multiphase systems (TMS) to enable a staged “catalyst separation + amine isolation” strategy; several aliphatic tertiary amines were recovered from complex mixtures with purities up to 97.3 wt%, while nonpolar byproducts were largely retained in the solvent phase. This highlights SHAPE as a robust alternative to distillation for high-boiling product streams.

dieter.vogt@tu-dortmund.de
thomas.seidensticker@tu-dortmund.de

Publications:
Riemer, T.B.; Kulaš, M.; Baba, M-A; Vogt, D.; Seidensticker, T. Switchable Hydrophilicity Amine Product Extraction: Efficient Separation of Tertiary Amines via Carbon Dioxide-Induced Polarity Switch in Homogeneous Catalysis. ACS Sustainable Chemistry & Engineering 2025 (published online). https://doi.org/10.1021/acssuschemeng.4c07757

Process Intensification for Continuous Multiphase Reactions.

Coupling Gas Permeation with Gas-Consuming Reactions in Slug-Flow Capillaries for Continuous, Selective Biodiesel Hydrogenation

Florian Lehmann, Niclas von Vietinghoff, Peter Pey, Karl Steffen Wulle, Thomas Seidensticker

Multiphase reactions are often rate-limited by mass transfer resistances; therefore, reactor design for optimal mixing is crucial. Capillary reactors enable slug flow, where alternating liquid and gas segments create strong internal mixing with a defined residence time, and a high surface-to-volume ratio that improves mass and heat transfer. For gas-liquid reactions, low gas solubility and rapid consumption often lead to shrinking gas segments, disrupting the flow pattern, and changing residence times, which can reduce selectivity when follow-up reactions occur. Continuous gas replenishment into slug flow by permeation through fluorinated capillary walls was already demonstrated, but it has rarely been applied together with catalytic reactions. Selective partial hydrogenation towards monounsaturated species is a useful exemplary gas-liquid reaction, where full saturation must be avoided. Here, gas permeation is integrated into a capillary slug-flow reactor for continuous selective partial hydrogenation of fatty acid methyl esters, and the influence of gas supply and operating mode is evaluated.

A capillary slug-flow reactor concept with integrated hydrogen permeation to enable stable continuous operation of gas-consuming multiphase reactions is presented using the selective partial hydrogenation of soybean-derived fatty acid methyl esters as a model gas-liquid reaction. The key challenge addressed is that hydrogen consumption in conventional reactive slug flow causes gas-bubble shrinkage, destabilizing segmentation and altering residence time. To overcome this, hydrogen is continuously replenished through the gas-permeable fluoropolymer capillary wall, maintaining a stable flow regime. Several different reactor concepts and operating modes apart from a batch reaction are investigated and are summarized in Figure 1, including the presence or absence of additional gas slugs.

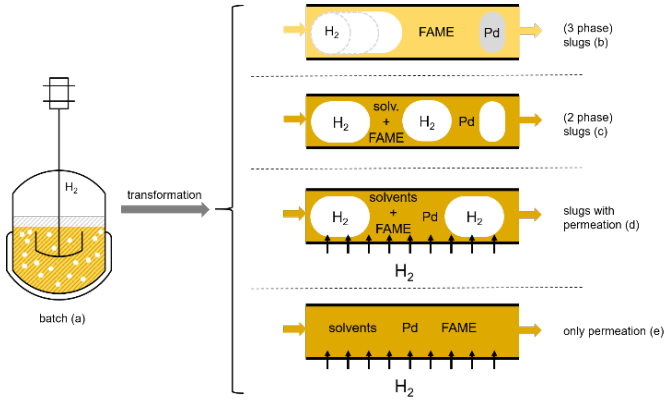

Figure 1. Schematic and enlarged (not to scale) possibilities of investigated reactor concepts. (a) Batch reaction with one or two liquid phases and one gas phase. (b) Reaction in capillary with three phases, shrinking gas slugs and without additional solvent. (c) Reaction in capillary with two phases, shrinking gas slugs, and additional solvent. (d) Reaction in capillary with two phases, additional solvent, and gas replenishment by permeation leading to gas slugs with roughly constant size. (e) Reaction in capillary with one phase, additional solvent, and permeation, without additional gas slugs.

A solvent-stabilized Pd nanoparticle catalyst in propylene carbonate is employed, and conditions are optimized to favor the formation of the monounsaturated compound while suppressing overhydrogenation. Direct transfer of a typical batch protocol to the capillary setup necessitates the use of an additional solvent to establish a stable two-phase slug flow.

Applying hydrogen permeation, the product composition remained essentially unchanged relative to slug flow without permeation, but flow stability improved, with more uniform slug sizes and reduced residence time, consistent with mitigated bubble shrinkage.

Kinetic evaluation indicated a >9-fold rate increase for the formation of the monounsaturated compound from the twice unsaturated one relative to a batch reaction under the same conditions and a TOF20-equivalent of 257,000 h^{-1}. No mass-transport limitations are observable anymore under these conditions. At the same time, capillary slug flow without permeation still leads to an intensified reaction compared to batch.

Overall, reaction gas permeation was established as a practical tool to stabilize reactive slug flow and intensify the selective hydrogenation of a renewable feedstock, offering transferability of the concept to any other mass-transport-limited gas/liquid reaction in a slug-flow regime.

florian.lehmann@tu-dortmund.de
thomas.seidensticker@tu-dortmund.de

Publications:
Lehmann, F.; von Vietinghoff, N.; Pey, P.; Wulle, K.S.; Seidensticker, T., "Integrating Gas Permeation with Gas-Consuming Reactions in Slug-Flow Capillaries: Continuous and Selective Hydrogenation of Biodiesel", ACS Sustainable Chem. Eng. 2025, 13, 20242–20252,
DOI: 10.1021/acssuschemeng.5c09302.

Sustainable Transfer Hydrogenation.

Formic Acid from Waste-Derived Aqueous Streams as a Hydrogen Donor, Catalysed by the SulfoShvo Catalyst

Justus Diekamp, Milan D. Kulaš, Jakob Albert, and Thomas Seidensticker

As the chemical industry shifts from fossil to renewable feedstocks, more reduction reactions will be needed because many bio-based molecules are oxygen-rich. While electrolysis-derived hydrogen will likely dominate, storage and safety issues - plus the chance to use waste streams - make liquid hydrogen carriers attractive. Formic acid is a promising hydrogen surrogate, especially when produced from biomass via the commercial OxFA process, which can use varied carbon sources and delivers a 50–60 wt% aqueous formic acid solution that is usually concentrated before use. Direct use of this crude aqueous solution would avoid resource-intensive separation, but many homogeneous transfer-hydrogenation catalysts are not compatible with water and acidic conditions. Here, this limitation is addressed using a highly water-soluble Shvo-type catalyst (sulfoShvo) that operates without added base and is better suited to acidic media, enabling direct application of OxFA formic acid in transfer hydrogenation.

In this article, the direct use of waste-derived aqueous formic acid (FA) solutions as a hydrogen donor for catalytic transfer hydrogenation was demonstrated, thereby avoiding the energy- and resource-intensive concentration and purification steps typically required to obtain commercial-grade FA. The study was motivated by the OxFA process, which generated crude FA streams of roughly 50–60 wt% in water from biomass-derived byproducts (e.g., raw glycerol), but for which classical downstream separation would normally dominate process burdens. A decisive enabling element was the highly hydrophilic and acid-stable sulfoShvo catalyst, which remained active at pH ≈ 1 and did not require base activation, making direct utilization of strongly acidic, aqueous FA realistic. The integrated valorization concept which linkis biomass oxidation (OxFA) to catalytic reduction without external H_2 is outlined in Figure 1. Direct conversion of oxidized feedstocks into reduced, bio-based platform chemicals is depicted, with CO_2 arising as the benign byproduct of FA dehydrogenation.

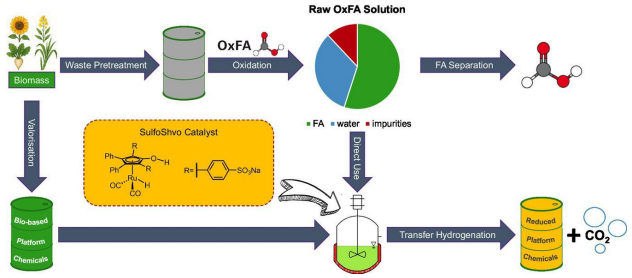

Figure 1. Flow scheme of the production of reduced, bio-based platform chemicals through utilisation of the raw OxFA solution without an external hydrogen source as proposed in this publication.

Levulinic acid (LA) was selected as a model substrate because its hydrogenation intermediate (4-hydroxyvaleric acid) rapidly cyclized under acidic conditions to γ-valerolactone (GVL), providing a robust readout for conversion and selectivity. To operate above the boiling points of water and FA, reactions were performed in pressure autoclaves, and a temperature screening (70–170 °C) identified 130 °C as an effective compromise between activity and catalyst integrity. At higher temperatures (≥150 °C), the formation of black Ru-containing particles indicated catalyst decomposition. Under optimized conditions, catalyst loadings as low as 0.2 mol% enabled rapid full conversion at 130 °C. Importantly, a crude glycerol-derived OxFA solution exhibited performance comparable to an artificial 55 wt% FA/H_2O mixture, indicating substantial tolerance toward typical OxFA impurities and supporting the premise that FA purification was not mandatory for high catalytic performance.

The impact of headspace composition was also assessed. When N_2 was replaced by CO_2 pressure, still a high yield with a reduced rate was observed, consistent with partial inhibition or altered gas–liquid equilibria in the closed system. Catalyst stability was evaluated by recycling and low-loading studies: while recycling at 130 °C showed pronounced deactivation, markedly improved long-term performance was obtained at 100 °C.

Finally, a broader substrate scope was demonstrated for several water-soluble carbonyl and olefinic compounds, underscoring the general applicability of the OxFA/sulfoShvo system for sustainable reductions that upgrade diluted, waste-derived FA streams into valuable products without external hydrogen supply.

justus.diekamp@tu-dortmund.de
thomas.seidensticker@tu-dortmund.de

Publications:
Diekamp, J.; Kulaš, M.D.; Albert, J.; Seidensticker, T Transfer Hydrogenation with Waste-Derived Aqueous Solutions of Formic Acid Catalysed by the SulfoShvo Catalyst. ChemSusChem 2025 (published online).
https://doi.org/10.1002/cssc.202501832

2025

Peer-Reviewed Journal Articles

Diekamp, J., Kŭlas, M. D., Albert, J., Seidensticker, T.
Transfer Hydrogenation with Waste-Derived Aqueous Solutions of Formic Acid Catalysed by the SulfoShvo Catalyst.
ChemSusChem, 18, e202501832 (2025).
https://doi.org/10.1002/cssc.202501832

Lehmann, F., von Vietinghoff, N., Pey, P., Wulle, K. S., Seidensticker, T.
Integrating Gas Permeation with Gas-Consuming Reactions in Slug-Flow Capillaries: Continuous and Selective Hydrogenation of Biodiesel.
ACS Sustainable Chem. Eng., Volume 13, Issue 46, 20242–20252 (2025)
https://doi.org/10.1021/acssuschemeng.5c09302

Kost, N., Lehmann, F., Guo, R., Loza, K., Heggen, M., Seidensticker, T., Epple, M.
Catalytic Activity of Water-Dispersed Palladium Nanoparticles with Different Sizes and Shapes in the Semihydrogenation of Alkynes.
ChemCatChem, e01164 (2025)
https://doi.org/10.1002/cctc.202501164

Lehmann, F., Wegener, H. W., Brede, N., Seidensticker, T.
Combining Partial Hydrogenation of Soybean-Derived Biodiesel and Methoxycarbonylation Using a Single Palladium Source.
Eur. J. Lipid Sci., e70073 (2025)
https://doi.org/10.1002/ejlt.70073

Rienhoff, B., Oppenberg, N., Zolthoff, F., Vogt, D., Seidensticker, T.
Selective Ammonium Carbamate Crystallization: An Innovative Approach for Catalyst Recycling in Homogeneously Catalyzed Primary Amine Synthesis.
ChemCatChem, e00989 (2025)
https://doi.org/10.1002/cctc.202500989

Rienhoff, B., Mede, D., Schöler, M., Vogt, D., Seidensticker, T.
Selective and Waste-Free Isolation of High Purity Primary Amines from Amine and Reaction Mixtures by Selective Ammonium Carbamate Crystallization.
Chem. Eur. J., e202500059 (2025)
https://doi.org/10.1002/chem.202500059

Obst, S., Köhnke, K., Seidensticker, T., Leitner, W., Vorholt, A. J.
Development of a Highly Active Catalyst System with Tuneable Selectivity for the Hydroformylation of the Renewable 1,3-Diene β-Myrcene.
ChemCatChem, e00553 (2025)
https://doi.org/10.1002/cctc.202500553

Windisch, A., Pey, P., Seidensticker, T.
CO-Degassing in a Segmented Slug Flow Reactor Enables Continuous Linear Alcohol Formation from Alkenes using a single, non-assisted Rh-catalyst by Switching Between Hydroformylation and Aldehyde Reduction.
ChemRxiv, (2025)
https://doi.org/10.26434/chemrxiv-2025-r5jz4

Kondratiuk, M., Spiekermann, M. L., Seidensticker, T., Gooßen, L.
Sustainable Diesel from Rapeseed Oil Esters by Sequential Semi-Hydrogenation, Double Bond Isomerization, and Metathesis.
Chem. Eur. J., e202500523 (2025)
https://doi.org/10.1002/chem.202500523

Fromme, T., Spiekermann, M. L., Lehmann, F., Barcikowski, S., Seidensticker, T., Reichenberger, S.
Preferential enrichment and extraction of laser-synthesized nanoparticles in organic phases.
Beilstein J. Nanotechnol., Volume 16, 254–263 (2025)
https://doi.org/10.3762/bjnano.16.20

Riemer, T. B., Kulaš, M. D., Baba, M.-A., Vogt, D., Seidensticker, T.
Switchable Hydrophilicity Amine Product Extraction: Efficient Separation of Tertiary Amines via Carbon Dioxide-Induced Polarity Switch in Homogeneous Catalysis.
ACS Sustainable Chem. Eng., Volume 13, Issue 4, 1544–1553 (2025)
https://doi.org/10.1021/acssuschemeng.4c07757

Wegener, H. W., Reichert, R., Brede, N., Gierse, A., Spiekermann, M. L., Vogt, D., Seidensticker, T.
Mechanistic Insights Into the Methoxycarbonylation of Technical Grade Oleochemicals: Catalytical and Structural Analysis of Conjugated Fatty Acid Methyl Esters.
Eur. J. Lipid Sci. Technol., e202400198 (2025)
https://doi.org/10.1002/ejlt.202400198

Roth, T. F. H., Averbeck, T., Daalmann, M., Vogt, D., Seidensticker, T.
Continuous Production of Bifunctional Platform Chemicals From Plant Oils in Water by Cyclodextrin-Mediated Hydroformylation.
ChemSusChem, e202402421 (2025)
https://doi.org/10.1002/cssc.202402421

Diekamp, J., Schmidt, A., Holstein, J. J., Strohmann, C., Seidensticker, T.
Synthesis and catalytic testing of the first hydrophilic derivative of Shvo's catalyst.
Chem. Commun., 61, 117–120 (2025)
https://doi.org/10.1039/D4CC04390A

2024

Peer Reviewed Journal Articles

Roth, T. F. H., Spiekermann, M., Kühl, A., Wegener, H., Seidensticker, T.
Biodiesel as a sustainable platform chemical enabled by selective partial hydrogenation: Compounds outplace Combustion?!
ChemSusChem, 17, 13, e202400036 (2024)
https://doi.org/10.1002/cssc.202400036

Roth, T. F. H., Spiekermann, M. L., Lütkenhaus, D., Niefer, F., Vogt, D., Seidensticker, T.
The effect of polyunsaturation – insights into the hydroformylation of oleochemicals.
Catal. Sci. Technol., 14, 5551-5558
https://doi.org/10.1039/D4CY00839A

Söderholm, V., Stajer, M., Savage, C., Splittgerber L., Vogt, D.
Towards continuous Rh-hydroformylation of long chain alkenes: handling methodology for the long-term stability of Biphephos in a continuous reactor with an attached membrane separation unit.
Catal. Sci. Technol., 15, 592-604
https://doi.org/10.1039/D4CY01148A

Wegener, H. W., Diekamp, J., Seidensticker, T.
A Perspective on Aldoximes as Platform Chemicals: Rethinking C−N Bond Formation.
ChemCatChem, e202401206
https://doi.org/10.1002/cctc.202401206

Riemer, T.B., Windisch, A.M., Vogt, D., Seidensticker, T.
Robust and flexible continuous operation of homogeneous catalysis in thermomorphic multiphase systems − On-stream switching of substrates and reactions in amine production.
Chem. Eng. J. (497) 154643
https://doi.org/10.1016/j.cej.2024.154643

Ferreira, M., Bricout, H., Roth, T. F.H., Seidensticker, T., Tilloy, S., Monflier, E.
Aqueous biphasic hydroformylation and hydroaminomethylation assisted by cyclodextrins: From benchtop to industrial perspective.
Catal. Today, 442, 113951
https://doi.org/10.1016/j.cattod.2024.114951

Roth, T. F.H., Häusler, M., Vogt, D., Seidensticker, T.
Advancing the aqueous biphasic hydroformylation of oleochemicals in

the loop: Continuous reaction and separation using a jet-loop reactor concept.
Catal. Today, 439, 114803
https://doi.org/10.1016/j.cattod.2024.114803

Kampwerth, A., Riemer, T. B., Pöttker-Menke, J., Oppenberg, J., Windisch, A. M., Vogt, D., Seidensticker, T.
Hydroaminomethylation of methyl 10-undecenoate with integrated catalyst recycling *via* a thermomorphic multiphase system for the continuous production of renewable amines.
RSC Sustain., 2, 1797-1808
https://doi.org/10.1039/D4SU00109E

Averbeck, T., Sadowski, G., Held, C., Seidensticker, T.
Neural Network-Based Tensor Completion: Advancing Predictions of Activity Coefficients and Beyond.
Ind. Eng. Chem. Res. 63, 28, 12648–12655
https://doi.org/10.1021/acs.iecr.4c00352

Spiekermann, M. L., Seidensticker, T.
Catalytic processes for the selective hydrogenation of fats and oils: reevaluating a mature technology for feedstock diversification.
Catal. Sci. Technol. 14, 4390-4419
https://doi.org/10.1039/D4CY00488D

Hares, K., Wegener, H. W., Roth, T. F. H., Reichert, R., Vogt, D., Seidensticker, T.
Primary amines from alkenes and carbonyl compounds: highly selective hydrogenation of oximes using a homogeneous Ru-catalyst.
Catal. Sci. Technol., 14, 2940-2950
https://doi.org/10.1039/D4CY00368C.

Köhler, T., Rienhoff, B., Vogt, D.
Nickel(BiPhePhos)-Catalyzed Hydrocyanation of Styrene—Highly Increased Catalytic Activity by Optimized Operational Procedures.
Catalysts, 14(3), 210
https://doi.org/10.3390/catal14030210.

Roth, T. F. H., Kühl, A., Spiekermann, M. L., Wegener, H. W., Seidensticker,T.
Biodiesel as a Sustainable Platform Chemical Enabled by Selective Partial Hydrogenation: Compounds Outplace Combustion?!
ChemSusChem, e202400036
https://doi.org/10.1002/cssc.202400036.

Gottu Mukkul, A. R., Riemer, T. B., Kühl, A., Vogt, D., Engell, S.
Iterative real-time optimization of a reductive amination process in a thermomorphic multiphase system.
Chem. Eng. Sci., 287(119662)
https://doi.org/10.1016/j.ces.2023.119662.

2023

Seifert, A. I., Wegener, H. W., Brühl, K., Seidensticker, T., Wohlgemuth, K.
Polymer-Grade Bio-Monomers from Oleochemicals by Combining Homogeneous Catalysis and Selective Product Crystallization in an Integrated Process.
Processes, 11(10), 2861
https://doi.org/10.3390/pr11102861

Riemer, T. B., P. Lapac, P., Vogt, D., Seidensticker, T.
Stable and Continuous Production of Amines via Reductive Amination in a Green Switchable Solvent System with Efficient Water Removal.
ACS Sustainable Chem. Eng., 11, 12959–12966
https://doi.org/10.1021/acssuschemeng.3c02320

Javed, S., Ropel, D., Vogt, D.
Sodium ethoxide as an environmentally benign and cost-effective catalyst for chemical depolymerization of post-consumer PET waste.
Green Chem., 25, 1442-1452
https://doi.org/10.1039/D2GC04548F

Javed, S., Vogt, D.
Development of Eco-Friendly and Sustainable PET Glycolysis Using Sodium Alkoxides as Catalysts.
ACS Sustainable Chem. Eng., 11, 31, 11541–11547

https://doi.org/10.1021/acssuschemeng.3c01872

Vondran, J., Moeschke, R., Deysenroth, T., Seidensticker, T.
Pushing Boundaries—Selective Cooling Crystallization as Tool for Selectivity Compensation and Product Purification Using a Recyclable Pd/Xantphos Catalyst in the Methoxycarbonylation of Methyl 10-Undecenoate.
Eur. J. Lipid Sci. Technol., 125, 2200126
https://doi.org/10.1002/ejlt.202200126

Heider, C., Menk, M., Terhorst, M., Vogt, D., Seidensticker, T.
Synthesis of Tertiary Fatty Amines in Water: The Dual Role of Dimethylamine as Reagent and Phase Mediator in the Homogeneously Catalyzed Fatty Alcohol Amination.
ACS Sustainable Chem. Eng. 11, 31, 11359–11363
https://doi.org/10.1021/acssuschemeng.3c02764

Diekamp, J., Seidensticker, T.
Synthesis Strategies towards Tagged Homogeneous Catalysts To Improve Their Separation.
Angew. Chem. Int. Ed. 2023, e202304223
https://doi.org/10.1002/anie.202304223

Roth, T., Evertz, R., Kopplin, N., Tilloy, S., Monflier, E., Vogt, D., Seidensticker, T.
Continuous production of amines directly from alkenes via cyclodextrin-mediated hydroaminomethylation using only water as the solvent.
Green Chem., 25, 3680-3691
https://doi.org/10.1039/D2GC04847G

Kampwerth, A., Terhorst, M., Kampling, N., Vogt, D., Seidensticker, T.
Synthesis of biobased amines via Pd-catalysed telomerisation of the renewable β-myrcene in a water/ethanol multiphase system: catalyst recycling enabled by a self-separating product phase.
Green Chem. 25, 6345-6354
https://doi.org/10.1039/D3GC00453H

Heider, C., Winter, A., Voß, V., Vogt, D., Seidensticker, T.
Homogeneous Catalysis at its Edge: High-Temperature Ru-Catalysed Amination of Alcohols under Continuous Flow Conditions.
ChemCatChem e202201307
https://doi.org/10.1002/cctc.202201307

Metzger, J. O., Biermann, U., Seidensticker, T.
Fats and Oils as Renewable Feedstock for the Chemical Industry.
Eur. J. Lipid Sci. Technol. 125, 5, 1438-7697
https://doi.org/10.1002/ejlt.202300038

Javed, S., Vogt, D.
Kinetic Investigation for Chemical Depolymerization of Post-Consumer PET Waste Using Sodium Ethoxide.
Ind. Eng. Chem. Res. 62(10), 4328–4336
https://doi.org/10.1021/acs.iecr.2c04308

von Vietinghoff, N., Immken, A., Seidensticker, T., de Caro, P., Thiebaud Roux, S., Agar, D. W.
Gas Introduction by Permeation into Long Fluorinated Ethylene Propylene Capillaries with Slug Flow.
Chem Eng Technol 46(5), 1047-1051
https://doi.org/10.1002/ceat.202200557

Javed, S., Fisse, J., Vogt, D.
Optimization and Kinetic Evaluation for Glycolytic Depolymerization of Post-Consumer PET Waste with Sodium Methoxide.
Polymers 15(3), 687
https://doi.org/10.3390/polym15030687

Thermodynamics (TH)

The more the better? – Vitamin E TPGS as release enhancer for Ritonavir/PVPVA ASDs

Ineke Fahrig[1], Stefanie Walter[2], Samuel Kyerematenq[2], Matthias Degenhardt[2], Gabriele Sadowski[1], Christoph Brandenbusch[1]

[1] TU Dortmund, Department of Biochemical and Chemical Engineering, Laboratory of Thermodynamics

[2] AbbVie Deutschland GmbH & Co. KG, Development Sciences, R&D

Amorphous solid dispersions (ASDs) are state-of-the-art formulation strategies for improving the solubility and release of poorly water-soluble small-molecule active pharmaceutical ingredients (APIs). Yet elevated drug loads (DLs) frequently result in a loss of release (LoR). This study delivers a mechanistic insight on the concentration-dependent role of Vitamin E TPGS in high DL ritonavir (RIT)/poly(vinyl pyrrolidone-co-vinyl acetate) (PVPVA) ASDs. The results reveal the existence of a distinct design window in which TPGS effectively stabilizes the formulation and preserves release performance. However, excessive TPGS amounts re-promote destabilization and LoR. Using a thermodynamics-based design approach, rather than a "the more the better" principle, this work provides a rational framework for optimizing next-generation high-DL ASDs.

At low DL (~ 20 wt.% in the system studied here), ASDs typically demonstrate complete release of both the API and the polymer (see Figure 1A). However, at higher DLs (> 30 wt.%), the API release drops significantly, leading to an incomplete or collapsed API release. Phase separation within the ASD hinders API release by forming a continuous API-rich phase (see Figure 1B).

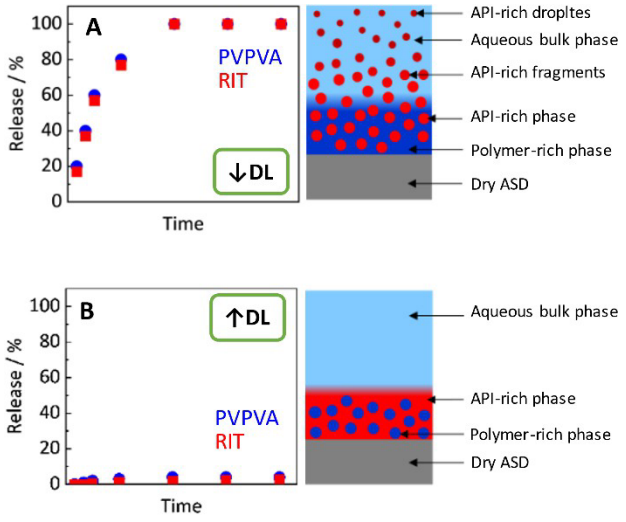

Figure 1. Release profiles and schematic illustration of the phase separation in ASDs with complete release (A) and minimal release behavior (B).

Adding 3 wt.% Vitamin E TPGS increases the release, with both RIT and PVPVA released completely. However, at 40 wt.% DL, even high Vitamin E TPGS concentrations (up to 10 wt.%) fail to achieve full release. Our results suggest, that appropriate concentrations of Vitamin E TPGS stabilize discrete API-rich domains and hinder their coalescence during phase separation in the ASD, enabling complete release. However, excessive Vitamin E TPGS reduces this stabilization potential.

The system can no longer maintain its two-phase liquid-liquid phase behavior. Instead, an even more complex three-phase demixing occurs (see Figure 2), where API, polymer, and surfactant separate into distinct phases:

an API-rich phase, a polymer-rich phase and a surfactant-rich phase. This disrupts the established stabilization mechanism, resulting in incomplete RIT release.

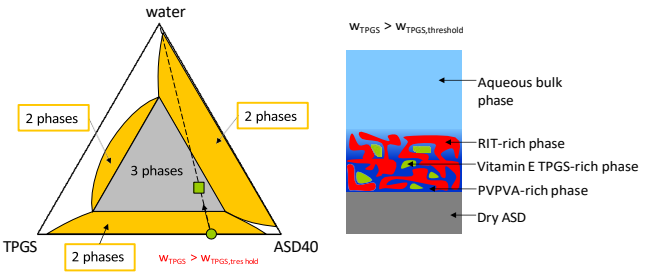

Figure 2. Schematic pseudo ternary phase diagram for the system of RIT/PVPVA at fixed ratio of RIT to PVPVA 40:60 (ASD 40), Vitamin E TPGS, and water (left) and schematic illustration of the three-phase demixing in ASDs (right) above a threshold concentration of Vitamin E TPGS.

Overall, this study highlights the critical role of surfactants like Vitamin E TPGS in optimizing ASD formulations, while emphasizing challenges that arise at high surfactant concentrations. These insights are valuable for the development of formulations where optimizing API release must be balanced with other critical factors, such as long-term stability or manufacturability.

ineke.fahrig@tu-dortmund.de
gabriele.sadowski@tu-dortmund.de
christoph.brandenbusch@tu-dortmund.de

Publication:
Fahrig, I.; Walter, S.; Kyerematenq, S.; Degenhardt, M.; Sadowski, S.; Brandenbusch, C., The more the better? – Vitamin E TPGS as release enhacer for Ritonvair/PVPVA ASDs. Molecular Pharmaceutics 2025, 22, 9, 5592-5602.
https://doi.org/10.1021/acs.molpharmaceut.5c00620

Predicting solvation properties of ions in mixed solvents.

Further advancing the electrolyte equation of state ePC-SAFT

Paul Figiel, Gangqiang Yu, Christoph Held

Electrolyte solutions are omnipresent in the chemical industry, biotechnology and in the energy sector. They are used in batteries, electrolysis and carbon capture, and many more. Electrolyte solutions involve both, aqueous and organic solvent systems which often consist of mixtures of different solvents. However, literature data for mixed solvent electrolyte solutions is scarce. Modeling tools such as ePC-SAFT can help to minimize the required experimental effort by predicting thermodynamic properties of these solutions. In this work, the ion-dipolar interactions (the Born term) within ePC-SAFT are characterized more quantitatively correct in order to be able to predict crucial properties of mixed solvent electrolyte systems very accurately.

ePC-SAFT is an equation of state that incorporates Helmholtz-energy contributions based on physical molecular interactions. The ion-dipolar Born-energy contribution within the ePC-SAFT framework has a very strong influence on the results of the modeled thermodynamic properties of ions at infinite dilution. In previous works, an ion-specific diameter as well as an averaged dielectric constant of the bulk liquid phase were introduced as input into the Born term. In this work, modifications to the averaging mixing rule and to the Born term on the modeling results were explored. We found that a very easy mixing rule for the relative dielectric constant ε_r allows describing the experimental data of different salts in water, methanol and ethanol surprisingly well. The results of the new mixing rule for ε_r are compared to the results with the mixing rule for ε_r of previous works in Figure 1.

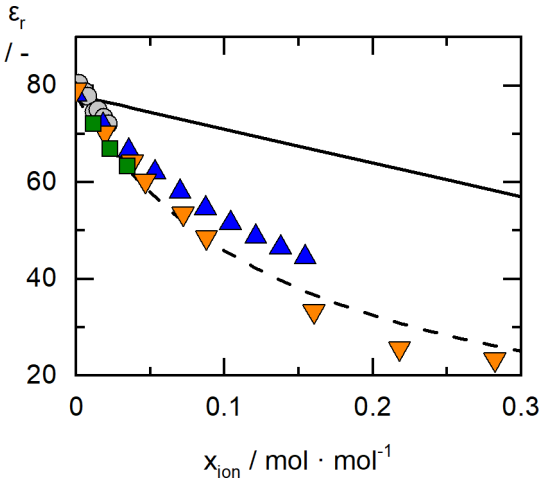

Figure 1. Relative dielectric constant ε_r of aqueous electrolyte solutions at 298.15 K and 1 bar. Solid line: old mixing rule; dashed line: new mixing rule; symbols: experimental data points taken from literature (details: see publication).

Further, the Born term was modified by considering two additional effects in the ion solvation. The first effect is the formation of a solvation shell of solvent molecules around an ion. This was implemented in the Born term by considering the solvation-shell diameter instead of the Born diameter, since the latter neglects the kind of the solvating molecules. The second modification deals with the dielectric constant within the solvation shell, where a lower dielectric constant compared to the bulk phase is expected. This effect is called dielectric saturation and was considered in ePC-SAFT.

These developments allowed for quantitative descriptions of electrolyte solutions at infinite dilution in pure solvents as well as for accurate predictions in mixed-solvent systems. The results of the Gibbs energy of transfer from water to water-methanol mixtures for the potassium ion is shown in Figure 2.

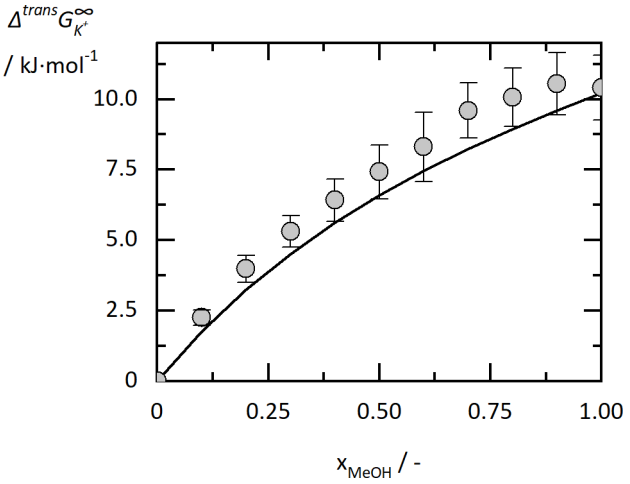

Figure 2. Gibbs energy of transfer from water to water-methanol mixtures of the potassium ion at infinite dilution at 298.15K and 1 bar. The circles are data taken from the literature (details: see publication) and the line was predicted using ePC-SAFT.

Additionally, properties of concentrated solutions (e.g. activity coefficients) of electrolytes in mixed solvent systems were predicted. The predictions were in good agreement with literature data. Overall, the modifications to ePC-SAFT allowed for better description of properties of electrolyte solutions at infinite dilution while retaining the ability of ePC-SAFT to predict properties of concentrated electrolyte systems.

paul.figiel@tu-dortmund.de
yugq@bjut.edu.cn
christoph.held@tu-dortmund.de

Publications:
Figiel, P.; Yu, G.; Held, C.,
Predicting Thermodynamic Properties of Ions in Single Solvents and in Mixed Solvents Using a Modified Born Term within the ePC-SAFT Framework.
Ind. Eng. Chem. Res. 64 (2025) 9406.
https://doi.org/10.1021/acs.iecr.5c00475

Predicting solubilization of hydrophobic compounds by surfactants

A new thermodynamic modelling framework showing nearly quantitative predictive capabilities

Milan Völkel, Gabriele Sadowski

The amphiphilic nature of surfactant molecules enables the solubilization of hydrophobic compounds via micellar aggregate formation once the critical micelle concentration (CMC) is exceeded. This is of particular interest for pharmaceutical formulations in which oil-swollen surfactant aggregates serve as effective carrier systems for poorly water-soluble drugs. We present a new thermodynamic approach for modelling micellar solubilization, which has been shown to accurately predict the drastic improvement in water solubility of long-chain hydrocarbons by surfactants.

In the new modelling approach, we apply a mass-action law describing the formation of mixed aggregates comprising surfactants and solute molecules. The aggregation equilibrium is described via an infinite number of parallel reactions according to the formalism depicted in Figure 1.

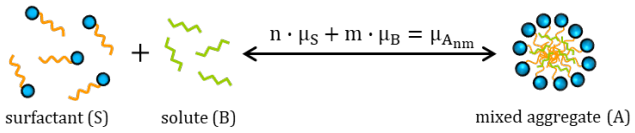

Figure 1. Equilibrium between free surfactants and solute molecules in the aqueous bulk phase and their corresponding mixed aggregates

The chemical potentials of all involved components are calculated using the PC-SAFT equation of state. Herein, mixed aggregates are treated as distinct species, which are allowed to vary in both size and composition. Conformational changes, steric effects, and Gibbs energies of mixing inside the aggregates are considered as additional contributions to the mixed aggregates' chemical potentials, such that effects of their size, geometry, and composition are explicitly accounted for.

This allowed for almost-quantitative predictions (Figure 2) of liquid-liquid equilibria (LLEs) in ternary systems containing water, polyethoxylated alkyl ethers (C_iE_j) as surfactants, and linear hydrocarbons as hydrophobic components.

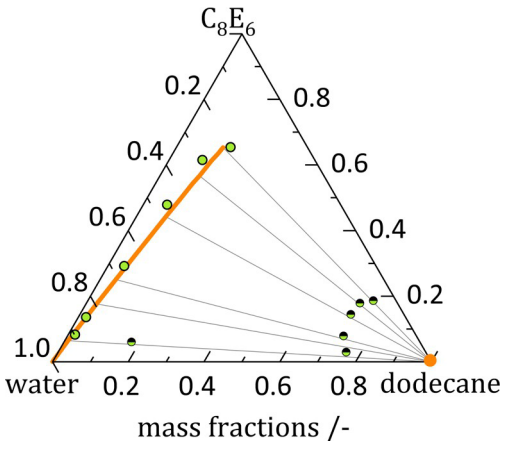

Figure 2. LLE of the system water + C_8E_6 + n-dodecane at 298.15 K. Green circles and half-black circles: Experimental binodal curve and mixing points, respectively (ref. for exp. data see publication). Orange and grey lines: Predicted binodal curve and tie lines, respectively.

Our approach is furthermore capable of quantitatively modelling the CMC which is predicted as the decisive threshold beyond which the solutes' aqueous solubility increases sharply (Figure 3).

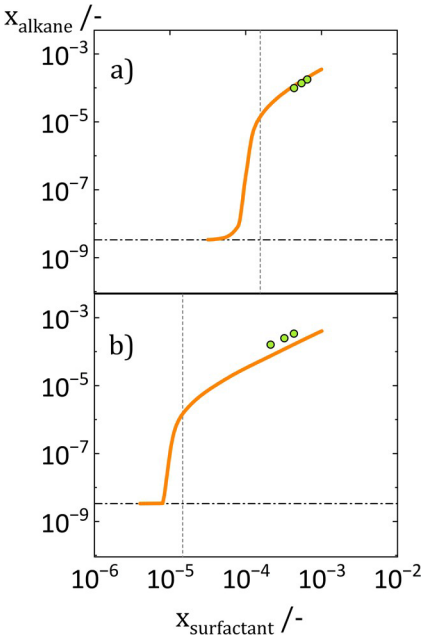

Figure 3. Equilibrium compositions of the aqueous phases in the systems water + C_8E_6 + n-decane (a) and water + $C_{10}E_6$ + n-decane (b) all at 298.15 K. Green circles: Experimental data (for ref. see publication). Orange lines: Model predictions. Vertical dotted lines mark the CMC. Horizontal dashed lines mark the solubility of n-decane in surfactant-free water.

The novel approach provides a predictive design tool for surfactant formulations as a mean to overcome solubility limitations of poorly water-soluble target compounds. It therefore represents a promising step towards in-silico screening methods of surfactants as suitable solubilizing agents.

milan.voelkel@tu-dortmund.de
gabriele.sadowski@tu-dortmund.de

Publications:
Völkel, M.; Sadowski, G., Modelling liquid-liquid equilibria and aggregate formation in aqueous surfactant solutions. Fluid Phase Equilib. 602 (2026) 114608. https://doi.org/10.1016/j.fluid.2025.114608

Völkel, M.; Sadowski, G., Predicting the Solubilization of Hydrocarbons in Aqueous Surfactant Solutions. J. Chem. Eng. Data. (2026). https://doi.org/10.1021/acs.jced.5c00738

Lithium extraction from salt-lake brines using dicationic ionic liquids.

ePC-SAFT modeling and molecular mechanisms.

Gangqiang Yu, Paul Figiel, Christoph Held

This work proposes a novel strategy for enhancing Li^+ extraction from salt-lake brines with the high Mg^{2+}/Li^+ ratio using dicatonic ionic liquid (DIL)-based extractants. The ternary mixture of the DIL [DOMIM][Tf_2N]$_2$, tributyl phosphate (TBP) and dichloromethane (DCM) as a diluent achieved a higher single-stage Li+ extraction efficiency (E_{Li+}≈86.40%) and separation selectivity of Li^+/Mg^{2+} (≈302.37) compared with the ternary mixture based on monocationic IL [OMIM][Tf_2N] instead of the DIL. ePC-SAFT was used to qualitatively predict activity coefficients of Li^+ and Mg^{2+} in the organic phase of the so-called "organic–inorganic complex strong electrolyte system". The DIL-enhanced extraction mechanisms at the molecular level (i.e., Li^+ extracted the form of $2Li^+$+3TBP+2[Tf_2N]$^-$ complex) was revealed by slope analysis spectrum characters and quantum chemical (QC) calculations.

The IGM analyses were performed to further understand the molecular-level mechanism for Li^+ extraction. The Li^+-[Tf_2N]- system, the $Li^+\cdots$O=S interactions can present between Li^+ and oxygens of O=S groups. It can be visually observed that Li^+-[Tf_2N]$^-$ has two interaction sites, while $2Li^+$-2[Tf_2N]$^-$ has six interaction sites, which results in the DIL -based extractant has the stronger affinity with Li^+. Meanwhile, the similar phenomena are also presented in the IGM distributions of H_2O-[OMIM]$^+$ and $2H_2O$- [DOMIM]$^{2+}$ indicating the DIL can increase affinity with H_2O to improve the cation exchange for Li^+ extraction.

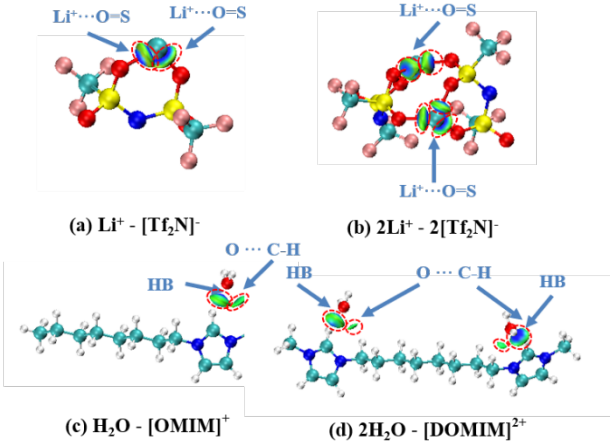

Figure 1. IGM visualization of complex: Li^+-[Tf_2N]- (a), $2Li^+$-2[Tf_2N]- (b) and IGM visualization of ion hydration H_2O-[OMIM]$^+$ (c), $2H_2O$-[DOMIM]$^{2+}$(d)

In ePC-SAFT modeling, Mg^{2+}-related binary interaction parameters were set to zero. The inverse infinite-dilution activity coefficient ($1/\gamma^{\infty}$) was used to represent extraction capacity. the predicted $\ln(1/\gamma^{\infty})$ values align well with experimental distribution ratios (D_{Li+}) for both ions. With increasing V_{IL} and V_{TBP} extraction increased significantly before leveling off, whereas Mg^{2+} extraction showed a continuous increasing trend. These results confirm that ePC-SAFT can qualitatively describe the thermodynamics of this complex organic–inorganic electrolyte system using minimal interaction parameters.

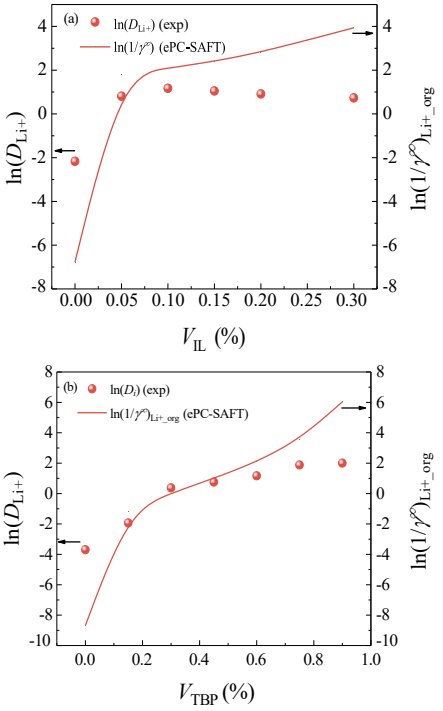

Figure 2. Comparison of the calculated (lines) and experimental (points) on the effects of the volume fraction of DIL(V_{IL}) (Mg^{2+}/Li^+ = 46:1; and pH = 7 and V_{IL} = 0-30%) (a) and the TBP volume concertation(V_{TBP}) (Mg^{2+}/Li^+ = 46:1; and pH = 7 and V_{TBP} = 0-100%)(b) on Li^+ extraction efficiency with [DOMIM][Tf_2N]$_2$ + TBP+DCM as extraction system and the parameters were fitted to E_{Li+} at O/A = 1:1 and 298.15 K, i.e., all other modeling lines are predictions.

To conclude, integrating experimental validation with ePC-SAFT predictions and quantum chemical calculations demonstrates that the novel [DOMIM][Tf_2N]$_2$-based system significantly enhances Li^+ extraction via a stable $2Li^+$+3TBP+2[Tf_2N]$^-$ complex, offering superior selectivity and for complex brine treatment compared to monocationic analogues.

yuqq@bjut.edu.cn (G. Yu)
christoph.held@tu-dortmund.de (C. Held)

Publications:
Yu, G.Q.; Li, Y.F.; Zhang, X.H.; Jovein, I.B.; Figiel, P.; Chen, B.H.; Ji, Y.H.; Sadowski, G.; Held, C. Lithium extraction from salt-lake brines using dicatonic ionic liquids: ePC-SAFT modeling and molecular mechanisms. AIChE Journal, 71 (2025), 9.
https://doi.org/10.1002/aic.18907

2025

Peer Reviewed Journal Articles – TH

Schlüter, M., Held, C., Wohlgemuth, K.
BHET Crystallization in Water-Free PET Glycolysis Systems.
Industrial & Engineering Chemistry Research 64 (2), 1189–120 (2025)
https://doi.org/10.1021/acs.iecr.4c03250

Zäh, M., Brandenbusch, C., Artusio, F., Sadowski, G., Pisano, R.
DSC Reveals the Excipient Impact on Aggregation Propensity of Pharmaceutical Peptides during Freezing.
European Journal of Pharmaceutical Sciences 204, 106954 (2025)
https://doi.org/10.1016/j.ejps.2024.106954

Borrmann, D., Friedrich, P., Smuda, J., Sadowski, G.
Counteracting the Loss of Release for Indomethacin-Copovidone ASDs.
Journal of Pharmaceutical Sciences 114 (1), 449–457 (2025)
https://doi.org/10.1016/j.xphs.2024.10.022

Kerkhoff, J., Borrmann, D., Sadowski, G.
Co-Sorption of Volatile Components in Polymer-Based Pharmaceutical Formulations.
Fluid Phase Equilibria 589, 114247 (2025)
https://doi.org/10.1016/j.fluid.2024.114247

Ascani, M., Sadowski, G., Held, C.
Molecular Thermodynamics of Complex Coacervate Systems. Part I: Modeling of Polyelectrolyte Solutions Using pePC-SAFT.
Fluid Phase Equilibria 591, 114304 (2025)
https://doi.org/10.1016/j.fluid.2024.114304

Ascani, M., Lipínski, W. P., Smokers, I. B. A., Neethirajah, P., Vogel, M., Spruijt, E., Sadowski, G., Held, C.
Molecular Thermodynamics of Complex Coacervate Systems. Part II: Measuring and Modeling of the Phase Envelope Using pePC-SAFT.
Fluid Phase Equilibria 591, 114305 (2025)
https://doi.org/10.1016/j.fluid.2024.114305

Zäh, M., Brandenbusch, C., Groël, S., Winter, G., Sadowski, G.
Water Activity as an Indicator for Antibody Storage Stability in Lyophilized Formulations.
Molecular Pharmaceutics 22 (2), 918–926 (2025)
https://doi.org/10.1021/acs.molpharmaceut.4c01106

Schlüter, M., Zimmer, J., Held, C., Wohlgemuth, K.
Enhancing Sustainability in PET Glycolysis by Closed-Loop Recycling.
Chemical Engineering Science 307, 121337 (2025)
https://doi.org/10.1016/j.ces.2025.121337

Jovein, I. B., Baco, S., Sadowski, G., Doghieri, F., Baschetti, M. G., Yu, G., Leveneur, S., Legros, J., Held, C.
Comprehensive Compilation on Esterification Reactions and Predicting Reaction Kinetics and Equilibrium Using PC-SAFT.
ACS engineering Au 5 (3), 234–246 (2025)
https://doi.org/10.1021/acsengineeringau.5c00002

Rother, M., Sadowski, G.
Hydrophobic Interactions Described Using Hetero-Segmented PC-SAFT: 2. Surfactants and Their Aqueous Solutions.
Fluid Phase Equilibria 593, 114342 (2025)
https://doi.org/10.1016/j.fluid.2025.114342

Zhang, X., Li, Y., Chen, B., Sadowski, G., Held, C., Yu, G.
Magnesium Extraction from Salt Lake Brines by Hydrophobic Eutectic

Solvents: Experimental and Molecular Insights.
Chemical Engineering Science 306 (2025)
https://doi.org/10.1016/j.ces.2025.121285

Kerkhoff, J., Opitz, N., Borrmann, D., Sadowski, G.
Drying Kinetics of Polymer-Based Pharmaceutical Formulations.
Fluid Phase Equilibria 594, 114390 (2025)
https://doi.org/10.1016/j.fluid.2025.114390

Kerkhoff, J., Opitz, N., Peters, L., Borrmann, D., Sadowski, G.
Water-Assisted Drying of PVPVA-Based Amorphous Solid Dispersions.
Molecular Pharmaceutics 22 (7), 3771–3781 (2025)
https://doi.org/10.1021/acs.molpharmaceut.5c00033

Guo, Y., Zhang, X., Chen, B., Sadowski, G., Held, C., Yu, G., Sadowski, G.
Π-Electron-driven Ionic Liquids to Enhance Lithium Recovery from Spent Batteries: Experimental and Mechanistic Insights.
AIChE Journal 71(8), e18860 (2025)
https://doi.org/10.1002/aic.18860

Yu, G., Fu, Y., Mu, W., Wang, N., Jovein, I. B., Chen, B., Sadowski, G., Ji, X., Held, C.
CO2 Capture with Hydrophobic Halogen-free Natural Deep Eutectic Solvents: Perturbed-chain Statistical Associating Fluid Theory Modeling and Molecular Insights.
AIChE Journal 71 (8), e18878 (2025)
https://doi.org/10.1002/aic.18878

Yu, G., Li, Y., Zhang, X., Jovein, I. B., Figiel, P., Chen, B., Ji, Y., Sadowski, G., Held, C. Lithium Extraction from Salt-lake Brines Using Dicationic Ionic Liquids:
ePC-SAFT Modeling and Molecular Mechanisms.
AIChE Journal 71 (9), e18907 (2025)
https://doi.org/10.1002/aic.18907

Fritschka, E., Sadowski, G.
The Hidden Crux of Correctly Determining Octanol–Water Partition Coefficients.
Molecular Pharmaceutics 22 (8), 4930–4939 (2025)
https://doi.org/10.1021/acs.molpharmaceut.5c00552

Peveling, S., Kühl, H.-D.
Numerical Optimization of Metal Felt Regenerators with Axially Varying Matrix Structures for Stirling Engines.
International Journal of Thermofluids 29, 101338 (2025)
https://doi.org/10.1016/j.ijft.2025.101338

Fahrig, I., Walter, S., Kyerematen, S., Degenhardt, M., Sadowski, G., Brandenbusch, C.
The More the Better?—Vitamin E TPGS as a Release Enhancer for Ritonavir/PVPVA Amorphous Solid Dispersions.
Molecular Pharmaceutics 22(9), 5592–5602 (*2025*)
https://doi.org/10.1021/acs.molpharmaceut.5c00620

Zäh, M., Knappstein, P. L., Brandenbusch, C., Sadowski, G.
Thermodynamic Insights into Annealing-Assisted Lyophilization.
Industrial & Engineering Chemistry Research 2025, 64 (32), 15857–15865
https://doi.org/10.1021/acs.iecr.5c01121

Mehrparvar, S., Klinksiek, M., Gauld, R. M., Wolf, J., Poliyodath Mohanan, M., Vonnemann, C., Haase, J., Papagna, R., Völkel, M., Däschlein-Gessner, V. H., Held, C., Huber, S. M.
Halogen Bonding in Solution: Under Pressure.
Journal of the American Chemical Society 147 (33), 29659–29665 (2025)
https://doi.org/10.1021/jacs.5c11036

Zhang, X., Li, Y., Chen, B., Lei, Z., Sadowski, G., Held, C., Yu, G., Sadowski, G.
Enhancing Lithium Extraction with Π-electron Donor-based Ionic Liquids: Molecular Thermodynamics and Dynamic Insights.

AIChE Journal 72 (1), e70063 (2025)
https://doi.org/10.1002/aic.70063

Fritschka, E., Sadowski, G., Sadowski, G.
Simultaneous Influence of Electrolytes and PH on Solubility and Distribution Coefficients of Ionizable Pharmaceuticals.
Industrial & Engineering Chemistry Research 64 (44), 21307–21315 (2025)
https://doi.org/10.1021/acs.iecr.5c03013

Yu, G., Li, Y., Jovein, I. B., Figiel, P., Chen, B., Sadowski, G., Held, C., Sadowski, G.
Olefin Separation from FCC Naphtha by Deep Eutectic Solvents: PC-SAFT Modeling and Molecular Insights.
AIChE Journal 72 (2), e70114 (2025)
https://doi.org/10.1002/aic.70114

Sadowski, G., Kontogeorgis, G. M., Artusio, F., Gerogiorgis, D. I., De Angelis, G., ten Kate, A., de Hemptinne, J.-C., Sadowski, G.
The Thermodynamic Pharma Challenge: A Cross-Cutting Perspective.
European Journal of Pharmaceutical Sciences 212, 107178 (2025)
https://doi.org/10.1016/j.ejps.2025.107178

Gerlach, M., Huxoll, F., Jameel, F., Stein, M., Seidel-Morgenstern, A., Hamel, C., Sadowski, G.
Activity-Based Approach to Predict the Effect of Solvent Composition on the Reaction Kinetics of Hydroformylation.
Chemical Engineering Journal 513, 162959 (2025)
https://doi.org/10.1016/j.cej.2025.162959

Perez Erviti, J. A., Almeida Hernández, Y., Mieres Pérez, J., Gajardo-Parra, N., Winter, R., Held, C., Sadowski, G., Sánchez García, E.
Effect of Trimethylamine-N-oxide (TMAO) and Sorbitol on the Catalytic Activity of Candida Boidinii Formate Dehydrogenase.
ChemCatChem 17 (11), e202401961 (2025)
https://doi.org/10.1002/cctc.202401961

Habicht, J., Sadowski, G., Brandenbusch, C.
An Adaptive ML Framework to Predict PC-SAFT Parameters for Mixtures.
Industrial & Engineering Chemistry Research 64 (46), 22413–22427 (2025)
https://doi.org/10.1021/acs.iecr.5c03062

Baco, S., Mignot, M., Held, C., Legros, S., Leveneur, S.
Dissecting steric and polar substituent effects in linear free energy Relationships: Re-Assessment of the Taft equation with Temperature-Dependent kinetic modeling.
Chemical Engineering Science 320, Part C, 122700 (2025)
https://doi.org/10.1016/j.ces.2025.122700

Zhang, W.H., Gao, J., Zhang, C., Held, C., Yu, G., Meng, H.
Ionic Liquids for olefin extractive separation from fluid catalytic cracking naphtha: Thermodynamics and molecular mechanisms.
Green Energy & Environment 2025
https://doi.org/10.1016/j.gee.2025.09.005

Zuo, Z., Cao, M., Mu, W., Jovein, I.B., Held, C., Chen, B., Yu, G.
Selective absorption of fluorinated gases by deep eutectic solvents: Thermodynamics and molecular insights.
Separation and Purification Technology, 364, Part 1, 132342 (2025)
https://doi.org/10.1016/j.seppur.2025.132342

Figiel, P., Yu, G., Held, C.
Predicting Thermodynamic Properties of Ions in Single Solvents and in Mixed Solvents Using a Modified Born Term within the ePC-SAFT Framework.
Industrial & Engineering Chemistry Research 64(18), 9406–9418 (2025)
https://doi.org/10.1021/acs.iecr.5c00475

Klinksiek, M., Baco, S., Leveneur, S., Legros, J., Held, C.
Predicting Proton Activity and Acid Dissociation Equilibria in Mixed-Solvent Systems, and Their Impact on Esterification Kinetics of Levulinic Acid.
Industrial & Engineering Chemistry Research, 64(11), 6188–6202 (2025)
https://doi.org/10.1021/acs.iecr.5c00115

Gajardo-Parra, N.F., Cea-Klapp, E., Chandra, A., Canales, R.I., Garrido, J.M., Held, C., Guajardo, N.
Assessing the Effect of Deep Eutectic Solvents on α-Chymotrypsin Thermal Stability and Activity.
ChemSusChem 18 (5), e202401414 (2025)
https://doi.org/10.1002/cssc.202401414

2024

Peer Reviewed Journal Articles - TH

Schick, D., Chen, Q., Hellfajer, L., Strangmann, A., Figiel, P., Trusler, J. P. M., Sadowski, G., Held, C.
Influence of Solvents and Salts on CO2 Solubility and the Impact on an Esterification Reaction.
Journal of chemical & engineering data 69 (2), 560–572 (2024)
https://doi.org/10.1021/acs.jced.3c00178

Habicht, J., Sadowski, G., Brandenbusch, C.
Fitting Error vs Parameter Performance – How to Choose Reliable PC-SAFT Pure-Component Parameters by Physics-Informed Machine Learning.
Journal of chemical & engineering data 69 (2), 482–494 (2024)
https://doi.org/10.1021/acs.jced.3c00411

Ostermeier, L., Ascani, M., Gajardo-Parra, N., Sadowski, G., Held, C., Winter, R.
Leveraging Liquid-Liquid Phase Separation and Volume Modulation to Regulate the Enzymatic Activity of Formate Dehydrogenase.
Biophysical chemistry 304 (2024)
https://doi.org/10.1016/j.bpc.2023.107128

Grönniger, B., Kimpe, K., Singh, A., Sadowski, G.
Simultaneous Water Sorption and Crystallization in ASDs 1: Stability Studies Lasting for Two Years.
Molecular pharmaceutics 2024
https://doi.org/10.1021/acs.molpharmaceut.3c01056

Pyka, T., Bieberle, A., Loll, R., Held, C., Schubert, M., Schembecker, G.
Distributor Effects on Liquid Hold-up in Rotating Packed Beds.
Industrial & engineering chemistry research 63 (4), 2000–2010 (2024)
https://doi.org/10.1021/acs.iecr.3c03996

Anjum, F., Wessner, M., Witte, B. D., Al-Rifai, N., Collas, A., Sadowski, G.
Tailoring the Use of Excipients in Bottom-up Production of Naproxen Crystal Suspensions via Membrane Technology.
International journal of pharmaceutics 652 (2024)
https://doi.org/10.1016/j.ijpharm.2024.123846

Yu, G., Zhang, X., Hubach, T., Chen, B., Held, C.
Highly Efficient Lithium Extraction from Magnesium-Rich Brines with Ionic Liquid-Based Collaborative Extractants: Thermodynamics and Molecular Insights.
Chemical engineering science 286 (2024)
https://doi.org/10.1016/j.ces.2023.119682

Fischer, F., Kühl, H.-D.
Generation of Compressed Air by Overdriven Free-Displacer Thermocompressors – Experimental Investigation of a Single Stage.
Applied thermal engineering 244 (2024)
https://doi.org/10.1016/j.applthermaleng.2024.122712

Anjum, F., Viville, T., Nandi, S., Wessner, M., Witte, B. D., Collas, A., Sadowski, G.
Bottom-up Production of Injectable Itraconazole Suspensions Using Membrane Technology.
International journal of pharmaceutics 654 (2024)
https://doi.org/10.1016/j.ijpharm.2024.123977

Wang, S., Sadowski, G., Ji, Y.
Strategy of Coupling Artificial Intelligence with Thermodynamic Mechanism for Predicting Complex Polymer Viscosities.
ACS sustainable chemistry & engineering 12 (11), 4631–4643 (2024)
https://doi.org/10.1021/acssuschemeng.3c08185

Brandenbusch, C., Lu, X.
Enders, S. Editorial for the Special Issue in Honor of Gabriele Sadowski on the Occasion of Her 60th Birthday.
In Journal of chemical & engineering data, ACS Publ.: Washington, DC Vol. 69, pp 289–290 (2024)
https://doi.org/10.1021/acs.jced.4c00014

Deac, A., Lübbert, C., Qi, Q., Courtney, R. M., Indulkar, A. S., Gao, Y., Zhang, G. G. Z., Sadowski, G., Taylor, L. S.
Dissolution Mechanisms of Amorphous Solid Dispersions: Application of Ternary Phase Diagrams to Explain Release Behavior.
Molecular pharmaceutics 21 (4), 1900–1918 (2024)
https://doi.org/10.1021/acs.molpharmaceut.3c01179

Schlüter, M., Bhutani, S., Bahr, J., Wohlgemuth, K., Held, C.
Measurement and PC-SAFT Modeling of the Solubility of the BHET Monomer, the BHET Dimer, and PET in Single Solvents.
Journal of chemical & engineering data 69 (3), 1326–1334 (2024)
https://doi.org/10.1021/acs.jced.3c00627

Kloc, A. P., Anjum, F., Wessner, M., Hudson, S., Fernandes, P., Witte, B. D., Sadowski, G.
PC-SAFT-Assisted Design of Antisolvent Naproxen Crystallization in the Presence of Polymers.
Crystal growth & design 24 (8), 3419–3429 (2024)
https://doi.org/10.1021/acs.cgd.4c00143

Grönniger, B., Fritschka, E., Kimpe, K., Singh, A., Sadowski, G.
Simultaneous Water Sorption and Crystallization in ASDs 2: Modeling Long-Term Stabilities.
Molecular pharmaceutics 21 (6), 2908–2921 (2024)
https://doi.org/10.1021/acs.molpharmaceut.4c00055

Fritschka, E., Sadowski, G.
Rigorous Modeling the PH-Dependent Solubility of Weak Acids, Weak Bases and Their Salts.
Fluid phase equilibria, 580 (2024)
https://doi.org/10.1016/j.fluid.2024.114039

Cui, C., Wu, H., Sadowski, G., Ji, Y.
Solubility Measurement and Thermodynamic Modeling of Bifendate in 13 Pure Solvents at Temperatures from 293.15 to 333.15 K.
Journal of chemical & engineering data 2024
https://doi.org/10.1021/acs.jced.4c00239

Baco, S., Klinksiek, M., Mignot, M., Held, C., Legros, J., Leveneur, S.
Temperature Effect on the Steric and Polar Taft Substituent Parameter Values.
Reaction chemistry & engineering 9 (4), 833–841 (2024)
https://doi.org/10.1039/d3re00500c

Oliva, R., Ostermeier, L., Jaworek, M., Del Vecchio, P., Gajardo-Parra, N., Cea-Klapp, E., Held, C., Petraccone, L., Winter, R.
Modulation of Protein-Saccharide Interactions by Deep-Sea Osmolytes under High Pressure Stress.
International journal of biological macromolecules 255 (2024)
https://doi.org/10.1016/j.ijbiomac.2023.128119

Schlüter, M., Bhutani, S., Wohlgemuth, K., Held, C.
Predicting Kinetics of the PET Glycolysis Reaction Using an Activity-Based Model and Experimental Validation.
Industrial & engineering chemistry research, 63 (35), 15458–15465 (2024)
https://doi.org/10.1021/acs.iecr.4c02382

Schlüter, M., Enomoto, R., Makino, S., Weihs, L., Stamm, C. L., Wohlgemuth, K., Held, C.
Boosting the Kinetics of PET Glycolysis.
Reaction chemistry & engineering 2024
https://doi.org/10.1039/d4re00235k

Fischer, F., Kühl, H.-D.
Generation of Compressed Air by Overdriven Free-Displacer Thermocompressors: Experimental Investigation of a Three-Stage Cascade.
Applied thermal engineering 257 (A) (2024)
https://doi.org/10.1016/j.applthermaleng.2024.124193

Rother, M., Sadowski, G.
Hydrophobic Interactions Described Using Hetero-Segmented PC-SAFT: 1. Alcohol/Water Mixtures.
Fluid phase equilibria 582 (2024)
https://doi.org/10.1016/j.fluid.2024.114102

Averbeck, T., Sadowski, G., Held, C., Seidensticker, T.
Neural Network-Based Tensor Completion: Advancing Predictions of Activity Coefficients and Beyond.
Industrial & engineering chemistry research 63 (28), 12648–12655 (2024)
https://doi.org/10.1021/acs.iecr.4c00352

Sadowski, G., Huang, L., Ji, X., Ji, Y.
Preface to the Special Issue in Honor of Xiaohua Lu.
Journal of chemical & engineering data, 69 (12), 4259–4260 (2024)
https://doi.org/10.1021/acs.jced.4c00648

Schlüter, M., Held, C., Wohlgemuth, K.
BHET Crystallization in Water-Free PET Glycolysis Systems.
Industrial & engineering chemistry research 2024
https://doi.org/10.1021/acs.iecr.4c03250

2023

Peer Reviewed Journal Articles - TH

Kroll, P., Exner, L., Brandenbusch, C., Sadowski, G.
Influence of Hydrophobic and Hydrophilic Chain Length of CiEj Surfactants on the Solubilization of Active Pharmaceutical Ingredients.
Molecular pharmaceutics, 20 (2), 1296–1306 (2023)
https://doi.org/10.1021/acs.molpharmaceut.2c00941

Klinksiek, M., Baco, S., Leveneur, S., Legros, J., Held, C.
Activity-based Models to Predict Kinetics of Levulinic Acid Esterification.
ChemPhysChem 24 (4) (2023)
https://doi.org/10.1002/cphc.202200729

Ascani, M., Sadowski, G., Held, C.
Simultaneous Predictions of Chemical and Phase Equilibria in Systems with an Esterification Reaction Using PC-SAFT.
Molecules 28 (4) (2023)
https://doi.org/10.3390/molecules28041768

Anjum, F., Wessner, M., Sadowski, G.
Membrane-Based Solvent Exchange Process for Purification of API Crystal Suspensions.
Membranes 13 (3), 263 (2023)
https://doi.org/10.3390/membranes13030263

Grönniger, B., Fritschka, E., Fahrig, I., Danzer, A., Sadowski, G.
Water Sorption in Rubbery and Glassy Polymers, Nifedipine, and Their ASDs.
Molecular pharmaceutics 20 (4), 2194–2206 (2023)
https://doi.org/10.1021/acs.molpharmaceut.3c00006

Yu, G., Gajardo-Parra, N. F., Chen, M., Chen, B., Sadowski, G., Held, C.
Aromatic Volatile Organic Compounds Absorption with Phenyl-based Deep Eutectic Solvents: A Molecular Thermodynamics and Dynamics Study.
AIChE journal / American Institute of Chemical Engineers 69 (5) (2023)
https://doi.org/10.1002/aic.18053

Cordier, A., Klinksiek, M., Held, C., Legros, J., Leveneur, S.
Biocatalyst and Continuous Microfluidic Reactor for an Intensified Production of N-Butyl Levulinate : Kinetic Model Assessment.
Chemical engineering journal 451 (2023)
https://doi.org/10.1016/j.cej.2022.138541

Grönniger, B., Danzer, A., Kimpe, K., Singh, A., Sadowski, G.
Viscoelastic Behavior of Supercooled and Glassy ASDs at Humid Conditions Can Be Predicted.
Molecular pharmaceutics 20 (5), 2568–2578 (2023)
https://doi.org/10.1021/acs.molpharmaceut.3c00008

Krummnow, A., Danzer, A., Voges, K., Kyeremateng, S. O., Degenhardt, M., Sadowski, G.
Kinetics of Water-Induced Amorphous Phase Separation in Amorphous Solid Dispersions via Raman Mapping.
Pharmaceutics 15 (5) (2023)
https://doi.org/10.3390/pharmaceutics15051395

Janssen, L., Sadowski, G., Brandenbusch, C.
Continuous Phase Separation of Stable Emulsions from Biphasic Whole-cell Biocatalysis by Catastrophic Phase Inversion.
Biotechnology journal 18 (6) (2023)
https://doi.org/10.1002/biot.202200489

Habicht, J., Brandenbusch, C., Sadowski, G.
Predicting PC-SAFT Pure-Component Parameters by Machine Learning Using a Molecular Fingerprint as Key Input.
Fluid phase equilibria 565 (2023)
https://doi.org/10.1016/j.fluid.2022.113657

Dohrn, S., Kyeremateng, S. O., Bochmann, E., Sobich, E., Wahl, A., Liepold, B., Sadowski, G., Degenhardt, M.
Thermodynamic Modeling of the Amorphous Solid Dispersion-Water Interfacial Layer and Its Impact on the Release Mechanism.
Pharmaceutics 15 (5) (2023)
https://doi.org/10.3390/pharmaceutics15051539

Lingen, T. van, Bragoni, V., Dyga, M., Exner, B., Schick, D., Held, C., Sadowski, G., Gooßen, L. J.
Carboxylation of Acetylene without Salt Waste: Green Synthesis of C4 Chemicals Enabled by a CO2-pressure Induced Acidity Switch.
Angewandte Chemie International edition 62 (27) (2023)
https://doi.org/10.1002/anie.202303882

Hubach, T., Schlüter, S., Held, C.
Model-Based Optimization of Multi-Stage Nanofiltration Using the Solution-Diffusion–Electromigration Model.
Processes 11 (8) (2023)
https://doi.org/10.17877/de290r-23911

Loll, R., Nordhausen, L., Bieberle, A., Schubert, M., Pyka, T., Koop, J., Held, C., Schembecker, G.
Analysis of Flow Patterns in Structured Zickzack Packings for Rotating Packed Beds Using γ-Ray Computed Tomography.
Industrial & engineering chemistry research, 62 (38), 15625–15634 (2023)
https://doi.org/10.1021/acs.iecr.3c02252

Gajardo-Parra, N. F., Rodríguez, G., Arroyo-Avirama, A. F., Veliju, A., Happe, T., Canales, R. I., Sadowski, G., Held, C.
Impact of Deep Eutectic Solvents on Kinetics and Folding Stability of Formate Dehydrogenase.
Processes 11 (10) (2023)
https://doi.org/10.3390/pr11102815

Hubach, T., Pillath, M., Knaup, C., Schlüter, S., Held, C.
Li+ Separation from Multi-Ionic Mixtures by Nanofiltration Membranes: Experiments and Modeling.
Modelling 4 (3), 408–425 (2023)
https://doi.org/10.3390/modelling4030024

Fischer, F., Peveling, S., Kühl, H.-D.
Simulation and Stability Analysis of a Thermocompressor Cascade with Overdriven Free Displacers.
Thermal science and engineering progress 44 (2023)
https://doi.org/10.1016/j.tsep.2023.102037

Zäh, M., Brandenbusch, C., Winter, G., Sadowski, G.
Predicting the Amorphous-Phase Composition during Lyophilization.
International journal of pharmaceutics 636 (2023)
https://doi.org/10.1016/j.ijpharm.2023.122836

Held, C., Liang, X.
100 Years from the Debye-Hückel Theory and Beyond.
In Fluid phase equilibria, Elsevier: Amsterdam Vol. 575 (2023)
https://doi.org/10.1016/j.fluid.2023.113931

Aravena, P., Cea-Klapp, E., Gajardo-Parra, N., Held, C., Garrido, J. M., Canales, R. I.
Effect of Water and Hydrogen Bond Acceptor on the Density and Viscosity of Glycol-Based Eutectic Solvents.
Journal of molecular liquids 389 (2023)
https://doi.org/10.1016/j.molliq.2023.122856

Kruber, K. F.; Kroll, M.; Held, C.; Skiborowski, M.
Evaluation of the Potential of a Deep Eutectic Solvent for Liquid-Liquid Extraction of Furfural Using Optimization-Based Process Design.
In 33rd European Symposium on Computer Aided Process Engineering; Kokossis, A. C., Georgiadis, M. C., Pistikopoulos, S., Eds.; Elsevier: Amsterdam Vol. 52, pp 955–960 (2023)
https://doi.org/10.1016/b978-0-443-15274-0.50152-9

Pyka, T., Ressemann, A., Held, C., Schembecker, G., Repke, J.-U.
Impact of Vapor Bypasses on Separation Performance of Rotating Packed Beds in Distillation.
Industrial & engineering chemistry research 62 (33), 13274–13279 (2023)
https://doi.org/10.1021/acs.iecr.3c01947

Meneses, L., Gajardo-Parra, N., Cea-Klapp, E., Garrido, J. M., Held, C., Duarte, A. R., Paiva, A.
Improving the Activity of Horseradish Peroxidase in Betaine-Based Natural Deep Eutectic Systems.
RSC sustainability 1 (4), 886–897 (2023)
https://doi.org/10.1039/d2su00127f

Arroyo-Avirama, A. F., Carreño-Guzmán, S., Lorenzo-Llanes, J., Gajardo-Parra, N., Santiago, R., Held, C., Palomar, J., Canales, R. I.
In Situ Product Recovery of β-Ionone from a Fermentation Broth: Computational Solvent Selection and Process Design of Its Extraction and Purification.
ACS sustainable chemistry & engineering 11 (24), 9065–9076 (2023)
https://doi.org/10.1021/acssuschemeng.3c01739

Martinez, F., Held, C., Siepmann, J. I.
Introducing JCED Associate Editor Fleming Martinez and Topic Editor Christoph Held - Some Remarks on Reporting on the Solubility of Organic Compounds and of Electrolytes.
In Journal of chemical & engineering data, ACS Publ.: Washington, DC Vol. 68, pp 1265–1266 (2023)
https://doi.org/10.1021/acs.jced.3c00278

Schick, D., Arrad, M., Sadowski, G., Figiel, P., Held, C.
Modeling the Temperature-Dependent Solubility of Salts in Organic Solvents.
Fluid phase equilibria 572 (2023)
https://doi.org/10.1016/j.fluid.2023.113828

Pyka, T., Brunert, M., Koop, J., Bieberle, A., Held, C., Schembecker, G.
Novel Liquid Distributor Concept for Rotating Packed Beds.

Industrial & engineering chemistry research 62 (14), 5984–5994 (2023)
https://doi.org/10.1021/acs.iecr.3c00248

Schick, D., Bierhaus, L., Strangmann, A., Figiel, P., Sadowski, G., Held, C.
Predicting CO2 Solubility in Aqueous and Organic Electrolyte Solutions with EPC-SAFT Advanced.
Fluid phase equilibria 567 (2023)
https://doi.org/10.1016/j.fluid.2022.113714

Delgado, J., Vásquez Salcedo, W. N., Devouge-Boyer, C., Hebert, J.-P., Legros, J., Renou, B., Held, C., Grenman, H., Leveneur, S.
Reaction Enthalpies for the Hydrogenation of Alkyl Levulinates and Levulinic Acid on Ru/C– Influence of Experimental Conditions and Alkyl Chain Length.
Process safety and environmental protection 171, 289–298 (2023)
https://doi.org/10.1016/j.psep.2023.01.025

Espinoza-Cartagena, F., Ormazábal-Latorre, S., Pazo-Carballo, C., Gajardo-Parra, N., Núñez, G. A., Garrido, J. M., Cea-Klapp, E., Santiago, R., Held, C., Canales, R. I.
Separation of Isoeugenol from Methylcyclohexane as a Model Mixture of Biojet Fuel Purification: Solvent Selection and Liquid–Liquid Equilibrium.
Industrial & engineering chemistry research 62 (30), 12006–12020 (2023)
https://doi.org/10.1021/acs.iecr.3c01440

Koop, J., Bera, N., Quickert, E., Schmitt, M., Schlüter, M., Held, C., Schembecker, G.
Separation of Volatile Organic Compounds from Viscous Liquids with RPB Technology.
Industrial & engineering chemistry research 62 (334), 13637–13645 (2023)
https://doi.org/10.1021/acs.iecr.3c01597

Cea-Klapp, E., Arroyo-Avirama, A. F., Ormazábal-Latorre, S., Gajardo-Parra, N. F., Gajardo-Parra, N., Pazo-Carballo, C., Quinteros-Lama, H., Marzialetti, T., Held, C., Canales, R. I., Garrido, J. M.
Separation of Furfuryl Alcohol from Water Using Hydrophobic Deep Eutectic Solvents.
Journal of molecular liquids 384 (2023)
https://doi.org/10.1016/j.molliq.2023.122232

Tsurko, E. N., Held, C., Kunz, W.
Thermodynamic Modeling of Aqueous Guanidinium Chloride/Sodium l-Aspartate (Na-l-Asp) Mixtures.
Journal of solution chemistry 52 (10), 1157–1175 (2023)
https://doi.org/10.1007/s10953-023-01306-y

Chen, Q., Weng, J., Sadowski, G., Ji, Y.
Influence Mechanism of Polymeric Excipients on Drug Crystallization: Experimental Investigation and Chemical Potential Gradient Model Analysis and Prediction.
Crystal growth & design 23 (5), 3862–3872 (2023)
https://doi.org/10.1021/acs.cgd.3c00314

Ge, K., Paus, R., Penner, V., Sadowski, G., Ji, Y.
A Novel Theoretical Strategy for Predicting Dissolution Kinetics and Mechanisms of Pharmaceuticals in Complex Biorelevant Media.
International journal of pharmaceutics 648 (2023)
https://doi.org/10.1016/j.ijpharm.2023.123594

Wolbert, F., Luebbert, C., Sadowski, G.
The Shelf Life of ASDs: 2. Predicting the Shelf Life at Storage Conditions.
International journal of pharmaceutics: X 6 (2023)
https://doi.org/10.1016/j.ijpx.2023.100207

Kloc, A. P., Danzer, A., Sadowski, G.
Solubility of Naproxen and Indomethacin in Supercritical Carbon Dioxide/Ethyl Acetate Mixtures.
The journal of supercritical fluids 200 (2023)
https://doi.org/10.1016/j.supflu.2023.105990

Pyka, T., Backhaus, V., Held, C., Schembecker, G.
Impact of Number of Rotors in Rotating Packed Beds on Separation Performance in Distillation.
Industrial & engineering chemistry research 62 (46), 19855–19861 (2023)
https://doi.org/10.1021/acs.iecr.3c03173

Lingen, T. van, Bragoni, V., Dyga, M., Exner, B., Schick, D., Held, C., Sadowski, G., Gooßen, L. J.
Salzabfall-freie Carboxylierung von Acetylen: grüne Synthese von C4-Chemikalien durch einen CO2-Druck-induzierten Aciditätsswitch.
Angewandte Chemie 135 (27) (2023)
https://doi.org/10.1002/ange.202303882

Grenningloh, K., Wessner, M., Brandenbusch, C., Sadowski, G.
Influence of Process Parameters and Composition on Long-Term Stability of Lipid
Nanocarrier Formulations, 2023
https://aiche.confex.com/aiche/2023/meetingapp.cgi/Paper/663071

Transport Processes (TP)

An extended approach to multiscale simulation of structured heat exchang-ers for enhanced battery cooling.

Simon Baier, Michael-David Fischer, Norbert Kockmann, Alba Dieguez-Alonso

In recent years, EV battery demand experienced rapid growth. To avoid accelerated aging of widely used lithium-ion packs, temperatures must be maintained within roughly 15–35 °C. This paper develops a multiscale simulation approach that couples CFD and FEM on representative unit cells, requiring only the flow pattern and inlet temperature to compute detailed temperature and pressure fields for an entire battery pack. Applied to a 448-cell 18650 pack with sinusoidal cooling channels, the model reproduces full-scale heat-flow and pressure-drop results within about 3 % and 1 %, respectively, showing both its accuracy and computational efficiency.

The multiscale simulation framework divides the battery-pack heat-exchanger into representative “unit cells” and models them individually using CFD-FEM; each unit cell comprises 16 18650 lithium-ion battery cells (18 mm × 65 mm), thermally conductive paste, and a sinusoidally corrugated aluminum cooling plate, yielding a balanced compromise between heat-transfer enhancement and pressure drop. A two-dimensional finite-difference sub-model solves the temperature field within a cylindrical battery cell, allowing the detailed unit-cell model to be reduced to the coolant, plate and the thermal paste; results from these unit-cell simulations are then linked to construct a large-scale battery-pack model. The unit-cell model was evaluated over multiple geometries and inlet temperatures, revealing fully developed flow within half a unit cell, detachment vortices at channel extrema producing local hot spots, and a pressure drop of roughly 11 Pa per cell.

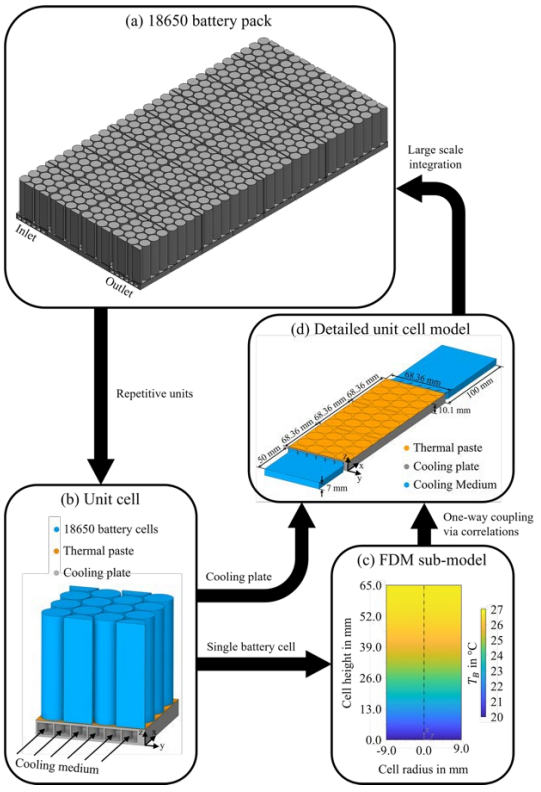

Figure 1. Model scheme of the multiscale simulation method introduced in this work.

By interconnecting 32 unit cells in a large-scale model the entire battery pack was simulated. This multiscale approach was validated using a full-scale CFD-FEM simulation, showing temperature fields within 0.5 % error and cooling-power and pressure-drop predictions within about 3 %, with discrepancies mainly at channel bends.

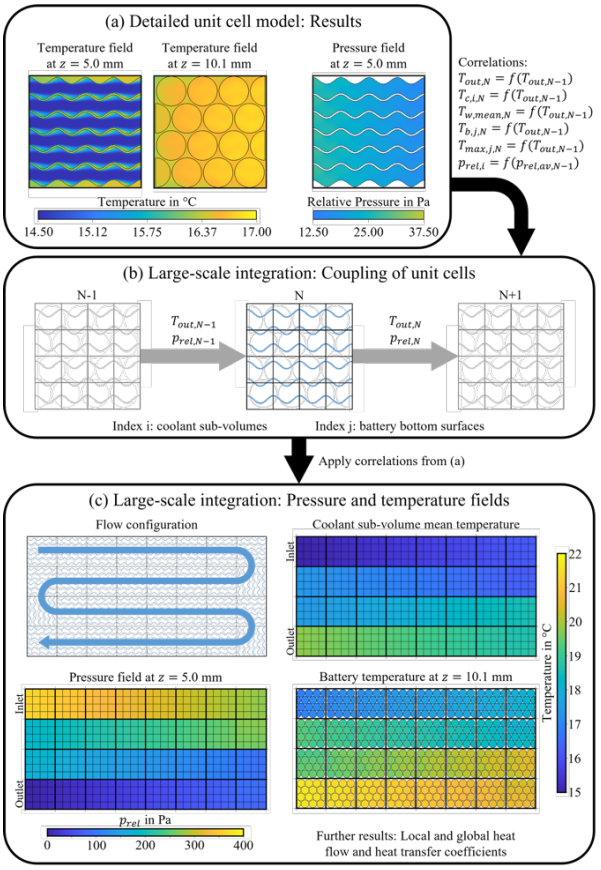

Figure 1. Illustration of the large-scale integration procedure used to describe the entire battery pack.

Parametric studies indicated that battery temperatures are most sensitive to heat generation; increasing coolant flow raises the heat-transfer coefficient but also the pressure drop, and adjusting inlet temperature and flow enables pack designs that keep cell temperatures in the required 15–35 °C range while balancing thermal and hydraulic performance.

simon.baier@tu-dortmund.de
alba.dieguez@tu-dortmund.de

Publication:
Baier, S.; Fischer, M-D.; Kockmann, N.; Dieguez-Alonso, A., An extended approach to multiscale simulation of structured heat exchangers for enhanced battery cooling, International Journal of Heat and Mass Transfer 263 (2026) 128683.

2025

Peer Reviewed Journal Articles

A. Dernbecher, S. Bhaskaran, N. Vorhauer-Huget, J. Seidenbcher, S. Gopalkrishna, L. Briest, A. Dieguez-Alonso, **Investigation on the intra-particle anisotropic transport properties of a beech wood particle during pyrolysis**, *Particuology* 98, 172-190, 2025. https://doi.org/10.1016/j.partic.2025.01.006

JJ Rico, A. Dernbecher, JM de la Rosa, L Hilfert, H Almuina-Villar, N Kulak, S Lucia, A Dieguez-Alonso, **Investigation on the impact of potassium and mild transport limitations on the pyrolysis behavior of beech wood and its macrocomponents**, *Journal of Analytical and Applied Pyrolysis* 192, 107201, 2025. https://doi.org/10.1016/j.jaap.2025.107201

2024

Peer Reviewed Journal Articles

S Hazratqulov, G von Ahlefeldt, R Liu, H Bessler, H Almuina-Villar, A Dieguez-Alonso, C Engels, **Processing Municipal Waste for Phytostabilization of Heavy Metal Contaminated Soils**, *Soil Systems* 8 (4), 109, 2024 https://doi.org/10.3390/soilsystems8040109

P Maziarka, N Kienzl, A Dieguez-Alonso, W Prins, PJ Arauzo, Ø Skreiberg, A Anca-Couce, JJ Manyà, F Ronsse, **Part 2 – Tailoring of Pyrolytic Char Properties with a Singel Particle CFD Model with a Focus on the Impact of Shrinkage, Vapor Cracking, and Char Permeability**, *Energy & Fuels* 38 (11), 9772-9793, 2024 https://doi.org/10.1021/acs.energyfuels.4c00942

P Maziarka, N Kienzl, A Dieguez-Alonso, V Fierro, A Celzard, PJ Arauzo, N Hedin, W Prins, A Anca-Couce, JJ Manyà, F Ronsse, **Part 1 – Impact of pyrolysis temperature and wood particle length on vapor cracking and char porous texture in relation to the tailoring of char properties**, *Energy & Fuels* 38 (11), 9751-9771, 2024 https://doi.org/10.1021/acs.energyfuels.4c00937

N Vorhauer-Huget, J. Seidenbecher, S. Bhaskaran, F. Schenkel, L. Briest, S. Gopalkrishna, J. Barowski, A. Dernbecher, L. Hilfert, I. Rolfes, A. Dieguez-Alonso, **Dielectric and physico-chemical behavior of single thermally thick wood blocks under microwave assisted pyrolysis**, *Particuology* 86, 291-303, 2024 https://doi.org/10.1016/j.partic.2023.07.004

J. Seidenbecher, F. Herz, E. Specht, A. Dieguez-Alonso, **Contact heat transfer analysis in flighted rotary drums**, *Thermal Science and Engineering Progress* 2024, 47, 102265. https://doi.org/10.1016/j.tsep.2023.102265